FLOW PAST A THIN INFLATED LENTICULAR AEROFOIL

by

© MAN-CHUN TSE

A Thesis submitted to the Faculty of Graduate Studies and Research in partial fulfillment of the requirements for the degree of Master of Engineering.

Department of Mechanical Engineering
McGill University
Montreal, Quebec, Canada

August, 1979

SUMMARY

A theoretical and experimental investigation has been conducted on a simulation of a long inflated building.

Thin aerofoil theory using sources and sinks, combined with the equilibrium condition for the membrane, yields an integral equation. This has been solved by using a Fourier Sine series and the shape, membrane tension and pressure distribution are predicted.

Related experiments were carried out for various combinations of the independent parameters, Reynolds number (2.87×10^5 - 9.77×10^5), inflation pressure coefficient (-0.12 - 3.22), and ratio of excess length of membrane to chord length (0.56% - 5.2%). Results for tension in particular are in good accord with theory for values of height-to-chord up to 0.1. The tension coefficient is shown to be a unique function of a parameter which combines the inflation pressure coefficient and the excess length ratio.

RESUME

Une étude théorique et expérimentale a été conduite sur un long bâtiment gonflé.

La théorie des ailes fines, utilisant une distribution de puits et de sources, et l'analyse de tension de membrane ont été employées conjointement pour former une équation intégrale. Cette dernière a été resolue à l'aide des series Sinus de Fourier.

Des expériences ont été organisées avec une combinaison des paramètres indépendants, comme: nombre de Reynolds (2.87×10^5 - 9.77×10^5), coefficient de pression (-0.12 - 3.22) de gonflement, et un rapport "exces de longueur de la membrane sur la corde" ((l-c)/c) (0.56% - 5.2%). Ces résultats ont été en accord avec la théorie, spécialement pour le coefficient de tension jusqu'à valeur de hauteur/corde = 0.1. Le coefficient de tension était fonction unique de la combinaison de la pression de gonflement et du rapport excès de longueur sur corde.

ACKNOWLEDGEMENTS

I would like to express my gratitude to Dr. B.G. Newman for his great help, interest and guidance.

Thanks also to Mr. Joe Dubik who built the apparatus and made the experiment successful.

Above all, I would be very much in debt to my late grandmother who brought me up.

The work was supported by the National Research Council of Canada under the grant number (NRC, A7096).

TABLE OF CONTENTS

NOMENCLATURE

A_n	Fourier Sine coefficient
B_s	Solid blockage
B_t	Total blockage
B_w	Wake blockage
c	Chord length
C_D	Drag coefficient
Cp	Static pressure coefficient at the surface of the inflated aerofoil
Cp_i	$\frac{Pi-P_\infty}{\frac{1}{2}\rho U_\infty^2}$ inflation pressure coefficient
C_T	$\frac{T}{qc}$ induced tension coefficient
$Cp_i\left(\frac{\ell-c}{c}\right)^{-\frac{1}{2}}$	Normalized inflation pressure coefficient
d	Portion of the envelope extends outside the tunnel roof
F_c	Total end correction force
F_L	Total measured force on the leading wedge
F_T	Total measured force on the trailing edge
g(t)	Strength of source or sink per unit length
h	t/2, maximum height of the envelope
H	Tunnel working section height

ℓ	Length of membrane in chordwise direction
m	$-\frac{\delta_2^2}{\nu}\frac{dU}{ds}$, laminar flow separation parameter
N	Number of Fourier coefficient (also, equals to the number of chordwise position)
P	Local absolute static pressure at the inflated aerofoil surface
P_a	Atmospheric pressure
P_i	Inflation absolute pressure
Pig	Inflation gauge pressure
P_r	Tunnel reference pressure
P_s	Free stream static pressure without test model in the working section
P_t	Total pressure of the flow
q	$\frac{1}{2}\rho U_\infty^2$, free stream dynamic pressure
R	Radius of curvature
Re	Reynolds number
s	Distance along the surface, measured from leading edge
S_f	Shape factor
S_s	Laminar separation point
S_t	Transition point

t	Maximum thickness of the inflated aerofoil
T	Induced membrane tension per unit length in span direction
T_c	Induced tension per unit length by the circular arc profile of the envelope
u	Local wind velocity at the surface
u'	Perturbation velocity
U_∞	Free stream velocity
U	Free stream just outside the boundary layer
U_t	Velocity outside the boundary layer at transition
U_{ts}	Velocity outside the boundary layer at turbulence separation
W	Tunnel working section width
x, y	Cartesian coordinate

Greek Symbols

δ_2	Momentum thickness
θ	Chordwise position
θ_o	Leading or trailing edge angle (Theory)
θ_L	Leading edge angle (measured)
θ_T	Trailing edge angle (measured)
θ_c	The circular arc edge angle

Θ	$\delta_{2t}\left(\frac{U_t \delta_{2t}}{\nu}\right)^{\frac{1}{2}}$
ρ	Free stream density
ϕ	Angle substained by the circular arc element which is along the surface of the envelope

LIST OF TABLES

LIST OF FIGURES

1. INTRODUCTION

The use of air structures could be said to date back to the time of the Roman civilization when inflated animal skins were used as floats for crossing rivers [Ref. 1]. However, it was not until the eighteenth century that air structures were used in transportation. In 1783, the Montgolfier brothers introduced the hot air balloon made of paper and linen, and at the same time Meusnier suggested a design for an airship [Ref. 2]. These devices marked the beginning of pneumatic air-transportation.

Initial development of pneumatic buildings benefitted considerably from techniques used in balloon and airship design. The first known architectural attempt to apply these techniques to an earthbound structure was by the English engineer, Lanchester [Ref. 3]. In his patent of 1917 for a field hospital, the basic principles for an air supported structure were developed.

During the second world war, Steven, an American engineer, tried to promote Lanchester's idea; but the real break-through was achieved only after the war, at the Cornell Aeronautical Laboratory, by Bird who designed and built successful spherical radomes for early warning radar [Ref. 4]. His work was supported by research, and in particular was the wind tunnel testing of models. Since then, similar work has been done elsewhere especially in Germany, Britain, Japan and Sweden [Ref. 5]. In Germany, Beger and Macher

undertook wind tunnel investigations of model buildings of spherical and cylindrical shape, [Ref. 6] and similar experiments had been made by Niemann [Ref. 7].

The stress distribution in a flexible air structure is a function of the pressure distribution over the surface. For two-dimensional cases, under uniform inflation pressure, and without wind loading, equal stresses are developed at every point on the envelope. However, the varying pressure differential resulting from airflow across the surface of the unit causes a non-uniform loading and consequently causes deformation of the unit. As the membrane distorts, the wind pressure distribution varies with the change in shape until an equilibrium condition is reached or an instability may arise. The wind pressure distribution is therefore different from that over a solid body with the same profile as the flexible body with wind off.

In general, it was found that for thickness to chord ratios greater than or equal to half, it is necessary to relate the inflation gauge pressure Pig to the free stream dynamic pressure q to avoid vibration or even collapse. For instance, a 3/4 spherical shape requires $Pig/q > 1$, a hemispherical shape requires $Pig/q > 0.7$, and a cylindrical shape with 1/4 spherical ends requires $Pig/q > 0.6$ [Ref. 7].

Recently, Hoxey and Wells [Ref. 8] did a full scale wind pressure measurement on a twin-span greenhouse inflated-roof, the roof was a thin lenticular aerofoil. They pointed out it was

impractical to measure the shape. However, they predicted the shape indirectly from the pressure distribution. They also observed that a roof of increased slope was easily deformed by wind pressure.

The use of air structures has grown rapidly in recent years because they are light weight, portable, easily erected, and can provide column-free cover over a large area. However, it is a relatively new building technology and many technical problems remain to be solved.

The objective is the idealization of flow across an inflated building in two-dimensional flow with the effect of the boundary layer removed.

In the present work, a theoretical and experimental study was conducted on a thin inflated lenticular aerofoil in two-dimensional flow at zero flow incidence. Thin aerofoil theory [Ref. 9] and membrane stress analysis were employed together to predict the shape, surface pressure distribution and induced membrane tension.

A preliminary smoke tunnel investigation at $Re = 5 \times 10^3$ gave an indication of the maximum value of ℓ/c for which flow separation would be avoided. The experiments were carried out in a blower wind tunnel of closed working section of dimensions 0.762 m wide by 0.432 m high. Model sizes were restricted by consideration of wind tunnel blockage and flow separation on model. Methods of measuring pressure distribution and induced membrane tension were developed. Experiments were carried out for various combinations of the independent parameters: Reynolds number, inflation pressure coefficient and the excess length

of membrane over the chord length. The Reynolds number varied from 2.87×10^5 to 9.77×10^5, the inflation pressure coefficients varied from -0.12 to 3.22, and the excess length to chord ratio varied from 0.56% to 5.2% which approximately corresponded to wind-off height-chord ratios of 4.6% to 14% respectively.

2. THEORY

2.1 Thin Symmetrical Aerofoil at Zero Flow Incidence in Potential Flow

In potential flow theory, flow past a closed surface may be obtained by considering a number of sources and sinks located in a uniform stream as for instance in the Rankine oval and its degenerate case the circular cylinder. In these examples, modelling is done by introducing singularities of finite strength located at isolated points within the body.

To simulate the flow past a thin aerofoil at zero incidence, a continuous distribution of sources and sinks of strength $g(x)$ per unit length located along the chordline is considered [Ref. 9, 10]. Referring to [Fig. 12], orthogonal axes are used: the origin is at the leading edge with x the distance along the chordline measured from the leading edge, and y the distance perpendicular to the chordline. The aerofoil is symmetrical about the x-axis. Thus an element of length 'dx' has associated with it a source of strength $g(x)dx$ on the x-axis.

If the aerofoil is sufficiently thin the slope of the surface is small and for the purposes of determining the source distribution the flow velocity inside the aerofoil may be taken as U_∞.

Within the profile, the difference between the quantity of fluid flowing at x_1 and $x_1 + dx_1$ is equal to that emanating from the sources contained within this interval.

Hence,

$$g(x)dx_1 = 2\,U_\infty\left(y_1 + \frac{dy_1}{dx_1}\,dx_1\right) - 2\,U_\infty\,y_1$$

$$g(x) = 2\,U_\infty\,\frac{dy_1}{dx_1} \qquad (2.1.1)$$

Thus the required source distribution is simply determined by the shape of the aerofoil. The slope for the first half of the body is positive, which implies a continuous source distribution. The second half body has negative slope, which implies a continuous sink distribution.

If the thickness is small, the velocity induced at a point (x,y) on the surface of the profile by a fluid source or sink at the point $(x_1, 0)$ is approximately equal to that which would be induced at the point $(x, 0)$ by the same source or sink [Fig. 12]. Then the perturbation velocity at point (x, y) due to source at $(x_1,0)$ is given by:

$$du' = \frac{g(x_1)dx_1}{2\pi(x-x_1)} \qquad (2.1.2)$$

and the perturbation due to the combined effect of source and sink along the chord length is,

$$u' = \int_0^c \frac{g(x_1)dx_1}{2\pi(x-x_1)}$$

Using equation (2.1.1) gives

$$\frac{u'}{U_\infty} = \frac{1}{\pi}\int_0^c \frac{\frac{dy_1}{dx_1}\,dx_1}{(x-x_1)} \qquad (2.1.3)$$

and hence the total velocity at (x, y) is

$$u = U_\infty + u'$$

$$\text{i.e. } \frac{u}{U_\infty} = 1 + \frac{1}{\pi}\int_0^c \frac{\frac{dy_1}{dx_1}\,dx_1}{(x-x_1)} \tag{2.1.4}$$

2.2 Formulation of Inflated Lenticular Aerofoil

In [Fig. 13] let the chordwise tension per unit span of the inflated aerofoil be T. Due to ideal flow, the skin friction is zero, and tangential equilibrium requires that tension T must be constant throughout the membrane [Ref. 11, 12, 13].

Thus,

$$T = \text{constant} \tag{2.2.1}$$

The condition of normal equilibrium is,

$$2T \sin(\phi/2) + \Delta p \cdot 2R \sin(\phi/2) = 0 \tag{2.2.2}$$

where $\Delta p = p_i - p$

Hence

$$\Delta p = -T/R \tag{2.2.3}$$

where R is the radius of curvature and is given by:

$$\frac{1}{R} = \frac{\frac{d^2y}{dx^2}}{\left[1+\left(\frac{dy}{dx}\right)^2\right]^{3/2}} \tag{2.2.4}$$

with the assumption y is small from thin aerofoil theory, $\frac{dy}{dx}$ is small. Therefore $\left(\frac{dy}{dx}\right)^2$ can be neglected when comparing to unity and consequently,

$$\frac{1}{R} = \frac{d^2y}{dx^2} \tag{2.2.5}$$

combine (2.2.3) and (2.2.5),

$$\Delta p = -T \frac{d^2y}{dx^2} \tag{2.2.6}$$

$$\frac{\Delta p}{\frac{1}{2}\rho U_\infty^2} = \frac{(p_1 - p_\infty)}{\frac{1}{2}\rho U_\infty^2} - \frac{(p - p_\infty)}{\frac{1}{2}\rho U_\infty^2}$$

$$\text{i.e. } \frac{\Delta p}{q} = Cp_1 - Cp \tag{2.2.7}$$

where q is the free stream dynamic pressure,

Cp_1 is the inflation pressure coefficient.

Cp is the local surface pressure coefficient.

By Bernoulli's equation,

$$p_\infty + \frac{1}{2}\rho U_\infty^2 = p + \frac{1}{2}\rho u^2$$

hence,

$$Cp = 1 - \left(\frac{u}{U_\infty}\right)^2 \tag{2.2.8}$$

substitute (2.1.4) into (2.2.8) and neglecting the second power of perturbation, gives,

$$Cp = \frac{-2}{\pi} \int_0^c \frac{\frac{dy_1}{dx_1}\, dx_1}{(x - x_1)} \tag{2.2.9}$$

and consequently combine (2.2.7) and (2.2.9),

$$\frac{\Delta p}{q} = Cp_1 + \frac{2}{\pi} \int_0^c \frac{\frac{dy_1}{dx_1}\, dx_1}{(x - x_1)} \tag{2.2.10}$$

Normalize equation (2.2.6) by q, and combine with (2.2.10),

$$-\frac{T}{q}\frac{d^2y}{dx^2} = Cp_i + \frac{2}{\pi}\int_0^c \frac{\frac{dy_1}{dx_1}\,dx_1}{(x-x_1)} \qquad (2.2.11)$$

Equation (2.2.11) is the master equation for analysis; it relates the induced membrane tension, inflation pressure, and flow condition.

In order to solve this integral equation, Fourier Series and numerical matrix techniques are employed [Ref. 12]. x and y are transformed into parametric equations involving θ with y expressed as a Sine Series.

hence,

$$x = \frac{c}{2}(1 - \cos\theta) \qquad (2.2.12)$$

$$y = f(x) = c\sum_{n=1}^{\infty} A_n \sin(n\theta) \qquad (2.2.13)$$

where $0 \leq \theta \leq \pi$

$\theta = 0$ at leading edge

$\theta = \pi$ at trailing edge.

An's are the non-dimensional Fourier coefficients and c is the chord length. The use of Sine Series satisfies the boundary conditions at the leading and trailing edges, which require y equal to zero.

Taking the differential of (2.2.12) and (2.2.13), gives,

$$dx_1 = \frac{c}{2}\sin\theta_1\, d\theta_1$$

$$dy_1 = c\sum_{n=1}^{\infty} n A_n \cos(n\theta_1)\, d\theta_1$$

Substitute them into equation (2.1.3),

$$\frac{u'}{U_\infty} = \frac{2}{\pi}\int_0^{\pi} \sum_{n=1}^{\infty} \frac{n A_n \cos(n\theta_1)}{(\cos\theta_1 - \cos\theta)}\, d\theta_1 \qquad (2.2.14)$$

It is shown in the reference by Glauert (Ref. 14)

$$\int_0^{\pi} \frac{\cos(n\theta_1)\, d\theta_1}{(\cos\theta_1 - \cos\theta)} = \pi \frac{\sin(n\theta)}{\sin\theta} \qquad (2.2.15)$$

With the above integral result, equation (2.2.14) reduces to:

$$\frac{u'}{U_\infty} = 2 \sum_{n=1}^{\infty} n A_n \frac{\sin(n\theta)}{\sin\theta} \qquad (2.2.16)$$

hence,

$$\frac{u}{U_\infty} = 1 + 2 \sum_{n=1}^{\infty} n A_n \frac{\sin(n\theta)}{\sin\theta} \qquad (2.2.17)$$

Consequently, equation (2.2.9) and (2.2.11) give,

$$Cp = -4 \sum_{n=1}^{\infty} n A_n \frac{\sin(n\theta)}{\sin\theta} \qquad (2.2.18)$$

$$-\frac{T}{q}\frac{d^2y}{dx^2} = Cp_i + 4 \sum_{n=1}^{\infty} n A_n \frac{\sin(n\theta)}{\sin\theta} \qquad (2.2.19)$$

It can be shown that

$$\frac{d^2y}{dx^2} = -\frac{4}{c}\left[\sum_{n=1}^{\infty} n A_n \frac{\cos(n\theta)\cos(\theta)}{\sin^3\theta} + \sum_{n=1}^{\infty} n^2 A_n \frac{\sin(n\theta)}{\sin^2\theta}\right] \qquad (2.2.20)$$

Substitute (2.2.20) into (2.2.19) and rearrange,

$$\sum_{n=1}^{\infty} \left\{ \begin{array}{l} C_T[n\cos(n\theta)\cos(\theta) + n^2 \sin(n\theta)\sin\theta] \\ -\, n \sin(n\theta) \sin^2\theta \end{array} \right\} \left(\frac{A_n}{Cp_i}\right) = \frac{T}{4}\sin^3\theta \qquad (2.2.21)$$

where $C_T = \frac{T}{qc}$

It can be shown that the shape is symmetrical about the centre line of the chord [Appendix I], and this requires that for n even An's = 0.*

Equation (2.2.21) is the governing equation, it must satisfy the requirement of sharp edges (i.e. leading and trailing edge). Thus at the edges it is required that

$$\frac{dy}{dx} = \frac{2 \sum_{n=1}^{\infty} n A_n \cos(n\theta)}{\sin\theta} \qquad n \text{ is odd} \tag{2.2.22}$$

be finite.

At the leading edge ($\theta = o$), $\sin(\theta) = 0$ and for $\left(\frac{dy}{dx}\Big|_{x=o}\right)$ to be finite, requires

$$\sum_{n=1}^{\infty} n A_n = o \qquad n \text{ is odd} \tag{2.2.23}$$

For the trailing edge ($\theta = \pi$), it gives the same end conditions as (2.2.23).

The length of the surface in chordwise direction is given by:

$$\ell = \int_o^c \left[1 + \left(\frac{dy}{dx}\right)^2\right]^{\frac{1}{2}} dx \tag{2.2.24}$$

this can be linearized, and yields the excess length to chord ratio $(\ell - c)/c$

$$\frac{\ell - c}{c} = \frac{1}{2c} \int_o^c \left(\frac{dy}{dx}\right)^2 dx \tag{2.2.25}$$

* From now on, it is understood that all summation signs are for n = 1, 3, 5, 7, ...∞ (odd terms only).

To find the relation of the edge angle as a function of the tension parameter C_T, equation (2.2.19) is used,

$$-C_T\, c \frac{d^2y}{dx^2} = Cp_i + 4 \sum_{\substack{n=1 \\ \text{odd}}}^{\infty} n A_n \frac{\sin(n\theta)}{\sin\theta} \qquad (2.2.26)$$

integrating once [Appendix II].

$$\frac{1}{Cp_i}\frac{dy}{dx} = \frac{1}{2C_T}\left[1 + 4 \sum_{\substack{n=1 \\ \text{odd}}}^{\infty} \frac{A_n}{Cp_i} \cos\left(n \cos^{-1}\left(1-\frac{2x}{c}\right)\right)\right] - \frac{x}{C_T c} \qquad (2.2.27)$$

at the leading edge, $x = 0$, this gives

$$\frac{1}{Cp_i}\left.\frac{dy}{dx}\right|_{x=0} = \frac{1}{2C_T}\left[1 + 4 \sum_{n=1}^{\infty} \frac{A_n}{Cp_i}\right] \qquad n \text{ is odd} \qquad (2.2.28)$$

since $\left.\frac{dy}{dx}\right|_{x=0}$ = slope at leading edge

$= \tan(\theta_0)$

where θ_0 is the leading edge angle.*

Rearranging (2.2.28) gives

$$\frac{Cp_i}{\tan\theta_0} = 2\left[1 + 4 \sum_{n=1}^{\infty} \frac{A_n}{Cp_i}\right]^{-1} C_T \quad , n \text{ is odd} \qquad (2.2.29)$$

To obtain the relation of excess length as a function of the tension coefficient C_T, substitute (2.2.27) into (2.2.25) and carry out the integral [Appendix III]. It gives

$$\frac{Cp_i}{\sqrt{\frac{\ell-c}{c}}} = \sqrt{24}\left\{1 - 24 \sum_{n=1}^{\infty} \frac{1}{(n^2-4)} + 48 \sum_{m=1}^{\infty} \sum_{n=1}^{\infty} \left(\frac{A_m}{Cp_i}\right)\left(\frac{A_n}{Cp_i}\right)\left[\frac{1-n^2-m^2}{[(1-n)^2-m^2][(1+n)^2-m^2]}\right]\right\}^{\frac{1}{2}} C_T \qquad (2.2.30)$$

where m, n are odd.

* Due to symmetry leading and trailing edge angles are the same (Theory).

Eliminate C_T in (2.2.29) and (2.2.30),

$$\frac{Qp_i}{\tan\theta_o} = \frac{1}{\sqrt{6}} \left\{ \frac{1-24 \sum_{n=1}^{\infty} \frac{A_n}{Cp_i} \frac{1}{(n^2-4)} + 48 \sum_{m=1}^{\infty} \sum_{n=1}^{\infty} \frac{A_m}{Cp_i} \frac{A_n}{Cp_i} \frac{1-n^2-m^2}{[(1-n)^2-m^2][(1+n)^2-m^2]}}{\left[1 + 4 \sum_{n=1}^{\infty} \frac{A_n}{Cp_i}\right]} \right\}^{\frac{1}{2}} \times \frac{Cp_i}{\sqrt{\frac{\ell-c}{c}}} \qquad (2.2.31)$$

2.3 Numerical Solution and Discussion

The determination of the Fourier's coefficients involves the transformation of the master equation (2.2.21). Equation (2.2.21) is valid at any chordwise position. Thus a set of linear simultaneous equations can be obtained by specifying a number of chordwise positions in the equation (2.2.21).

Due to symmetry of the shape about the chordline centre, all positions can be chosen within $\theta = 0$ and $\theta = \pi/2$. The sharp edge condition requires that $\theta = 0$ must be included, and symmetry about the chordline centre requires $\theta = \pi/2$ be included. The rest of the positions are chosen to be equally spaced between 0 and $\pi/2$ [Ref. 14]. The magnitude of the interval is then equal to $\frac{\pi}{2} \frac{1}{(N-1)}$, where N, which is also the number of Fourier's coefficients chosen, is the number of chordwise positions. The use of equal intervals of θ was found to produce a well behaved and non-singular matrix. Some trials with non-equal intervals produced a nearly singular matrix and numerical inaccuracy.

In matrix form, equation (2.2.21) is rewritten as:

$$C_{n,m}\ S_n = D_m \qquad (2.3.1)$$

where: $C_{n,m} = C_T\,[n\cos(n\theta_m)\cos(\theta_m) + n^2\sin(n\theta_m)\sin(\theta_m)]$

$$- n\sin(n\theta_m)\sin^2(\theta_m)$$

$$S_n = A_n/Cp_i \quad , \quad \theta_m = \frac{\pi}{2}\,\frac{(m-1)}{(N-1)}$$

$$D_m = \tfrac{1}{4}\sin^3(\theta_m)$$

and $n = 1, 3, 5, 7, - - - - (2N-1)$

$m = 1, 2, 3, 4, - - - - N$

In order to find the sufficient number of coefficients which gives acceptable accuracy, the work by Nielsen [Ref. 12] was used as a guide.

For a given C_T, the matrix was solved for different numbers of N's, say $N_1 < N_2 < N_3$ etc. Then the following comparisons were made: (1) the difference between each corresponding coefficient; (2) the difference in maximum thickness which was evaluated from the corresponding set of coefficients; (3) the difference in excess length to chord ratio. For comparison (2) within a practically acceptable tolerance, say 0.01% (Nielsen), the smallest value of N which gives such tolerance would be accepted as the optimum number of coefficients for analysis.

The matrix had been solved by truncation with N equal to 10, 15, 20 and 25 for various values of the tension parameter C_T.

Results had been compared and presented in Tables 1-7. It was seen that the successive coefficients decrease rapidly in magnitude, and only the first two coefficients are dominant.

Assuming for the moment that the 'true' values are given for N = 25, comparison for N = 20 shows that the percentage difference for $(h/c)/Cp_i$ is about 0.005% and for the excess length to chord ratio $\left(\frac{\ell-c}{c}\right)/Cp_i^2$ is about 0.05% for all values of C_T greater than 0.5. It is concluded that N = 20 gives a nearly asymptotic solution and provides a sufficiently accurate solution. *

Once the Fourier coefficients are known, all the characteristics of the inflated aerofoil can be obtained.

It is interesting to note that the numerical solution gives values of An/Cp_i and not An. [Fig. 14], shows C_T is a unique function of $Cp_i\left(\frac{\ell-c}{c}\right)^{-\frac{1}{2}}$ as given by equation (2.2.30). The value of C_T equals to about 0.5 separates positive and negative value of Cp_i. $Cp_i\left(\frac{\ell-c}{c}\right)^{-\frac{1}{2}}/C_T$ achieves the asymptotic value $\sqrt{24}$, which corresponds to wind off when C_T reaches very large value.

In [Fig. 15], for C_T greater than 0.5, the normalized shape $(y/c)/Cp_i$ starts with cusps at the edges for low value of C_T, and tends to become a circular arc profile as C_T increases.

In [Fig. 16], for values of C_T less than about 0.5, the normalized shapes $(y/c)/Cp_i$ are negative, except for C_T = 0.2 and C_T = 0.125 which cross over the zero line. In the range of C_T between 0.49847 and 0.28438, the shapes are only different in amplitude

* All theoretical results are obtained for N = 20.

They are geometrically similar with only one peak at the centre. At C_T equals to 0.28438, the shape has zero slope at the leading and trailing edges. For C_T from 0.28438 to 0.2, the shapes start to cross over the zero line near the edges. The amplitude of the cross over as well as the width grow rapidly, and have their maximum case at C_T equals to 0.2. Further decrease of C_T from 0.2 to 0.17625, changes the shapes in such a way that they are inverse of the case for C_T equals to 0.2 but with smaller amplitudes. When C_T reaches 0.125, it crosses over the zero line again with more ripples and smaller amplitude. For C_T less than 0.125 until 0.05 the shape becomes negative, and once again more ripples and smaller amplitude. *

In [Fig. 17], this provides a direct estimate of the tension in the membrane for a given flow speed, inflation pressure and height-to-chord ratio. It shows that the smaller the height-to-chord ratio, the higher the induced membrane tension. However, the percentage of increase is larger for large height-to-chord ratio.

In [Fig. 18], as a practical example, the change of shape for a particular ℓ corresponding to wind off height-to-chord ratio 0.14, $\left(\frac{\ell-c}{c} = 0.05\right)$, has been determined for various values of Cp_i. Their corresponding induced tension is also given in the figure. As the inflation pressure coefficient goes from large to small, the corresponding shapes are once again seen to change from almost a circular arc to a cusp shape.

* The wavy shapes in Fig. 16 were not achieved experimentally.

3. EXPERIMENT

3.1 Wind Tunnel Description and Calibration

The general arrangement of the blower wind-tunnel is as shown in [Fig. 1]. The tunnel is of the blower type, and has an open jet exit of 0.762 m wide by 0.432 m high (30" x 17"). The contracting section which leads to the working section [Fig. 2, 3] is a two-dimensional type having a contraction ratio of 6:1 [Ref.15].

The test model extended through the roof and floor, located at the centre of the working section. The model was aligned in flow direction by means of pressure taps at front of leading edge wedge. A device which carried a static tube for the measurement of surface pressure distribution was attached to the plexiglas window. It could be moved parallel to flow direction.

The tunnel calibration involved two pressure taps located on each side of the vertical walls of the settling chamber, one foot from the upstream end. These tubes were connected to give an average pressure Pr for the determination of wind speed.

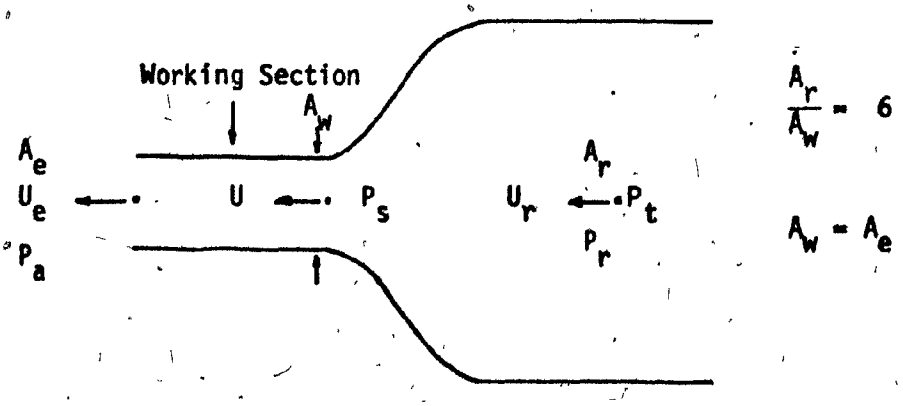

Pitot-static tube, which was located at the centre of the working section, was used to measure the values of (Pr-Pa), (Pt-Pa), and (Ps-Pa) simultaneously. Inclined alcohol (S.G. 0.8) manometers were used for these measurements. Results were presented by plotting (Pt-Ps)/(Pr-Pa) and (Ps-Pa)/(Pr-Pa) versus $[(Pr-Pa)/\rho\nu^2]^{\frac{1}{2}}$, where ν is the kinematic viscosity [Fig. 10]. The value $[(Pr-Pa)/\rho\nu^2]^{\frac{1}{2}}$ when multiplied by unit length is a measurement of the Reynolds number.

The calibration curves had been fitted by linear regression method to give the following expressions.

$$\frac{Pt-Pa}{Pr-Pa} = 1.029$$

$$\frac{Pt-Ps}{Pr-Pa} = [9583.052 + 0.575324 \times 10^{-4}\ Re + 0.495353 \times 10^{-10}\ Re^2 - 0.21716 \times 10^{-6}\ Re^3] \times 10^{-4}$$

$$\frac{Ps-Pa}{Pr-Pa} = [750.296 - 0.184041 \times 10^{-3}\ Re + 0.49051 + 10^{-10}\ Re^2 - 0.274852 \times 10^{-17}\ Re^3] \times 10^{-4}$$

where $Re = [(Pr-Pa)/\rho\nu^2]^{\frac{1}{2}}$/metre

and $2.5 \times 10^5 < Re < 18 \times 10^5$/metre

3.2 Model Design and Accessory Measurement Devices

The chord length was chosen to avoid separation ahead of the trailing edge. The method to determine laminar and transition was by the following equations [Ref. 16].

$$\frac{U\delta_2^2}{\nu} = \frac{0.45}{U^5} \int_0^c U^5 \, ds \qquad (3.2.1)$$

$$m = -\frac{\delta_2}{\nu} \frac{dU}{ds} \qquad (3.2.2)$$

where U is the free stream velocity just outside boundary layer

ν is the kinematic viscosity

δ_2 momentum thickness

s. is the distance along the surface,

and together with [Fig. 11] of "boundary layer Reynolds number at transition plotted against the pressure parameter", which was obtained from L.F. Crabtree [Ref. 17]. Laminar separation occurs when m = 0.09.

When no laminar separation occurs; the procedure of calculating the transition point is as follows: m and $Re\delta_2$ at points along the surface are calculated and plotted on Crabtree's diagram. So long as this curve lies to the left of Crabtree's critical curve, the boundary layer is laminar; transition occurs where the curves cross.

After determining the transition point, the turbulent separation is found approximately by Spence's method,

$$1.829\, U_{ts}^2 = U_t^2 - 0.00135 \int_{S_t}^{S_s} \frac{U^2}{\text{Ⓗ}} \, ds \qquad (3.2.3)$$

where $\text{Ⓗ} = \delta_{2t}\left(\frac{U_t \ \delta_{2t}}{\nu}\right)^{\frac{1}{4}}$,

and U_t, U_{ts} are the velocity outside the boundary layer at transition and the turbulence separation points. S_t, S_s are their corresponding locations along the surface.

Based on the above consideration, and avoiding the merge of the boundary layer growth at the roof and floor along the surface, the chord was chosen about 0.38 m (h/c was assumed 0.05). It was found that this dimension of chord was satisfactory for experiments.

Only solid and wake blockage were considered for determining the model sizes. The blockages can be estimated by [Ref. 18 and 19],

Total blockage $$B_t = B_s + B_w \qquad (3.2.4)$$

Wake blockage $$B_w = \frac{1}{4}\left(\frac{c}{w}\right)^2 C_D \qquad (3.2.5)$$

Solid blockage $$B_s = \frac{\pi^2}{12}\left(\frac{t}{w}\right)^2 S_f \qquad (3.2.6)$$

Shape factor $$S_f = \frac{4}{\pi}\int_0^c \frac{u}{U_\infty} y \frac{ds}{t^2} \qquad (3.2.7)$$

Corrected velocity $$u_c = u_t (1 + B_t) \qquad (3.2.8)$$

where w width of tunnel

t maximum thickness of object

c chord length

y ordinate of the surface measured from the chordline

u local velocity of the surface at a distance s from the leading edge

C_D measured drag coefficient. (It was assumed 0.01 from NACA0010-35)

u_t measured tunnel wind velocity

u_c corrected tunnel wind velocity

Total blockage was estimated for a few chord to thickness ratios, for instance,

when c/t = 10, B_t 0.01

c/t 5.5, B_t 0.02

c/t 4, B_t 0.027

They provided a guide for determining the c/t ratio. These were applied for the correction of measured inflation pressure coefficient (Cp_i), tension parameter (C_T), and Reynolds number (Re).

The design of the test model consisted of an envelope made of Stablekote II Nylon (25 gm/m^2) [Fig. 4, 5] wrapped around two steel wedges in order to achieve aerofoil shape when inflated. Wedge angle was restricted to about 10°, because large wedge angle would affect the edge angle of the envelope during the experiments. The wedges together with the end edges of the envelope extended through the tunnel roof and floor via the bicircular arc holes. The holes' sizes were made to closely resemble the inflated aerofoil so as to minimize the amount of leakage of tunnel flow.

The ends of the wedges were each held by flexures which were specially designed [Fig. 6] to allow very small and parallel movement in the direction of the main stream flow when forces act on the wedges. To each flexure, a full bridge connection of strain gauges was attached for force measurement [Fig. 7, 8.] The flexures were attached to the roof and floor [Fig. 8] of the working section.

The test model was two-dimensional, and required that there should be no induced membrane tension in the spanwise direction of the envelope. Thus two plexiglas plates were used which attached the ends of the envelope and served as end plates to reduce the escape of air from the inside of the aerofoil [Fig. 4].

The inflation pressure was supplied from both ends of a 0.0127 m (0.5") diameter pipe which extended through the covers. The pipe was designed to give uniform inflation pressure. Holes were drilled in it with varying spacing so as to give a uniform distribution of pressure inside [Ref. 20].

3.3 Measurement

The measurement of parameters included Cp_i, local Cp, and the excess length-to-chord ratio.

Measurements of inflation pressure, surface pressure distribution and tunnel speed give Cp_i and Cp. The measurements of wedge forces together with both leading and trailing edge angles give the value of C_T.

The inflation pressure was measured using 3 small tubes (0.318 cm). Two open ended and one static tubes were inserted inside the envelope from both top and bottom covers. There was negligible difference with readings from these tubes. They were however, connected together and measured by an inclined manometer.

A device was designed [Fig. 9] which allowed a mounted static tube (0.16 cm diameter) to be rotated or moved in and out so as to align the static tube parallel to the inflated surface at any chosen chordwise position. The device itself was mounted on the plexiglas window, and could be adjusted in the chordwise direction of the aerofoil. Again, the pressures were measured on an inclined manometer.

The forces on the leading edge and trailing edge were measured by the strain gauges attached to the supporting flexures, and the complete systems were individually calibrated with dead weights (Fig. 41). The outputs of the strain gauges were picked up by a B and K type 1562 strain indicator. The leading and trailing edge angles were determined from orientation of the static tube at these locations.

Since the shape of the membrane outside the tunnel was different from that affected by the wind, it was impossible to photograph the shape directly i.e. longitudinally. Some idea of the change of shape with speed was obtained from oblique photographs.

3.4 Experiment Procedure

To start the experiment, it was necessary to calibrate the membrane length, induced tension versus inflation pressure with wind off, because the fabric stretched slightly under tension. This was done with wind off by measuring the thickness of the circular arc aerofoil using calipers. This information combined with the measured internal pressure enabled the radius of curvature and membrane length (ℓ) to be determined. The information was also used to correct the wind-on readings for the effect of the ends which were outside the tunnel. Sample calibration curves are shown in [Fig. 19A, 19B].

Ambient temperature and pressure were recorded and used to calculate the corresponding density and kinematic viscosity of air.

For each envelope and combination of tunnel speed and inflation pressure, oblique photographs of the membrane shape were taken, and the corresponding surface pressure distribution and membrane tension were recorded.

Different excess length to chord ratios were obtained mainly by changing the size of the envelope, although slight adjustments were possible by changing the chord length.

Cases with negative Cp_i could be run by starting initially with a positive internal pressure and then, with wind on, reducing this to a value less than that in the working section.

The correction for the end effects on the measurement of tension was necessary. Since, with wind off the envelope had a circular arc profile over the whole length, with wind on, the portion of the envelope within the tunnel changed shape and the portion outside the tunnel also did, but presumably to a less extent. To make the correction for the end effects, it was assumed that the outside portion of the envelope remained a circular arc profile when wind was on. Thus the measured force would be due to two parts, namely the tunnel portion affected by the air flow, and the outside portion which was surrounded by effectively still air. For a given inflation pressure, the value of $\frac{\ell-c}{c}$ can be found from the calibration curve [Fig. 19A]. With the value of $\frac{\ell-c}{c}$ and [Fig. 19B], the tension per unit length may be determined. The total correction force is given by

$$F_c = (2\ Tc \cos \theta_c)d,$$

where d is the total distance of the wedge extended outside the floor and ceiling.

θ_c is the circular arc edge angle

Tc is the induced tension per unit length by the circular arc profile.

Let F_L and F_T be the total measured forces on the leading wedge and trailing wedge due to combined effect of wind and inflation pressure. The central portion of the aerofoil affected by the tunnel air is:

$$T_L = (F_L - F_c)/(2H \cos\theta_L) \quad *$$

$$T_T = (F_T - F_c)/(2H \cos\theta_T)$$

where θ_L, θ_T, are the measured leading and trailing edge angles, H is the height of the tunnel.

It has been assumed in the theory that the tension should be uniform throughout the membrane. Thus the average of T_L and T_T was taken as the induced tension (T) per unit length. In fact their difference was usually less than 1%.

* Where T_L, T_T are the induced tension per unit length in spanwise direction at the leading and trailing edge of the inflated envelope respectively.

4. EXPERIMENTAL RESULTS AND DISCUSSION

4.1 Comparison of Experimental Results with Theory

Comparison of equation (2.2.30) and experimental results are shown in [Fig. 20], where the tension coefficient C_T is plotted against $Cp_i\left(\frac{\ell-c}{c}\right)^{-\frac{1}{2}}$. The agreement is very good. Experimental results nearly all collapse convincingly on the theoretical curve within about 3%. The results are for a range of Reynolds number from 2.87×10^5 to 8.02×10^5, and indicate that they are insensitive to the change of Reynolds number. In all cases with positive inflation pressure [Fig. 20] the membrane appeared to be stable.

Some results for suction cases (negative Cp_i) were obtained also [Fig. 21]. These results, however, are less accurate because the portion of the membrane outside the tunnel was usually partially collapsed, and thus the end correction for the measured tensions were uncertain. Nevertheless, the results are still in fairly good agreement with the theoretical curve. Partial or total collapse occurred at the value of C_T less than about 0.4. The less the value of $(\ell-c)/c$, the more readily it is subjected to collapse. To avoid collapse, it should keep C_T greater than about 0.4, which corresponds to $Cp_i\left(\frac{\ell-c}{c}\right)^{-\frac{1}{2}}$ about -0.45.

The actual phenomenon of the membrane behaviour for negative Cp_i was a gradual process. When the inflation pressure was reduced

to the critical value which corresponds to a given flow speed and excess length to chord ratio, the envelope oscillated with very small amplitude but high frequency. There were no prominent wavy ripples observed. With further decrease of pressure, the membrane oscillated with larger amplitude but lower frequency. Finally, when the applied suction pressure was large enough for the given conditions, the envelope collapsed in such a way that the maximum thickness propagated rearwards to the trailing edge as one simple pulse wave [Fig. 40]. After collapse, the two surfaces of the envelope contacted each other tightly. However, when the suction pressure was removed, the envelope was inflated again. Also, the envelope could recover its stable state from oscillation when the flow speed increased, which is really an increase of Cp_i. High flow speed is favourable for stability, even for a small amount of suction. It was true for different $(\ell\text{-}c)/c$ even up to 0.038.

Edge slopes given by equation (2.2.31) as a function of the $Cp_i \left(\frac{\ell-c}{c}\right)^{-\frac{1}{2}}$ is compared in [Fig. 22]. In theory, the curve will achieve a slope of $(6)^{-\frac{1}{2}}$ for high value of $Cp_i \left(\frac{\ell-c}{c}\right)^{-\frac{1}{2}}$. There is good agreement for low value of $Cp_i \left(\frac{\ell-c}{c}\right)^{-\frac{1}{2}}$ below 4, and is still fairly good even up to 10. However, discrepancy between theory and experiment increases as $Cp_i \left(\frac{\ell-c}{c}\right)^{-\frac{1}{2}}$ beyond 10. Such disagreement is most probably due to measurement of angles when they are small. Similar features happened in [Fig. 23] where the edge slopes plotted against the tension coefficient C_T. The theoretical curve achieved a slope of 2 for high C_T. In both figures, disagreement between theory and experiment begins when $Cp_i/\tan(\theta o)$ is above 4.5.

Consider the pressure distributions which are shown in [Fig. 24-35]. They show that for low height to chord ratio, experiment and theory in general are in good accord [Fig. 24, 25]. However, as height to chord ratio is increased, the agreement is worse in some local regions [Fig. 28, 29]. Around the region of s/ℓ equals 0.075 to 0.3, the theory gives lower pressures and larger values in the region 0.35 to 0.8. It may be noted that although there is considerable disagreement at $s/\ell = 0.8$, the agreement surprisingly improves towards the trailing edge. This could be due to flow separation and reattachment near $s/\ell = 0.8$. For even thicker cases [Fig. 34, 35], separation bubble has moved forward and becomes larger as would be expected. The flow pattern around the region were investigated quantitatively using a tuft attached to a hand held wand, and light tufts attached to the surface of the membrane itself. The pressure distribution discrepancy for the forward part of the aerofoil can only be partially explained as an error in the potential flow analysis. In [Fig. 36], for potential flow, the present linearized theory for a lenticular aerofoil with circular arc gives more negative pressures for s/ℓ in the region 0.05 to 0.3 and vice versa in the region 0.4 to 0.5, as compared with Karman-Trefftz's method. The latter method is a conformal transformation of a circle and in the potential flow theory is exact. The comparison shown in [Fig. 36] indicates that the linearized theory gives satisfactory results for height to chord ratios of perhaps up to 0.1. This gives maximum reasonable h/c.

A second reason for the discrepancy over the rear half of the aerofoil could be the effect of the boundary layer build up over the surface. It would effectively thicken the shape of the aerofoil especially over the downstream half where there are unfavourable pressure gradients. Thus the pressure is reduced in these regions because of the wake. An additional effect of the lower pressure on the back of the aerofoil is to move the maximum thickness of the membrane rearwards and thus further reduce the pressure on the rear half surface. It also has the effect of increasing the pressure on the front half surface as is observed [Fig. 35].

The leading edge angle is always slightly less than the trailing edge angle.

4.2 Estimation of the Error in the Measured Coefficients

From [Fig. 20], it appears that $Cp_1 \left(\frac{\ell-c}{c}\right)^{-\frac{1}{2}}$ and C_T have been measured to an accuracy of somewhere between 2% to 3%. Cp_1 involved the measurement of internal pressure and tunnel dynamic pressure using manometers which could have been measured to an accuracy of 1%. The remains inaccuracy in $(\ell-c)/c$ is therefore between 2% and 4%. This corresponds to an error in the wind off t/c of about 1% and 2%.

It is somewhat surprising that such accuracy was achieved in the measurement of t using calipers. The measurement of C_T is inaccurate due to inaccuracy in T and q. The force on the wedges was measured to an accuracy of about 1% and the edge angles were relatively unimportant

for determining T since the cosine was taken. Thus with a small additional error from tunnel dynamic pressure, C_T may well have been measured to an accuracy better than 2%.

5. CONCLUSION

Idealization of flow over a long low inflated building with the effect of the earth's boundary layer removed has been studied successfully both in theory and experiment.

The tension coefficient C_T is a unique function of the collapsed parameter $Cp_i \left(\frac{\ell-c}{c}\right)^{-\frac{1}{2}}$ obtained theoretically and confirmed experimentally. The relation is insensitive to the Reynolds number, and applies for $(\ell-c)/c$ less than approximately 0.05. (about $h/c = 0.14$, with wind off).

The membrane was found to be stable for all positive values of Cp_i. $Cp_i \left(\frac{\ell-c}{c}\right)^{-\frac{1}{2}}$ should be greater than about -0.45 which corresponds to C_T about 0.4 to avoid partial or total collapse.

The non-dimensional shape $[(y/c/Cp_i)]$ of the membrane is determined uniquely by $Cp_i \left(\frac{\ell-c}{c}\right)^{-\frac{1}{2}}$, and the actual dimension is scaled accordingly to Cp_i.

The induced absolute tension is higher for low heights, however, the proportional increase with wind speed is less.

The measured pressure distribution broadly agrees with the theory although there appears to be some effect of the boundary layer built up on the aerofoil which results in a movement rearwards of the point of maximum thickness.

The theory is good for h/c up to 0.1 for design purposes.

REFERENCES

1. H. BOUGLAS, 'Military Bridges'. London, 1853.

2. B. CLARK, 'The History of Airships'. Jenkins, London, 1961.

3. CEDRIX PRICE and FRANK NEWLY, 'Air Structure'.

4. CORNELL AERONAUTICAL LABORATORY, 'Design Manual for Spherical Air-Supported Radomes'. Report No. UB-909-D-2, March, 1956.

5. Proceedings of International Symposium on Pneumatic Structure. Delft - 1972.

6. G. BEGER and E.T. MACHER, 'Results of Wind-Tunnel Tests on Some Pneumatic Structures'. Proceedings of 1st International Colloquium on Pneumatic Structures, Stuttgart, 1967.

7. H.J. NIEMANN, 'Wind-Tunnel Experiments on Aeroelastic Models on Air Supported Structures: Results and Conclusions'. Proceedings of International Symposium on Pneumatic Structure, Delft - 1972.

8. R.P. HOXEY and D.A. WELLS, 'Full-Scale Wind Pressure Measurement on a Twin-Span 12.2 m x 12.2 m Inflated Roof Greenhouse'. Journal of Industrial Aerodynamics 2 (1977) pp. 211-221.

9. B. THWAITES, 'Incompressible Aerodynamics'. Oxford University Press, 1960.

10. H. JULIAN ALLEN, 'General Theory of Airfoil Section Having Arbitrary Shape or Pressure Distribution'. NACA Tech. Report 833, 1945.

11. B. THWAITES, 'The Aerodynamic Theory of Sails I Two-Dimensional Sails'. Proceedings of the Royal Society of London Series A. Vol. 261, 1961. P. 402-422

12. J.N. NIELSEN, 'Theory of Flexible Aerodynamic Surface'. P. 431-442 ASME Transaction Journal Applied Mechanics, Sept. 1963.

13. J.D. MYALL and S.A. BERGER, 'Recent Progress in the Analytical Study of Sails'. AIAA 2nd Symposium Hydronautics of Sailing. P. 9-19

14. M.B. GLAUERT, 'The Elements of Aerofoil and Airscrew Theory'. Cambridge University Press, 1947.

15. I. WYGNANSKI, and I.S. GARTSHORE, 'General Description and Calibration of McGill 17 in x 30 in Blower Cascade Wind Tunnel'. McGill University Mech. Eng. Res. Labs. Tech. Note 63-7, 1963.

16. J.C. COOKE and G.G. BREBNER, 'The Nature of Separation and its Prevention of Geometric Design in a Wholly Subsonic Flow'. Boundary Layer and Flow Control (G.V. Lachman) Vol. 1.

17. L.F. CRABTREE, 'Prediction of Transition in the Boundary Layer on an Aerofoil'. Journal of the Royal Aeronautical Society Vol. 62, July 1958. P. 525-528

18. A. POPE, 'Wind Tunnel Testing', John Wiley, Second edition, 1954.

19. R.C. PANKHURST and D.W. HOLDER, 'Wind Tunnel Technique'. Pitman, London 1952.

20. J.D. KELLER, 'Manifold Problems'. Journal of Applied Mechanics, March 1949. P. 77-85

APPENDIX I

Thin inflated lenticular aerofoil in potential flow at zero incidence is symmetrical in shape.

The governing equation for the analysis is given by equation (2.2.21).

$$\sum_{n=1}^{\infty} \left[\begin{array}{l} C_T[n\cos n\theta \cos\theta + n^2 \sin n\theta \sin\theta] \\ -n\sin n\theta \sin^2\theta \end{array} \right] \left(\frac{A_n}{Cp_i}\right) = \tfrac{1}{4}\sin^3\theta \qquad (2.2.21)$$

Replace θ by $(\pi-\theta)$:

sin is unchanged

$\sin n\theta \rightarrow \sin n\theta$ n is odd

$-\sin n\theta$ n is even

$\cos\theta \rightarrow -\cos\theta$

$\cos n\theta \rightarrow -\cos n\theta$ n is odd

$\cos n\theta$ n is even

hence (2.2.21) becomes:

$$\sum_{n=1}^{\infty} \left[\begin{array}{l} C_T[n(\mp\cos n\theta)(-\cos\theta) + n^2(\pm\sin n\theta)\sin\theta] \\ -n(\pm\sin n\theta)\sin^2\theta \end{array} \right] \left(\frac{A_n}{Cp_i}\right) = \tfrac{1}{4}\sin^3\theta \qquad (I.1)$$

If n is odd:

equation (I.1) is identical to (2.2.21) and this implies equation (2.2.21) is symmetrical.

If n is even:

get:
$$\sum_{n=2}^{\infty} \left[\begin{array}{l} C_T[-n\cos n\theta \cos\theta - n^2 \sin n\theta \cdot \sin\theta] \\ + n \sin n\theta \sin^2\theta \end{array} \right] \left(\frac{A_n}{Cp_i}\right) = 0 \qquad (I.2a)$$

Rearrange (I.2a)

$$\tfrac{1}{2}\sum_{n=2}^{\infty} n\left(\frac{A_n}{Cp_1}\right)\left[\begin{array}{l}-C_T[(n+1)\cos(n-1)\theta-(n-1)\cos(n+1)\theta] \\ +\sin(n\theta)-\tfrac{1}{2}[\sin(n-2)\theta+\sin(n+2)\theta]\end{array}\right] = 0 \qquad \text{(I.2b)}$$

take $\int_0^{\pi}$ (I.2b) x $\cos m\theta d\theta$: (I.3)

the typical terms will be:

$$\int_0^{\pi}\cos(n\pm1)\theta\cdot\cos m\theta d\theta = 0$$

$$\int_0^{\pi}\sin n\theta\cos m\theta d\theta = \begin{cases}\frac{1}{n+m}+\frac{1}{n-m} & m = \text{odd, } n \text{ even} \\ 0 & m = \text{even, } n \text{ even}\end{cases}$$

Hence (I.3) is reduced to

$$\tfrac{1}{2}\sum_{n=2}^{\infty} n\,\frac{A_n}{Cp_1}\left[\frac{1}{n+m}+\frac{1}{n-m}-\frac{1}{2}\left(\frac{1}{n+m+2}+\frac{1}{n-m+2}+\frac{1}{n+m-2}+\frac{1}{n-m-2}\right)\right] = 0 \qquad \text{(I.4)}$$

for all odd m

Hence $A_n = 0$ for all n even.

Consequently, equation (2.2.21) becomes:

$$\sum_{\substack{n=1\\ n=\text{odd}}}^{\infty}\left[\begin{array}{l}C_T[n\cos(n\theta)\cos\theta+n^2\sin(n\theta)\sin\theta] \\ -n\sin(n\theta)\sin^2\theta\end{array}\right]\left(\frac{A_n}{Cp_1}\right) = \tfrac{1}{2}\sin^3\theta \qquad \text{(I.5)}$$

APPENDIX II

Derivation of relation between inflation pressure coefficient, tension coefficient and edge angle.

To obtain the relation

$$\frac{Cp_i}{y'(o)} = f(C_T)$$

From equation (2.2.19) and with $C_T = T/qc$,

$$-C_T\, cy'' = Cp_i + 4 \sum_{n=1}^{\infty} nA_n \frac{\sin(n\theta)}{\sin\theta} \quad n \text{ odd} \qquad \text{(II.1)}$$

$$\frac{-C_T c}{Cp_i} y'' = 1 + 4\sum_{n=1}^{\infty} n \frac{A_n}{Cp_i} \frac{\sin(n\theta)}{\sin\theta} \; *$$

Integrate once from $x = 0$ to $x = x$

$$\frac{-C_T c}{Cp_i} y' + K_1 = x + 4\left(\int_0^x \Sigma n \frac{A_n}{Cp_i} \frac{\sin(n\theta)}{\sin\theta} dz\right) \qquad \text{(II.2)}$$

where z is a dummy variable, K_1 is integration constant.

at $x = 0$,

$$\frac{y'(o)}{Cp_i} = \frac{K_1}{C_T c} \qquad \text{(II.3)}$$

Integrate (II.2) from $x = 0$ to $x = c$

$$-\frac{1}{Cp_i} y = -\frac{K_1}{C_T c} x \Big|_0^c + \frac{x^2}{2C_T c}\Big|_0^c + \frac{4}{C_T c} \cdot \int_0^c dx \int_0^x \Sigma \frac{A_n}{Cp_i} \frac{\sin(n\theta)}{\sin\theta} dz + K_2 \qquad \text{(II.4)}$$

* All Σ from n=1 to n=∞ for odd n.

At $x = o$, $y = o$, $\rightarrow K_2 = o$

At $x = c$, $y = o$,

$$\frac{K_1}{C_T} = \frac{c}{2C_T} + \frac{4}{C_T c} \cdot \int_o^c dx \left(\int_o^x \Sigma n \frac{A_n}{Cp_i} \frac{\sin(n\theta)}{\sin\theta} dz \right)$$

$$\frac{K_1}{C_T c} = \frac{1}{2C_T} + \frac{4}{C_T c^2} \cdot \int_o^c dx \left(\int_o^x \Sigma n \frac{A_n}{Cp_i} \frac{\sin(n\theta)}{\sin\theta} dz \right) \qquad \text{(II.5)}$$

Let $I_1 = \int_o^x \Sigma n \frac{A_n}{Cp_i} \frac{\sin(n\theta)}{\sin\theta}$ (II.6a)

where $\theta = \cos^{-1}\left(1 - \frac{2z}{c}\right)$

$$\cos\theta = \left(1 - \frac{2z}{c}\right)$$

$$dz = \frac{c}{2} \sin\theta d\theta$$

so: $I_1 = \frac{c}{2} \Sigma \frac{A_n}{Cp_i} \int_o^{\cos^{-1}\left(1-\frac{2x}{c}\right)} n \sin(n\theta)\, d\theta$

$$= \frac{c}{2} \Sigma \frac{A_n}{Cp_i} \left[1 - \cos\left(n \cos^{-1}\left(1-\frac{2x}{c}\right)\right) \right] \qquad \text{(II.6b)}$$

Substitute I_1 back into II.5:

$$\frac{K_1}{C_T c} = \frac{1}{2C_T} + \frac{4}{C_T c^2} \cdot \int_o^c dx \frac{c}{2} \Sigma \frac{A_n}{Cp_i} \left[1 - \cos\left(n \cos^{-1}\left(1 - \frac{2x}{c}\right)\right) \right]$$

$$= \frac{1}{2C_T} + \frac{2}{C_T} \Sigma \frac{A_n}{Cp_i} - \frac{2}{C_T} \Sigma \frac{A_n}{Cp_i} \int_o^c \cos\left(n \cos^{-1}\left(1-\frac{2x}{c}\right)\right) dx \qquad \text{(II.7)}$$

Let $I_2 = \Sigma \frac{A_n}{Cp_i} \int_o^c \cos\left(n \cos^{-1}\left(1-\frac{2x}{c}\right)\right) dx$ (II.8a)

also let:

$$u = n\cos^{-1}\left(1-\frac{2x}{c}\right),$$

at $x = 0 \quad u = 0$

$x = c \quad u = n\pi$

$$\cos\left(\frac{u}{n}\right) = \left(1-\frac{2x}{c}\right)$$

$$dx = \frac{c}{2n}\sin\left(\frac{u}{n}\right)du$$

$$I_2 = \Sigma \frac{A_n}{Cp_i}\ \frac{c}{2n} \cdot \int_0^{n\pi} \cos(u)\sin\left(\frac{u}{n}\right)du$$

$$= \frac{c}{2}\Sigma \frac{A_n}{Cp_i}\ \frac{1}{n}\left[-\frac{1}{2}\left(\frac{\cos\left(\frac{1}{n}-1\right)u}{\frac{1}{n}-1} + \frac{\cos\left(\frac{1}{n}+1\right)u}{\frac{1}{n}+1}\right)\right]_0^{n\pi}$$

$$= c\ \Sigma \frac{A_n}{Cp_i}\ \frac{(-1)}{4n}\ \frac{1}{\left(\frac{1}{n^2}-1\right)}\left[-\frac{2}{n} + \frac{1}{n}\left(\cos(\pi-n\pi) + \cos(\pi+n\pi)\right) + \cos(\pi-n\pi) - \cos(\pi+n\pi)\right]$$

$$= c\ \Sigma \frac{A_n}{Cp_i}\ \frac{-n^2}{4n\left(1-n^2\right)}\left[-\frac{2}{n} + \frac{2}{n}\cdot\cos\pi\cdot\cos n\pi + 2\cdot\sin\pi\cdot\sin n\pi\right]$$

$$= c\ \Sigma \frac{A_n}{Cp_i}\ \frac{-n^2}{4n\left(1-n^2\right)}\left[\frac{-2}{n}\cdot(1+\cos n\pi)\right]$$

$$= c\ \Sigma \frac{A_n}{Cp_i}\ \frac{(1+\cos n\pi)}{2\left(1-n^2\right)}$$

but n is odd $\rightarrow \cos n\pi = -1$

So $I_2 = 0$ (II.8b)

Substitute $I_2 = 0$ back into II.7,

$$\frac{K_1}{C_T c} = \frac{1}{2C_T} + \frac{2}{C_T}\Sigma \frac{A_n}{Cp_i} \qquad (II.9)$$

substitute (II.9) into (II.3),

$$\frac{y'(o)}{Cp_i} = \frac{1}{2C_T}\left[\, 1 + 4\,\Sigma\,\frac{A_n}{Cp_i}\right]$$

$$\text{i.e. } \frac{Cp_i}{y'(o)} = 2\left[\, 1 + 4\,\Sigma\,\frac{A_n}{Cp_i}\right]^{-1} C_T \qquad \text{(II.10)}$$

where $y'(o) = \tan\theta_o$, and θ_o is the edge angle.

APPENDIX III

Derivation of relation between excess length to chord ratio, inflation pressure coefficient and tension coefficient.

To obtain the relation

$$\frac{Cp_i}{\sqrt{\frac{\ell-c}{c}}} = f(C_T)$$

From (II.2) and (II.9), get

$$-\frac{1}{Cp_i}y' = -\frac{1}{C_T}\left(\tfrac{1}{4} + 2\Sigma\frac{A_n}{Cp_i}\right) + \frac{x}{C_T c} + \frac{4}{C_T c}\cdot\int_0^x \sum_{n=1}^{\infty} n\frac{A_n}{Cp_i}\frac{\sin(n\theta)}{\sin\theta}dz \qquad \text{(III.1)}$$

from appendix II, it has been shown that:

$$I_1 = \int_0^x \sum_{n=1}^{\infty} n\frac{A_n}{Cp_i}\frac{\sin(n\theta)}{\sin\theta}dz = \frac{c}{2}\Sigma\frac{A_n}{Cp_i}\left[1 - \cos\left(n\cos^{-1}\left(1 - \frac{2x}{c}\right)\right)\right]$$

Substitute I_1 into (III.1)

$$-\frac{1}{Cp_i}y' = -\frac{1}{2C_T} + \frac{x}{C_T c} - \frac{2}{C_T}\Sigma\frac{A_n}{Cp_i}\cos\left(n\cos^{-1}\left(1 - \frac{2x}{c}\right)\right) \qquad \text{(III.2)}$$

$$\left(\frac{y'}{Cp_i}\right)^2 = \left(\frac{1}{2C_T} - \frac{x}{C_T c}\right)^2 + \frac{4}{C_T^2}\left[\Sigma\frac{A_n}{Cp_i}\cos\left(n\cos^{-1}\left(1 - \frac{2x}{c}\right)\right)\right]^2$$

$$+ 2\left(\frac{1}{2C_T} - \frac{x}{C_T c}\right)\frac{2}{C_T}\Sigma\frac{A_n}{Cp_i}\cos\left(n\cos^{-1}\left(1 - \frac{2x}{c}\right)\right)$$

$$= \frac{1}{4C_T^2} + \frac{x^2}{C_T^2 c^2} - \frac{x}{C_T^2 c} + \frac{4}{C_T^2}\left[\Sigma\frac{A_n}{Cp_i}\cos\left(n\cos^{-1}\left(1 - \frac{2x}{c}\right)\right)\right]^2$$

$$+ \frac{2}{C_T^2}\Sigma\frac{A_n}{Cp_i}\cos\left(n\cos^{-1}\left(1 - \frac{2x}{c}\right)\right) - \frac{4}{C_T^2}\frac{x}{c}\Sigma\frac{A_n}{Cp_i}\cos\left(n\cos^{-1}\left(1 - \frac{2x}{c}\right)\right)$$

(III.3)

The equation of a length is given by

$$\ell = \int_0^c \sqrt{1 + \left(\frac{dy}{dx}\right)^2}\, dx \qquad \text{(III.4)}$$

Since $\frac{dy}{dx}$ is small, then by binomial expansion and rearrangement

$$\left(\frac{\ell - c}{c}\right) \frac{1}{Cp_i^2} = \frac{1}{2c} \int_0^c \left(\frac{1}{Cp_i} \frac{dy}{dx}\right)^2 dx \qquad \text{(III.5)}$$

Substitute (III.3) into (III.5),

$$\begin{aligned}
\left(\frac{\ell - c}{c}\right)\frac{1}{Cp_i^2} = \frac{1}{2c} \cdot \int_0^c \Bigg\{ & \frac{1}{4C_T^2} + \frac{-x^2}{C_T^2 c^2} - \frac{x}{C_T^2 c} + \frac{4}{C_T^2}\left[\Sigma \frac{A_n}{Cp_i} \cos\left(n \cos^{-1}\left(1 - \frac{2x}{c}\right)\right)\right]^2 \\
& + \frac{2}{C_T^2} \Sigma \frac{A_n}{Cp_i} \cos\left(n \cos^{-1}\left(1 - \frac{2x}{c}\right)\right) \\
& - \frac{4}{C_T^2} \frac{x}{c} \Sigma \frac{A_n}{Cp_i} \cos\left(n \cos^{-1}\left(1 - \frac{2x}{c}\right)\right) \Bigg\} dx \\
= \quad & \frac{1}{24C_T^2} + \frac{2}{C_T^2 c} \cdot \int_0^c \left[\Sigma \frac{A_n}{Cp_i} \cos\left(n \cos^{-1}\left(1 - \frac{2x}{c}\right)\right)\right]^2 dx \\
& + \frac{1}{C_T^2 c} \cdot \int_0^c \Sigma \frac{A_n}{Cp_i} \cos\left(n \cos^{-1}\left(1 - \frac{2x}{c}\right)\right) dx \\
& - \frac{2}{C_T^2 c} \cdot \int_0^c \Sigma \frac{A_n}{Cp_i} \frac{x}{c} \cos\left(n \cos^{-1}\left(1 - \frac{2x}{c}\right)\right) dx \qquad \text{(III.6)}
\end{aligned}$$

From (II.8a)

$$I_2 = \int_0^c \sum_{n=1}^{\infty} \frac{A_n}{Cp_1} \cos\left(n \cos^{-1}\left(1 - \frac{2x}{c}\right)\right) dx = 0$$

Let: $$I_3 = \int_0^c \Sigma \frac{A_n}{Cp_1} \frac{x}{c} \cos\left(n \cos^{-1}\left(1 - \frac{2x}{c}\right)\right) dx \qquad \text{(III.7)}$$

Let $u = n \cos^{-1}\left(1 - \frac{2x}{c}\right)$

At $x = 0 \quad u = 0$

$x = c \quad u = n\pi$

$$\cos\left(\frac{u}{n}\right) = \left(1 - \frac{2x}{c}\right)$$

$$dx = \frac{c}{2} \frac{1}{n} \sin\left(\frac{u}{n}\right) du$$

Hence

$$I_3 = \Sigma \frac{A_n}{Cp_1} \int_0^{n\pi} \tfrac{1}{2}\left(1 - \cos\frac{u}{n}\right) \cdot \cos u \cdot \left(\frac{c}{2n}\right) \cdot \sin\frac{u}{n}\, du$$

$$= \frac{c}{4} \Sigma \frac{A_n}{Cp_1} \frac{1}{n} \cdot \int_0^{n\pi} \left(\sin\frac{u}{n} \cos u - \sin\frac{u}{n} \cos\frac{u}{n} \cos u\right) du$$

$$= \frac{c}{4} \Sigma \frac{A_n}{Cp_1} \frac{1}{n} \cdot \int_0^{n\pi} \sin\frac{u}{n} \cos u\, du - \frac{c}{8} \Sigma \frac{An}{Cp_1} \frac{1}{n} \int_0^{n\pi} \sin\frac{2u}{n} \cos u\, du$$

$$\int_0^{n\pi} \sin\frac{u}{n} \cos u\, du = 0$$

$$\int_0^{n\pi} \sin\frac{2u}{n} \cos u\, du = \frac{4n}{4-n^2} \qquad \text{(with n's are odd)}$$

Hence

$$I_3 = -\frac{c}{8}\sum_{n}^{\infty}\frac{A_n}{Cp_f}\frac{1}{n}\left(\frac{4n}{4-n^2}\right)$$

$$I_3 = \frac{c}{2}\sum_{n}^{\infty}\frac{A_n}{Cp_f}\left(\frac{1}{n^2-4}\right)$$

Let: $$I_4 = \int_0^c\left[\sum_{n}^{\infty}\frac{A_n}{Cp_f}\cos\left(n\cos^{-1}\left(1-\frac{2x}{c}\right)\right)\right]^2 dx \qquad \text{(III.8)}$$

i.e. $$I_4 = \int_0^c\left[\sum_{m}^{\infty}\frac{A_m}{Cp_f}\cos\left(m\cos^{-1}\left(1-\frac{2x}{c}\right)\right)\right]\cdot\left[\sum_{n}^{\infty}\frac{A_n}{Cp_f}\cos\left(n\cos^{-1}\left(1-\frac{2x}{c}\right)\right)\right]dx$$

$$= \sum_{m}^{\infty}\sum_{n}^{\infty}\frac{A_m}{Cp_f}\frac{A_n}{Cp_f}\cdot\int_0^c\cos\left(m\cos^{-1}\left(1-\frac{2x}{c}\right)\right)\cos\left(n\cos^{-1}\left(1-\frac{2x}{c}\right)\right)dx$$

Let: $$u = \cos^{-1}\left(1-\frac{2x}{c}\right)$$

At $x = 0$ $u = 0$

$x = c$ $u = \pi$

$$\cos u = \left(1-\frac{2x}{c}\right)$$

$$dx = \frac{c}{2}\sin u\, du$$

Hence

$$I_4 = \frac{c}{2}\sum_{m}^{\infty}\sum_{n}^{\infty}\frac{A_m}{Cp_f}\frac{A_n}{Cp_f}\cdot\int_0^{\pi}\cos mu\cos nu\sin u\, du$$

by applying: $2\sin A\cos B = \sin(A-B) + \sin(A+B)$,

$$I_4 = \frac{c}{4}\sum_{m}^{\infty}\sum_{n}^{\infty}\frac{A_m}{Cp_f}\frac{A_n}{Cp_f}\cdot\int_0^{\pi}\left(\sin(1-n)u\cos mu + \sin(1+n)u\cos mu\right)du$$

by: $\int \sin px \cos qx \, dx = -\frac{1}{2}\left[\frac{\cos(p-q)x}{(p-q)} + \frac{\cos(p+q)x}{(p+q)}\right]$

and all m, n's are odd.

$$I_4 = \frac{c}{4} \sum_m^\infty \sum_n^\infty \frac{A_m}{Cp_i} \frac{A_n}{Cp_i} \left[\frac{2(1-n)}{(1-n)^2-m^2} + \frac{2(1+n)}{(1+n)^2-m^2} \right]$$

$$I_4 = c \sum_m^\infty \sum_n^\infty \frac{A_m}{Cp_i} \frac{A_n}{Cp_i} \left[\frac{1-n^2-m^2}{[(1-n)^2-m^2][(1+m)^2-m^2]} \right]$$

Substitute I_2, I_3, I_4 back into (III.6),

$$\left(\frac{\ell-c}{c}\right)\frac{1}{Cp_i^2} = \frac{1}{24C_T^2} + \frac{2}{C_T^2 c} \left\{ c \sum_m^\infty \sum_n^\infty \frac{A_m}{Cp_i} \frac{A_n}{Cp_i} \left[\frac{1-n^2-m^2}{[(1-m)^2-m^2][(1+n)^2-m^2]} \right] \right\}$$

$$+ \frac{1}{C_T^2 c} \cdot [0] - \frac{2}{C_T^2 c} \left[\frac{c}{2} \sum_n^\infty \frac{A_n}{Cp_i} \frac{1}{(n^2-4)} \right]$$

$$\left(\frac{\ell-c}{c}\right)\frac{1}{Cp_i^2} = \frac{1}{24C_T^2} \left[1 - 24 \sum \frac{A_n}{Cp_i} \frac{1}{(n^2-4)} + 48 \sum_m^\infty \sum_n^\infty \frac{A_m}{Cp_i} \frac{A_n}{Cp_i} \frac{1-n^2-m^2}{[(1-n)^2-m^2][(1+n)^2-m^2]} \right]$$

(III.9a)

or:

$$\frac{Cp_i}{\sqrt{\frac{\ell-c}{c}}} = \sqrt{24} \left[1-24 \sum_n^\infty \frac{A_n}{Cp_i} \frac{1}{(n^2-4)} + 48 \sum_m^\infty \sum_n^\infty \frac{A_m}{Cp_i} \frac{A_n}{Cp_i} \frac{1-n^2-m^2}{[(1-n)^2-m^2][(1+n)^2-m^2]} \right]^{-\frac{1}{2}} C_T$$

(III.9b)

from (II.10):

$$\frac{Cp_i}{y'(o)} = 2\left[1+4 \sum \frac{A_n}{Cp_i}\right]^{-1} C_T$$

Eliminate C_T between (II.10) and (III.9b)

$$\frac{Cp_i}{y'(o)} = \frac{1}{\sqrt{6}}\left[1-24\ \Sigma\frac{A_n}{Cp_i}\ \frac{1}{(n^2-4)} + 48\ \Sigma_m\ \Sigma_n\ \frac{A_m}{Cp_i}\ \frac{A_n}{Cp_i}\ \frac{1-n^2-m^2}{[(1-n)^2-m][(1+n)^2-m^2]}\right]^{\frac{1}{2}}$$

$$\cdot\left[1+4\ \Sigma\frac{A_n}{Cp_i}\right]^{-1}\cdot\ \frac{Cp_i}{\sqrt{\frac{\ell-c}{c}}} \qquad \text{(III.10)}$$

APPENDIX IV

Computer Program

This program solves for the coefficients (An/Cp_i) from the master equation (2.2.21), and hence the rest of the characteristics of the inflated lenticular aerofoil can be found by using equations (2.2.13), (2.2.17), (2.2.18), (2.2.19), (2.2.30) and (2.2.31).

List of symbols used in the computer program and sample program are shown on the following pages.

List of symbols used in the computer program

A(I, J)	to replace COA(M, N) i.e. COA(M, 2N-1) → A(M, N)
BS	solid blockage
BW	wake blockage
BT	BS + BW total blockage
C	chord length (cm)
C1	$-24\ \Sigma(An/Cp_i)\ (n^2 - 4)^{-1}$
C2	$48\ \Sigma\Sigma(An/Cp_i)\ (An/Cp_i)\ \frac{1-n^2-m^2}{[(1-n)^2-m^2][(1+n)^2-m^2]}$
C_D	drag coefficient (0.01)
CF2	C1 + C2
CF1	$4\ \Sigma(An/Cp_i)$
CT	tension coefficient
CPI	inflation pressure coefficient
CC(M, N)	$n\sin n\theta m\ \sin^2\theta m$
CL(M, N)	$n\cos(n\theta_m)\cos\theta_m + n^2\sin(n\theta_m)\sin\theta_m$
COA(M, N)	$= C_T$ * CL(M, N) - CL(M, N)
DXDYO	$Cp_i/y'(o)$
EST	$Cp_i\ (\frac{\ell-c}{c})^{-\frac{1}{2}}$ theoretical value
ESA	$Cp_i\ (\frac{\ell-c}{c})^{-\frac{1}{2}} = \sqrt{24}\ C_T$, asymptotic value
ITE	= 1: if both theoretical and experimental results desired i.e. Uo, C, Vis, inputs must have some value = 0: if only theoretical results desired i.e. Uo, C, VIS, inputs are zero
NDS	number of data sets inputed

NR	number of coefficients (An/Cp_i) desired
NT	2 * NR
RCP	Cp/Cp_i
RV	$(U/U_o-1)/Cp_i$
RYC	$(y/c)/Cp_i$
RE	Reynolds number base on chord length
RCT	c/t
RCW	c/w
RTW	t/w
S(M)	$\frac{1}{2}\sin^2(\theta m)$
SF	shape factor
SL	ℓ - membrane length (cm)
SOL(N)	solution of (An/Cp_i)
T	t inflated aerofoil thickness
TCP	C_p
TRV	u/Uo
TRYC	y/c
UO	free stream velocity
VIS	v kinematic viscosity (m^2/s)
W	tunnel width
SLEQN	this subroutine solves a system of linear equations by pivoting method
CHANGE	this subroutine interchanges the values of the variables
ESLOPE	this subroutine solves equation (2.2.29)
SLENGT	this subroutine solves equation (2.2.30)

BLOCKG	this subroutine to find the blockages
RXYUCP	this subroutine to solve equations (2.2.13), (2.2.17), (2.2.18)

All the rest are dummy variables

Sample Input

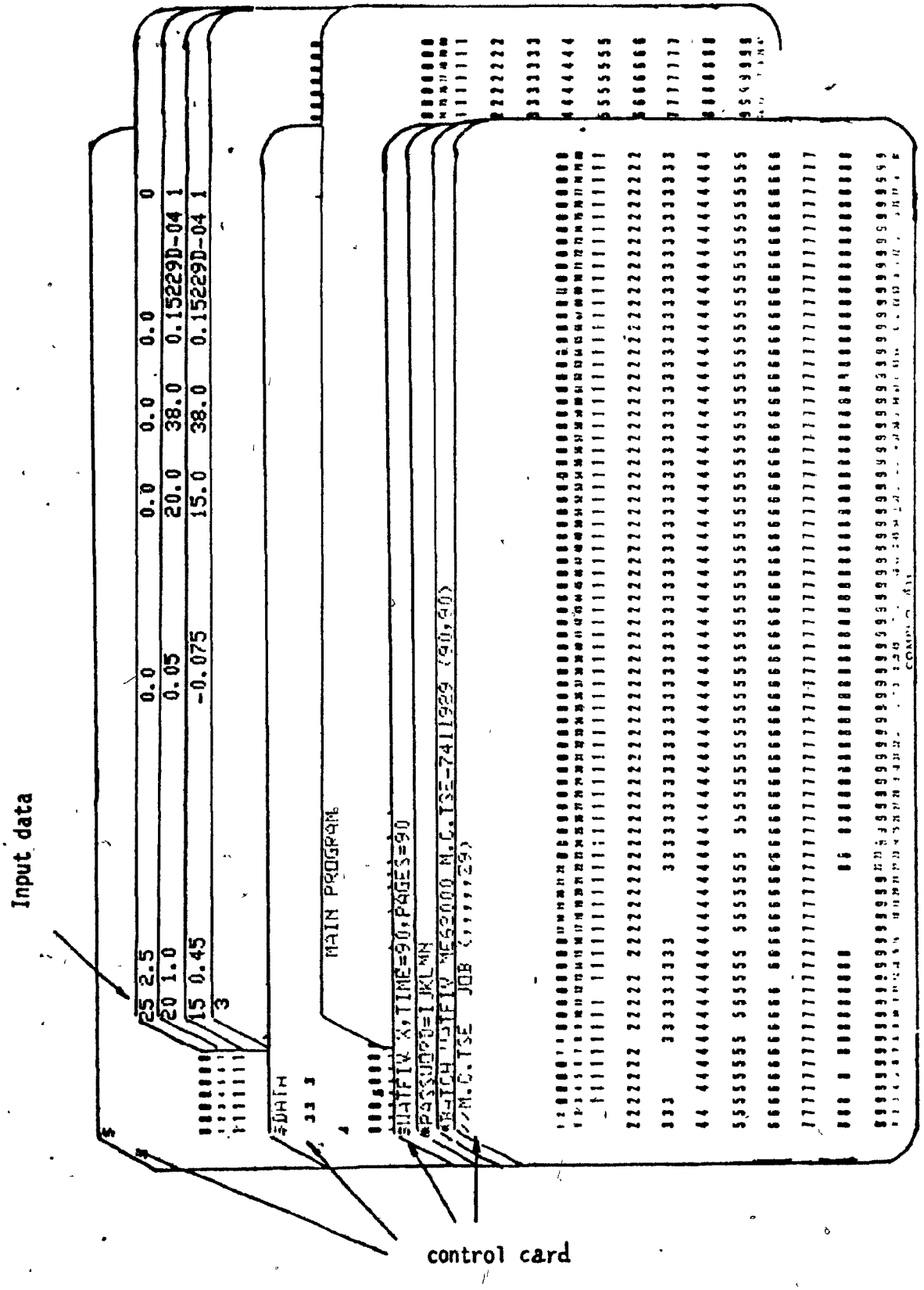

```
*BATCH WATFIV ME62000 M.C.TSE-7411929 (90,90)
*****************************************************************************

      $WATFIV X,TIME=90,PAGES=90
C
C
C     DATA INPUT
C
C
      IMPLICIT REAL*8 (A-H,O-Z)
      DOUBLE PRECISION CC(25,50),CL(25,50),COA(25,50),A(25,26),
     +S(25),SOL(50)
      W=76.2D0
      READ(5,101) NDS
  101 FORMAT(I2)
      DO 555 NTIME=1,NDS
      READ(5,100) NR,CT,CPI,U0,C,VIS,ITE
  100 FORMAT(I2,1X,D22.16,1X,D14.8,1X,D6.3,1X,D6.3,1X,D11.5,1X,I1)
      WRITE(6,200) CT,NR
  200 FORMAT(1H1,///////11X,'CT = ',D22.16,//11X,
     +'NO. OF COEFF. = ',I2,/)
C
C
C     TO GENERATE THE COEFF. OF A(N)/CPI N=ODD
C
C
      PI=DATAN(1.D0)*4.D0
      Q=DFLOAT(NR-1)
      D=(PI/2.D0)/Q
      X=0.0D0
      NT=NR+NR
      DO 1 M=1,NR
      S(M)=0.25D0*DSIN(X)**3
      DO 2 N=1,NT,2
      CC(M,N)=N*DSIN(N*X)*DSIN(X)**2
      CL(M,N)=N*DCOS(N*X)*DCOS(X)+N*N*DSIN(N*X)*DSIN(X)
      COA(M,N)=CL(M,N)*CT-CC(M,N)
    2 CONTINUE
      X=X+D
    1 CONTINUE
C
C
C     TO RE-ARRANGE THE COEFF. AS STARTING MATRIX ELEMENTS
C
      DO 3 I=1,NR
      J=1
      DO 4 N=1,NT,2
      IF(N.EQ.1) GO TO 50
      J=N-J
      A(I,J)=COA(I,N)
      GO TO 4
   50 A(I,1)=COA(I,1)
    4 CONTINUE
    3 CONTINUE
      NC=NR+1
      DO 5 I=1,NR
      A(I,NC)=S(I)
    5 CONTINUE
C
C
C     TO SOLVE THE MATRIX FOR A(N)/CPI N=ODD
```

```
C
      CALL SLEQN(NR,NC,A,CT)
C
CCCCC
      TO RE-ARRANGE THE SOLUTION
CCCCC
      I=1
      DO 20 K=1,NT,2
      IF(K.EQ.1) GO TO 51
      I=K-I
      SOL(K)=A(I,NC)
      GO TO 20
   51 SOL(1)=A(1,NC)
   20 CONTINUE
      WRITE(6,201)
  201 FORMAT(1H0,10X,'A( N)/CPI N=ODD',/)
      WRITE(6,202) (I,SOL(I),I=1,NT,2)
  202 FORMAT(11X,'A(',I2,')/CPI = ',D12.5)
C
CCCCC
      TO FIND MAXIMUM (Y/C)/CPI
CCCCC
      ANG=PI/2.D0
      RYC=0.D0
      DO 111 N=1,NT,2
      RYC=RYC+SOL(N)*DSIN(N*ANG)
  111 CONTINUE
      WRITE(6,210) RYC
      T=RYC*C*CPI
  210 FORMAT(1H0,/11X,'MAXIMUM (Y/C)/CPI        = ',D12.5)
C
CCCCC
      TO FIND CPI/DYDX AT X/C=0
CCCCC
      CALL ESLOPE(NT,SOL,CT,DXDY0,CF1)
      WRITE(6,213) CF1,DXDY0
  213 FORMAT(1H0,10X,'CFI  4*SUM(AN/CPI)          = ',D12.5,
     +//11X,'CPI/DYDX (X/C=0)          = ',D12.5)
C
CCCCC
      TO FIND  CPI/SQRT((L-C)/C)
CCCCC
      CALL SLENGT(NT,SOL,CT,CF2,EST)
      ESA=DSQRT(24.D0)*CT
      WRITE(6,214) CF2,EST,ESA
  214 FORMAT(1H0,10X,'CF2 (C1+C2)                = ',D12.5,
     +//11X,'CPI/SQRT((L-C)/C) T       = ',D12.5,
     +//11X,'CPI/SQRT((L-C)/C) A       = ',D12.5)
C
CCCCC
      TO FIND  X/C  S/L  (Y/C)/CPI  (U/U0-1)/CPI  CP/CPI  Y/C  U/U0  CP
CCCCC
      IF(ITE.NE.1) GO TO 999
C
      RE=U0*(C/1.D0,D0)/VIS
```

```
      SL=C*(1.D0+(CPI/EST)**2)
      WRITE(6,206) CT,CPI,RE,U0,C,SL
  206 FORMAT(1H1,//////15X,'CT = ',D23.16,/14X,'CPI = ',D15.8,/12X,
     +'RE(C) = ',D15.8,/10X,'U0(M/S) = ',D15.8,/12X,'C(CM) = ',D15.8,
     +/12X,'L(CM) = ',D15.8)
      WRITE(6,207)
  207 FORMAT(1H0,//5X,'X/C',9X,'S/L',7X,'(Y/C)/CPI',3X,
     +'(U/U0-1)/CPI',5X,'CP/CPI',9X,'Y/C',9X,'U/U0',10X,'CP',/)
      IT=1
      IE=41
      SSL=0.D0
      RSL=0.D0
      DO 23 I=IT,IE
      RV=0.D0
      RVC=0.D0
      RCP=0.D0
      RXC=0.025D0*I-0.025D0
      CALL RXYUCP(NT,SOL,RXC,RVC,RV,RCP)
      TRVC=RVC*CPI
      TRV=1.D0+RV*CPI
      TCP=RCP*CPI
      XX=RXC*C
      YY=TRVC*C
      IF(I.EQ.1) GO TO 929
      DYDX=(YY-YYI)/(XX-XXI)
      XXI=XX
      YYI=YY
      SSL=SSL+0.025D0*C*DSQRT(1.D0+DYDX**2)
      RSL=SSL/SL
      WRITE(6,208) RXC,RSL,RVC,RV,RCP,TRVC,TRV,TCP
  208 FORMAT(2X,D9.3,3X,D9.3,2X,D12.5,1X,D13.5,1X,D13.5,
     +1X,D12.5,1X,D12.5,1X,D12.5)
      GO TO 23
  929 XXI=XX
      YYI=YY
      WRITE(6,208) RXC,RSL,RVC,RV,RCP,TRVC,TRV,TCP
   23 CONTINUE
C
C
C     TO FIND SHAPE FACTOR,SOLID,WAKE & TOTAL BLOCKAGE.
C
      CALL BLOCKG(NT,SOL,CPI,C,T,W,SF,BS,BW,BT)
      WRITE(6,211) CT,CPI,SF,BS,BW,BT
  211 FORMAT(1H1,//////////////////8X,'CT = ',D23.16,//37X,'CPI = ',D15.8,
     +//23X,'SHAPE FACTOR (SF) = ',D12.5,//21X,'SOLID BLOCKAGE (BS) = ',
     +D12.5,//22X,'WAKE BLOCKAGE (BW) = ',D12.5,//21X,'TOTAL BLOCKAGE',
     +' (BT) = ',D12.5,///)
      GO TO 555
C
C
C     TO FIND   X/C  (Y/C)/CPI  (U/U0-1)/U  CP/CPI
C
C
  999 CONTINUE
      WRITE(6,300) CT
  300 FORMAT(1H1,/////////10X,'CT = ',D22.16,////14X,'X/C',8X,
     +'(Y/C)/CPI',4X,'(U/U0-1)/CPI',6X,'CP/CPI',/)
      IT=1
      IE=41
```

```
      DO 29 I=IT,IE
      RV=0.D0
      RYC=0.D0
      RCP=0.D0
      RXC=0.025D0*I-0.025D0
      CALL RXYUCP(NT,SOL,RXC,RYC,RV,RCP)
      WRITE(6,301) RXC,RYC,RV,RCP
  301 FORMAT(11X,D9.3,3(3X,D12.5))
   29 CONTINUE
C
  555 CONTINUE
C
C
      WRITE(6,212)
  212 FORMAT(1H1)
      STOP
      END


      SUBROUTINE $LEQN(NR,NC,A,CT)
      IMPLICIT REAL*8 (A-H,O-Z)
      DOUBLE PRECISION A(25,26)
      INTEGER IR(25),JC(25)
      EPS=0.1D-10
      N=NR
      B=0.0D0
      DO 6 K=1,NR
      IR(K)=K
      JC(K)=K
    6 CONTINUE
      DO 7 K=1,NR
      PIV=0.0D0
      DO 8 I=K,NR
      DO 8 J=K,NR
      G=DABS(A(I,J))
      PIV=DMAX1(PIV,G)
      IF((PIV-G).GT.EPS) GO TO 8
      II=I
      JJ=J
    8 CONTINUE
      DO 9 J=1,NC
    9 CALL CHANGE(A(K,J),A(II,J),N,N)
      DO 10 I=1,NR
   10 CALL CHANGE(A(I,K),A(I,JJ),N,N)
      CALL CHANGE(B,B,IR(K),IR(II))
      CALL CHANGE(B,B,JC(K),JC(JJ))
      PIV=A(K,K)
      IF(DABS(PIV).LT.EPS) GO TO 500
      DO 11 I=1,NR
      DO 11 J=1,NC
      IF(I.EQ.K) GO TO 11
      IF(J.NE.K) A(I,J)=A(I,J)-A(I,K)*A(K,J)/PIV
   11 CONTINUE
      DO 12 J=1,NC
      A(K,J)=A(K,J)/PIV
   12 CONTINUE
      DO 13 I=1,NR
      IF(I.NE.K) A(I,K)=-A(I,K)/PIV
      IF(I.EQ.K) A(K,K)=1.000/PIV
   13 CONTINUE
```

```
      7 CONTINUE
        DO 14 K=1,NR
        IF(IR(K).EQ.K) GO TO 14
        DO 15 I=1,NR
     15 IF(IR(I).EQ.K) L=I
        CALL CHANGE(B,B,IR(K),IR(L))
        DO 16 I=1,NR
     16 CALL CHANGE(A(I,K),A(I,L),N,N)
     14 CONTINUE
        DO 17 K=1,NR
        IF(JC(K).EQ.K) GO TO 17
        DO 18 I=1,NR
     18 IF(JC(I).EQ.K) L=I
        CALL CHANGE(B,B,JC(K),JC(L))
        DO 19 J=1,NC
     19 CALL CHANGE(A(K,J),A(L,J),N,N)
     17 CONTINUE
        GO TO 222
    500 WRITE(6,204) CT
    204 FORMAT(1H1,//////11X,'CT = ',D22.16,///11X,'DETERMINANT = 0.0',
       +////11X,'NO INVERSE MATRIX',///)
    222 RETURN
        END

        SUBROUTINE CHANGE(X,Y,I,J)
        DOUBLE PRECISION X,Y,Z
        Z=X
        X=Y
        Y=Z
        K=I
        I=J
        J=K
        RETURN
        END

        SUBROUTINE ESLOPE(NT,SOL,CT,DXDY0,CF1)
        IMPLICIT REAL*8 (A-H,O-Z)
        DOUBLE PRECISION SOL(NT)
        RANCPI=0.D0
        DO 25 N=1,NT,2
        RANCPI=RANCPI+SOL(N)
     25 CONTINUE
        CF1=4.D0*RANCPI
        DXDY0=CT*2.D0/(1.D0+4.D0*RANCPI)
        RETURN
        END

        SUBROUTINE SLENGT(NT,SOL,CT,CF2,EST)
        IMPLICIT REAL*8 (A-H,O-Z)
        DIMENSION SOL(NT)
        C1=0.D0
        C2=0.D0
        DO 26 M=1,NT,2
        P=DFLOAT(M)
        C1=C1+SOL(M)/(P*P-4.D0)
        SSAMAN=0.D0
        DO 27 N=1,NT,2
```

```
      Q=DFLOAT(N)
      CMN=(1.D0-Q*Q-P*P)/((1.D0-Q)**2-P*P)/((1.D0+Q)**2-P*P)
      SSAMAN=SSAMAN+SOL(N)*SOL(N)*CMN
   27 CONTINUE
      C2=C2+SSAMAN
   26 CONTINUE
      C1=-24.D0*C1
      C2=48.D0*C2
      CF2=C1+C2
      EST=CT*DSQRT(24.D0)/DSQRT(1.D0+CF2)
      RETURN
      END

      SUBROUTINE RXYUCP(NT,SOL,RXC,RYC,RV,RCP)
      IMPLICIT REAL*8 (A-H,O-Z)
      DOUBLE PRECISION SOL(NT)
      PI=DATAN(1.D0)*4.D0
      A=DARCOS(1.D0-2.D0*RXC)
      IF(RXC.EQ.0.5D0) A=PI/2.D0
      IF(RXC.LT.1.D-10) GO TO 53
      IF((1.D0-RXC).LT.1.D-10) GO TO 53
      DO 24 N=1,NT,2
      DD=SOL(N)*DSIN(N*A)
      RYC=RYC+DD
      RV=RV+N*DD
   24 CONTINUE
      RV=2.D0*RV/DSIN(A)
      RCP=-2.D0*RV
      GO TO 54
   53 DO 25 N=1,NT,2
      RYC=RYC+SOL(N)*DSIN(N*A)
      RV=RV+2.D0*N*SOL(N)*N
   25 CONTINUE
      RCP=-2.D0*RV
   54 CONTINUE
      RETURN
      END

      SUBROUTINE BLOCKG(NT,SOL,CPI,C,T,W,SP,RS,BW,BT)
      IMPLICIT REAL*8 (A-H,O-Z)
      DOUBLE PRECISION SOL(NT)
      CDT=0.01D0
      W=76.2D0
      PI=DATAN(1.D0)*4.D0
      RCT=C/T
      RCW=C/W
      RTW=T/W
      DIV=100.D0
      H=1.D0/DIV
      S=0.D0
      SVY=0.D0
      DO 1 M=1,99
      S=S+H
      A=DARCOS(1.D0-2.D0*S)
      IF(S.EQ.0.5D0) A=PI/2.D0
      RYC=0.D0
      V=0.D0
      DO 2 N=1,NT,2
```

```
      D=SOL(N)*DSIN(N*A)
      RYC=RYC+D
      V=V+N*D
    2 CONTINUE
      RYC=CPI*RYC
      V=1.D0+2.D0*CPI*V/DSIN(A)
      VY=V*RYC
      IF(M.EQ.M/2*2) GO TO 111
      SVY=SVY+4.D0*VY
      GO TO 1
  111 SVY=SVY+2.D0*VY
    1 CONTINUE
      SVY=SVY*H/3.D0
      SF=SVY*4.D0*RCT**2/PI
      BS=SF*RTW**2*PI**2/12.D0
      RW=RCW**2*COT/4.D0
      BT=BS+RW
      RETURN
      END

$DATA
```

CT = 0.45000000000000000D 00

NO. OF COEFF. = 15

A(N)/CPI N=ODD

A(1)/CPI = -0.20262D 01
A(3)/CPI = 0.62369D 00
A(5)/CPI = -0.20507D-01
A(7)/CPI = 0.92256D-02
A(9)/CPI = 0.39918D-02
A(11)/CPI = 0.22707D-02
A(13)/CPI = 0.14022D-02
A(15)/CPI = 0.92459D-03
A(17)/CPI = 0.64109D-03
A(19)/CPI = 0.46260D-03
A(21)/CPI = 0.34486D-03
A(23)/CPI = 0.26431D-03
A(25)/CPI = 0.20789D-03
A(27)/CPI = 0.12316D-02
A(29)/CPI = 0.98702D-03

MAXIMUM (Y/C)/CPI = -0.26772D 01

CF1 4*SUM(AN/CPI) = -0.56042D 01

CPI/DYDX (X/C=0) = -0.19547D 00

CF2 (C1+C2) = 0.79902D 02

CPI/SQRT((L-C)/C) T = 0.24510D 00

CPI/SQRT((L-C)/C) A = 0.22045D 01

CT = 0.450000000000000D 00
CPI = -0.750000000-01
RE(C) = 0.37428590D 06
U0(M/S) = 0.150000000 02
C(CM) = 0.380000000 02
L(CM) = 0.41556204D 02

X/C	S/L	(Y/C)/CPI	(U/U0-1)/CPI	CP/CPI	Y/C	U/U0	CP
0.0000 00	0.000D 00	0.000000 00	0.14143D 02	-0.28286D 02	0.000000 00	-0.60723D-01	0.21214D 01
0.2500-01	0.247D-01	-0.13823D 00	0.54251D 01	-0.10850D 02	0.103670-01	0.59312D 00	0.81376D 00
0.5000-01	0.500D-01	-0.29521D 00	0.37534D 01	-0.75068D 01	0.22141D-01	0.71849D 00	0.56301D 00
0.7500-01	0.756D-01	-0.46230D 00	0.26840D 01	-0.53680D 01	0.34672D-01	0.79870D 00	0.40260D 00
0.1000 00	0.102D 00	-0.64046D 00	0.15010D 01	-0.30021D 01	0.48035D-01	0.88742D 00	0.22516D 00
0.1250 00	0.127D 00	-0.81995D 00	0.77886D 00	-0.15577D 01	0.61497D-01	0.94159D 00	0.11683D 00
0.1500 00	0.154D 00	-0.10072D 01	-0.30755D 00	0.61509D 00	0.75537D-01	0.10231D 01	-0.46132D-01
0.1750 00	0.180D 00	-0.11942D 01	-0.12814D 01	0.25629D 01	0.89564D-01	0.10961D 01	-0.19221D 00
0.2000 00	0.206D 00	-0.13764D 01	-0.20220D 01	0.40441D 01	0.10323D 00	0.11517D 01	-0.30331D 00
0.2250 00	0.232D 00	-0.15562D 01	-0.28834D 01	0.57669D 01	0.11571D 00	0.12163D 01	-0.43252D 00
0.2500 00	0.258D 00	-0.17308D 01	-0.37949D 01	0.75898D 01	0.12981D 00	0.12846D 01	-0.56923D 00
0.2750 00	0.283D 00	-0.18946D 01	-0.45348D 01	0.90695D 01	0.14210D 00	0.13401D 01	-0.68022D 00
0.3000 00	0.308D 00	-0.20464D 01	-0.51674D 01	0.10335D 02	0.15348D 00	0.13876D 01	-0.77511D 00
0.3250 00	0.333D 00	-0.21863D 01	-0.58226D 01	0.11645D 02	0.16398D 00	0.14367D 01	-0.87340D 00
0.3500 00	0.358D 00	-0.23123D 01	-0.64479D 01	0.12896D 02	0.17342D 00	0.14836D 01	-0.96718D 00
0.3750 00	0.382D 00	-0.24210D 01	-0.69431D 01	0.13886D 02	0.18157D 00	0.15207D 01	-0.10415D 01
0.4000 00	0.405D 00	-0.25112D 01	-0.73221D 01	0.14644D 02	0.18834D 00	0.15492D 01	-0.10983D 01
0.4250 00	0.429D 00	-0.25828D 01	-0.76418D 01	0.15284D 02	0.19371D 00	0.15731D 01	-0.11463D 01
0.4500 00	0.452D 00	-0.26350D 01	-0.78950D 01	0.15790D 02	0.19763D 00	0.15921D 01	-0.11842D 01
0.4750 00	0.475D 00	-0.26667D 01	-0.80446D 01	0.16089D 02	0.20000D 00	0.16033D 01	-0.12067D 01
0.5000 00	0.498D 00	-0.26772D 01	-0.80905D 01	0.16181D 02	0.20079D 00	0.16068D 01	-0.12136D 01
0.5250 00	0.520D 00	-0.26667D 01	-0.80446D 01	0.16089D 02	0.20000D 00	0.16033D 01	-0.12067D 01
0.5500 00	0.543D 00	-0.26350D 01	-0.79950D 01	0.15790D 02	0.19763D 00	0.15921D 01	-0.11842D 01
0.5750 00	0.567D 00	-0.25828D 01	-0.76418D 01	0.15284D 02	0.19371D 00	0.15731D 01	-0.11463D 01
0.6000 00	0.590D 00	-0.25112D 01	-0.73221D 01	0.14644D 02	0.18834D 00	0.15492D 01	-0.10983D 01
0.6250 00	0.614D 00	-0.24210D 01	-0.69431D 01	0.13886D 02	0.18157D 00	0.15207D 01	-0.10415D 01
0.6500 00	0.638D 00	-0.23123D 01	-0.64479D 01	0.12896D 02	0.17342D 00	0.14836D 01	-0.96718D 00
0.6750 00	0.662D 00	-0.21863D 01	-0.58226D 01	0.11645D 02	0.16398D 00	0.14367D 01	-0.87340D 00
0.7000 00	0.687D 00	-0.20464D 01	-0.51674D 01	0.10335D 02	0.15348D 00	0.13876D 01	-0.77511D 00
0.7250 00	0.712D 00	-0.18946D 01	-0.45348D 01	0.90695D 01	0.14210D 00	0.13401D 01	-0.68022D 00
0.7500 00	0.738D 00	-0.17308D 01	-0.37949D 01	0.75898D 01	0.12981D 00	0.12846D 01	-0.56923D 00
0.7750 00	0.763D 00	-0.15562D 01	-0.28834D 01	0.57669D 01	0.11571D 00	0.12163D 01	-0.43252D 00
0.8000 00	0.789D 00	-0.13764D 01	-0.20220D 01	0.40441D 01	0.10323D 00	0.11517D 01	-0.30331D 00
0.8250 00	0.815D 00	-0.11942D 01	-0.12814D 01	0.25629D 01	0.89564D-01	0.10961D 01	-0.19221D 00
0.8500 00	0.842D 00	-0.10072D 01	-0.30755D 00	0.61509D 00	0.75537D-01	0.10231D 01	-0.46132D-01
0.8750 00	0.868D 00	-0.81995D 00	0.77886D 00	-0.15577D 01	0.61497D-01	0.94159D 00	0.11683D 00
0.9000 00	0.894D 00	-0.64046D 00	0.15010D 01	-0.30021D 01	0.48035D-01	0.88742D 00	0.22516D 00
0.9250 00	0.920D 00	-0.46230D 00	0.26840D 01	-0.53680D 01	0.34672D-01	0.79870D 00	0.40260D 00
0.9500 00	0.945D 00	-0.29521D 00	0.37534D 01	-0.75068D 01	0.22141D-01	0.71849D 00	0.56301D 00
0.9750 00	0.971D 00	-0.13823D 00	0.54251D 01	-0.10850D 02	0.10367D-01	0.59312D 00	0.81376D 00
0.1000 01	0.995D 00	-0.64795D-16	0.14143D 02	-0.28286D 02	0.63596D-17	-0.60723D-01	0.21214D 01

CT = 0.45000000000000D 00

CPI = -0.75000000D-01

SHAPE FACTOR (SF) = 0.52415D 01

SOLID BLOCKAGE (BS) = 0.43223D-01

WAKE BLOCKAGE (BW) = 0.62172D-03

TOTAL BLOCKAGE (BT) = 0.43845D-01

CT = 0.1000000000000000D 01

NO. OF COEFF. = 20

A(N)/CPI N=ODD

A(1)/CPI = 0.206250 00
A(3)/CPI = -0.483900-01
A(5)/CPI = -0.378390-02
A(7)/CPI = -0.149990-02
A(9)/CPI = -0.700130-03
A(11)/CPI = -0.382470-03
A(13)/CPI = -0.231480-03
A(15)/CPI = -0.150650-03
A(17)/CPI = -0.103490-03
A(19)/CPI = -0.741430-04
A(21)/CPI = -0.549270-04
A(23)/CPI = -0.418210-04
A(25)/CPI = -0.325770-04
A(27)/CPI = -0.258710-04
A(29)/CPI = -0.208900-04
A(31)/CPI = -0.171130-04
A(33)/CPI = -0.142020-04
A(35)/CPI = -0.119320-04
A(37)/CPI = -0.100620-03
A(39)/CPI = -0.857740-04

MAXIMUM (Y/C)/CPI = 0.25189D 00

CF1 4*SUM(AN/CPI) = 0.60213D 00

CPI/DYDX (X/C=0) = 0.12483D 01

CF2 (C1+C2) = 0.28161D 01

CPI/SQRT((L-C)/C) T = 0.25078D 01

CPI/SQRT((L-C)/C) A = 0.48990D 01

CT = 0.100000000000000D 01
CPI = 0.500000000-01
RE(C) = 0.499047870 06
U0(M/S) = 0.200000000 02
C(CM) = 0.380000000 02
L(CM) = 0.380151050 02

X/C	S/L	(Y/C)/CPI	(U/U0-1)/CPI	CP/CPI	Y/C	U/U0	CP
0.0000 00	0.0000 00	0.000000 00	-0.20958D 01	0.41916D 01	0.000000 00	0.89521D 00	0.20958D 00
0.2500-01	0.250D-01	0.20376D-01	-0.46995D 00	0.93990D 00	0.10188D-02	0.97650D 00	0.46995D-01
0.5000-01	0.500D-01	0.40747D-01	-0.24245D 00	0.48490D 00	0.20374D-02	0.98788D 00	0.24245D-01
0.7500-01	0.750D-01	0.60498D-01	-0.13872D 00	0.27744D 00	0.30249D-02	0.99306D 00	0.13872D-01
0.1000 00	0.1000 00	0.80277D-01	0.74271D-02	-0.14854D-01	0.40139D-02	0.10004D 01	-0.74271D-03
0.1250 00	0.125D 00	0.99020D-01	0.81710D-01	-0.16342D 00	0.49510D-02	0.10041D 01	-0.81710D-02
0.1500 00	0.150D 00	0.11744D 00	0.19050D 00	-0.38100D 00	0.58720D-02	0.10095D 01	-0.19050D-01
0.1750 00	0.175D 00	0.13457D 00	0.24194D 00	-0.48388D 00	0.67283D-02	0.10121D 01	-0.24194D-01
0.2000 00	0.200D 00	0.15115D 00	0.32576D 00	-0.65153D 00	0.75575D-02	0.10163D 01	-0.32576D-01
0.2250 00	0.225D 00	0.16650D 00	0.38144D 00	-0.76288D 00	0.83251D-02	0.10191D 01	-0.38144D-01
0.2500 00	0.250D 00	0.18069D 00	0.42628D 00	-0.85256D 00	0.90345D-02	0.10213D 01	-0.42628D-01
0.2750 00	0.275D 00	0.19396D 00	0.48668D 00	-0.97336D 00	0.96981D-02	0.10243D 01	-0.48668D-01
0.3000 00	0.300D 00	0.20580D 00	0.52297D 00	-0.10459D 01	0.10290D-01	0.10261D 01	-0.52297D-01
0.3250 00	0.325D 00	0.21635D 00	0.55530D 00	-0.11106D 01	0.10818D-01	0.10278D 01	-0.55530D-01
0.3500 00	0.350D 00	0.22575D 00	0.59476D 00	-0.11895D 01	0.11288D-01	0.10297D 01	-0.59476D-01
0.3750 00	0.375D 00	0.23366D 00	0.61913D 00	-0.12383D 01	0.11683D-01	0.10310D 01	-0.61913D-01
0.4000 00	0.400D 00	0.24014D 00	0.63713D 00	-0.12743D 01	0.12007D-01	0.10319D 01	-0.63713D-01
0.4250 00	0.425D 00	0.24530D 00	0.65751D 00	-0.13150D 01	0.12265D-01	0.10329D 01	-0.65751D-01
0.4500 00	0.450D 00	0.24898D 00	0.66987D 00	-0.13397D 01	0.12449D-01	0.10335D 01	-0.66987D-01
0.4750 00	0.475D 00	0.25115D 00	0.67544D 00	-0.13509D 01	0.12558D-01	0.10338D 01	-0.67544D-01
0.5000 00	0.500D 00	0.25189D 00	0.67800D 00	-0.13560D 01	0.12595D-01	0.10339D 01	-0.67800D-01
0.5250 00	0.525D 00	0.25115D 00	0.67544D 00	-0.13509D 01	0.12558D-01	0.10338D 01	-0.67544D-01
0.5500 00	0.550D 00	0.24898D 00	0.66987D 00	-0.13397D 01	0.12449D-01	0.10335D 01	-0.66987D-01
0.5750 00	0.575D 00	0.24530D 00	0.65751D 00	-0.13150D 01	0.12265D-01	0.10329D 01	-0.65751D-01
0.6000 00	0.600D 00	0.24014D 00	0.63713D 00	-0.12743D 01	0.12007D-01	0.10319D 01	-0.63713D-01
0.6250 00	0.625D 00	0.23366D 00	0.61913D 00	-0.12383D 01	0.11683D-01	0.10310D 01	-0.61913D-01
0.6500 00	0.650D 00	0.22575D 00	0.59476D 00	-0.11895D 01	0.11288D-01	0.10297D 01	-0.59476D-01
0.6750 00	0.675D 00	0.21636D 00	0.55530D 00	-0.11106D 01	0.10818D-01	0.10278D 01	-0.55530D-01
0.7000 00	0.700D 00	0.20580D 00	0.52297D 00	-0.10459D 01	0.10290D-01	0.10261D 01	-0.52297D-01
0.7250 00	0.725D 00	0.19396D 00	0.48668D 00	-0.97336D 00	0.96981D-02	0.10243D 01	-0.48668D-01
0.7500 00	0.750D 00	0.18069D 00	0.42628D 00	-0.85256D 00	0.90345D-02	0.10213D 01	-0.42628D-01
0.7750 00	0.775D 00	0.16650D 00	0.38144D 00	-0.76288D 00	0.83251D-02	0.10191D 01	-0.38144D-01
0.8000 00	0.800D 00	0.15115D 00	0.32576D 00	-0.65153D 00	0.75575D-02	0.10163D 01	-0.32576D-01
0.8250 00	0.825D 00	0.13457D 00	0.24194D 00	-0.48388D 00	0.67283D-02	0.10121D 01	-0.24194D-01
0.8500 00	0.850D 00	0.11744D 00	0.19050D 00	-0.38100D 00	0.58720D-02	0.10095D 01	-0.19050D-01
0.8750 00	0.875D 00	0.99020D-01	0.81710D-01	-0.16342D 00	0.49510D-02	0.10041D 01	-0.81710D-02
0.9000 00	0.900D 00	0.80277D-01	0.74271D-02	-0.14854D-01	0.40139D-02	0.10004D 01	-0.74271D-03
0.9250 00	0.925D 00	0.60498D-01	-0.13872D 00	0.27744D 00	0.30249D-02	0.99306D 00	0.13872D-01
0.9500 00	0.950D 00	0.40747D-01	-0.24245D 00	0.48490D 00	0.20374D-02	0.98788D 00	0.24245D-01
0.9750 00	0.975D 00	0.20375D-01	-0.46995D 00	0.93990D 00	0.10188D-02	0.97650D 00	0.46995D-01
0.1000 01	0.100D 01	-0.17580D-18	-0.20958D 01	0.41916D 01	-0.87900D-20	0.89521D 00	0.20958D 00

```
                    CT =  0.10000000000000000D 01
                   CPI =  0.50000000D-01
  SHAPE FACTOR (SF) =  0.66578D 02
SOLID BLOCKAGE (BS) =  0.21601D-02
 WAKE BLOCKAGE (BW) =  0.62172D-03
TOTAL BLOCKAGE (BT) =  0.27818D-02
```

```
CT = 0.2500000000000000D 01
NO. OF COEFF. = 25

A( N)/CPI N=ODD

A( 1)/CPI =  0.525350-01
A( 3)/CPI = -0.111480-01
A( 5)/CPI = -0.13271D-02
A( 7)/CPI = -0.455070-03
A( 9)/CPI = -0.208690-03
A(11)/CPI = -0.112920-03
A(13)/CPI = -0.679540-04
A(15)/CPI = -0.440590-04
A(17)/CPI = -0.301890-04
A(19)/CPI = -0.215860-04
A(21)/CPI = -0.159680-04
A(23)/CPI = -0.121430-04
A(25)/CPI = -0.944960-05
A(27)/CPI = -0.749760-05
A(29)/CPI = -0.604860-05
A(31)/CPI = -0.495030-05
A(33)/CPI = -0.410270-05
A(35)/CPI = -0.343820-05
A(37)/CPI = -0.290990-05
A(39)/CPI = -0.248470-05
A(41)/CPI = -0.213850-05
A(43)/CPI = -0.185410-05
A(45)/CPI = -0.161860-05
A(47)/CPI = -0.177310-04
A(49)/CPI = -0.156400-04

MAXIMUM (Y/C)/CPI          =  0.626750-01

CF1 4*SUM(AN/CPI)          =  0.156050 00

CPI/DYDX (X/C=0)           =  0.432510 01

CF2 (C1+C2)                =  0.534120 00

CPI/SQRT((L-C)/C) T        =  0.988820 01

CPI/SQRT((L+C)/C) A        =  0.122470 02
```

CT = 0.2500000000000000D 01

X/C	(Y/C)/CPI ,	(U/U0-1)/CPI	CP/CPI
0.000D 00	0.000000 00	-0.61980D 00	0.12396D 01
0.250D-01	0.57000D-02	-0.12487D 00	0.24974D 00
0.500D-01	0.11234D-01	-0.60125D-01	0.12025D 00
0.750D-01	0.16528D-01	-0.22876D-01	0.45753D-01
0.100D 00	0.21638D-01	0.14104D-01	-0.28209D-01
0.125D 00	0.26439D-01	0.36332D-01	-0.72664D-01
0.150D 00	0.30973D-01	0.54954D-01	-0.10991D 00
0.175D 00	0.35260D-01	0.74912D-01	-0.14982D 00
0.200D 00	0.39222D-01	0.87481D-01	-0.17496D 00
0.225D 00	0.42921D-01	0.10220D 00	-0.20440D 00
0.250D 00	0.46304D-01	0.11320D 00	-0.22640D 00
0.275D 00	0.49375D-01	0.12243D 00	-0.24486D 00
0.300D 00	0.52161D-01	0.13292D 00	-0.26584D 00
0.325D 00	0.54590D-01	0.13817D 00	-0.27634D 00
0.350D 00	0.56742D-01	0.14650D 00	-0.29300D 00
0.375D 00	0.58541D-01	0.15071D 00	-0.30143D 00
0.400D 00	0.60025D-01	0.15506D 00	-0.31011D 00
0.425D 00	0.61189D-01	0.15898D 00	-0.31796D 00
0.450D 00	0.62008D-01	0.16061D 00	-0.32121D 00
0.475D 00	0.62508D-01	0.16236D 00	-0.32472D 00
0.500D 00	0.62675D-01	0.16283D 00	-0.32566D 00
0.525D 00	0.62508D-01	0.16236D 00	-0.32472D 00
0.550D 00	0.62008D-01	0.16061D 00	-0.32121D 00
0.575D 00	0.61189D-01	0.15898D 00	-0.31796D 00
0.600D 00	0.60025D-01	0.15506D 00	-0.31011D 00
0.625D 00	0.58541D-01	0.15071D 00	-0.30143D 00
0.650D 00	0.56742D-01	0.14650D 00	-0.29300D 00
0.675D 00	0.54590D-01	0.13817D 00	-0.27634D 00
0.700D 00	0.52161D-01	0.13292D 00	-0.26584D 00
0.725D 00	0.49375D-01	0.12243D 00	-0.24486D 00
0.750D 00	0.46304D-01	0.11320D 00	-0.22640D 00
0.775D 00	0.42921D-01	0.10220D 00	-0.20440D 00
0.800D 00	0.39222D-01	0.87481D-01	-0.17496D 00
0.825D 00	0.35260D-01	0.74912D-01	-0.14982D 00
0.850D 00	0.30973D-01	0.54954D-01	-0.10991D 00
0.875D 00	0.26439D-01	0.36332D-01	-0.72664D-01
0.900D 00	0.21638D-01	0.14104D-01	-0.28209D-01
0.925D 00	0.16528D-01	-0.22876D-01	0.45753D-01
0.950D 00	0.11234D-01	-0.60125D-01	0.12025D 00
0.975D 00	0.57000D-02	-0.12487D 00	0.24974D 00
0.100D 01	-0.72196D-18	-0.61980D 00	0.12396D 01

CT = 0.10000D 00

NO. OF COEFF. =	N = 24	N = 20	N = 15	N = 10
MAX. (Y/C)/CPI =	-0.44885D 00	-0.44885D 00	-0.44883D 00	-0.44897D 00
CPI/SQRT((L-C)/C) =	0.63070D 00	0.63070D 00	0.63068D 00	0.63056D 00
A(M)/CPI M=ODD				
A(1)/CPI =	-0.30634D 00	-0.30634D 00	-0.30634D 00	-0.30634D 00
A(3)/CPI =	0.74481D-02	0.74483D-02	0.74493D-02	0.74563D-02
A(5)/CPI =	0.68185D-01	0.68186D-01	0.68188D-01	0.68203D-01
A(7)/CPI =	0.65025D-01	0.65025D-01	0.65027D-01	0.65041D-01
A(9)/CPI =	-0.90222D-01	-0.90222D-01	-0.90224D-01	-0.90236D-01
A(11)/CPI =	0.37430D-01	0.37430D-01	0.37431D-01	0.37439D-01
A(13)/CPI =	-0.90847D-02	-0.90847D-02	-0.90847D-02	-0.90862D-02
A(15)/CPI =	0.12636D-02	0.12636D-02	0.12639D-02	0.12688D-02
A(17)/CPI =	-0.23315D-03	-0.23311D-03	-0.23293D-03	-0.52105D-03
A(19)/CPI =	-0.40339D-04	-0.40302D-04	-0.40158D-04	-0.21524D-03
A(21)/CPI =	-0.39252D-04	-0.39218D-04	-0.39143D-04	
A(23)/CPI =	-0.28360D-04	-0.28331D-04	-0.28394D-04	
A(25)/CPI =	-0.21637D-04	-0.21612D-04	-0.21923D-04	
A(27)/CPI =	-0.16863D-04	-0.16847D-04	-0.12093D-03	
A(29)/CPI =	-0.13406D-04	-0.13401D-04	-0.93390D-04	
A(31)/CPI =	-0.10839D-04	-0.10854D-04		
A(33)/CPI =	-0.88927D-05	-0.89485D-05		
A(35)/CPI =	-0.73908D-05	-0.75398D-05		
A(37)/CPI =	-0.62146D-05	-0.60467D-04		
A(39)/CPI =	-0.52836D-05	-0.50525D-04		
A(41)/CPI =	-0.45448D-05			
A(43)/CPI =	-0.39737D-05			
A(45)/CPI =	-0.39828D-04			
A(47)/CPI =	-0.34464D-04			

Table 1

CT = 0.49800D 00

NO. OF COEFF. =	N = 24	N = 20	N = 15	N = 10
MAX. (Y/C)/CPI =	-0.27161D 03	-0.27178D 03	-0.27251D 03	-0.27687D 03
CPI/SQRT((L-C)/C) =	0.24021D-02	0.24004D-02	0.23937D-02	0.23541D-02

A(.M)/CPI M=ODD

A(1)/CPI =	-0.20939D 03	-0.20952D 03	-0.21006D 03	-0.21349D 03
A(3)/CPI =	0.60899D 02	0.60937D 02	0.61097D 02	0.62098D 02
A(5)/CPI =	-0.59880D 00	-0.59912D 00	-0.60050D 00	-0.60903D 00
A(7)/CPI =	0.10348D 01	0.10355D 01	0.10384D 01	0.10564D 01
A(9)/CPI =	0.47227D 00	0.47259D 00	0.47395D 00	0.48274D 00
A(11)/CPI =	0.26538D 00	0.26557D 00	0.26638D 00	0.27184D 00
A(13)/CPI =	0.16303D 00	0.16315D 00	0.16368D 00	0.16769D 00
A(15)/CPI =	0.10710D 00	0.10719D 00	0.10758D 00	0.11125D 00
A(17)/CPI =	0.74054D-01	0.74120D-01	0.74429D-01	0.38352D 00
A(19)/CPI =	0.53299D-01	0.53351D-01	0.53618D-01	0.27070D 00
A(21)/CPI =	0.39620D-01	0.39665D-01	0.39918D-01	
A(23)/CPI =	0.30245D-01	0.30285D-01	0.30557D-01	
A(25)/CPI =	0.23607D-01	0.23645D-01	0.24000D-01	
A(27)/CPI =	0.18777D-01	0.18814D-01	0.14215D 00	
A(29)/CPI =	0.15180D-01	0.15219D-01	0.11400D 00	
A(31)/CPI =	0.12446D-01	0.12490D-01		
A(33)/CPI =	0.10332D-01	0.10386D-01		
A(35)/CPI =	0.86720D-02	0.87541D-02		
A(37)/CPI =	0.73509D-02	0.73643D-01		
A(39)/CPI =	0.62874D-02	0.62666D-01		
A(41)/CPI =	0.54239D-02			
A(43)/CPI =	0.47221D-02			
A(45)/CPI =	0.49145D-01			
A(47)/CPI =	0.43032D-01			

Table 2

CT =	0.49850D 00			
NO. OF COEFF. =	N = 24	N = 20	N = 15	N = 10
MAX. (Y/C)/CPI =	0.50811D 04	0.50227D 04	0.47926D 04	0.37351D 04
CPI/SQRT((L-C)/C) =	0.12840D-03	0.12988D-03	0.13610D-03	0.17450D-03

A(M)/CPI M=ODD

A(1)/CPI =	0.39177D 04	0.38727D 04	0.36950D 04	0.28805D 04
A(3)/CPI =	-0.11389D 04	-0.11258D 04	-0.10741D 04	-0.83742D 03
A(5)/CPI =	0.10961D 02	0.10834D 02	0.10334D 02	0.80388D 01
A(7)/CPI =	-0.19378D 02	-0.19156D 02	-0.18279D 02	-0.14265D 02
A(9)/CPI =	-0.88463D 01	-0.87454D 01	-0.83461D 01	-0.65207D 01
A(11)/CPI =	-0.49706D 01	-0.49140D 01	-0.46904D 01	-0.36716D 01
A(13)/CPI =	-0.30533D 01	-0.30187D 01	-0.28821D 01	-0.22647D 01
A(15)/CPI =	-0.20059D 01	-0.19833D 01	-0.18942D 01	-0.15024D 01
A(17)/CPI =	-0.13869D 01	-0.13714D 01	-0.13104D 01	-0.51794D 01
A(19)/CPI =	-0.99818D 00	-0.98709D 00	-0.94403D 00	-0.36558D 01
A(21)/CPI =	-0.74200D 00	-0.73368D 00	-0.70281D 00	
A(23)/CPI =	-0.56642D 00	-0.56031D 00	-0.53798D 00	
A(25)/CPI =	-0.44211D 00	-0.43745D 00	-0.42253D 00	
A(27)/CPI =	-0.35165D 00	-0.34809D 00	-0.25027D 01	
A(29)/CPI =	-0.28428D 00	-0.28156D 00	-0.20071D 01	
A(31)/CPI =	-0.23309D 00	-0.23107D 00		
A(33)/CPI =	-0.19349D 00	-0.19216D 00		
A(35)/CPI =	-0.16240D 00	-0.16196D 00		
A(37)/CPI =	-0.13766D 00	-0.13625D 01		
A(39)/CPI =	-0.11775D 00	-0.11594D 01		
A(41)/CPI =	-0.10158D 00			
A(43)/CPI =	-0.88431D-01			
A(45)/CPI =	-0.92035D 00			
A(47)/CPI =	-0.80587D 00			

Table 3

CT = 0.50000D 00

NO. OF COEFF. =	N = 25	N = 20	N = 15	N = 10
MAX. (Y/C)/CPI =	0.84499D 02	0.84477D 02	0.84416D 02	0.83972D 02
CPI/SQRT((L-C)/C) =	0.77198D-02	0.77207D-02	0.77256D-02	0.77604D-02

A(M)/CPI M=ODD

A(1)/CPI =	0.65181D 02	0.65167D 02	0.65114D 02	0.64790D 02
A(3)/CPI =	-0.18919D 02	-0.18925D 02	-0.18900D 02	-0.18807D 02
A(5)/CPI =	0.17035D 00	0.17029D 00	0.17010D 00	0.16887D 00
A(7)/CPI =	-0.32318D 00	-0.32312D 00	-0.32291D 00	-0.32164D 00
A(9)/CPI =	-0.14769D 00	-0.14766D 00	-0.14758D 00	-0.14714D 00
A(11)/CPI =	-0.82958D-01	-0.82948D-01	-0.82916D-01	-0.82842D-01
A(13)/CPI =	-0.50953D-01	-0.50949D-01	-0.50942D-01	-0.51092D-01
A(15)/CPI =	-0.33471D-01	-0.33471D-01	-0.33478D-01	-0.33890D-01
A(17)/CPI =	-0.23141D-01	-0.23143D-01	-0.23160D-01	-0.11682D 00
A(19)/CPI =	-0.16654D-01	-0.16657D-01	-0.16683D-01	-0.82463D-01
A(21)/CPI =	-0.12379D-01	-0.12383D-01	-0.12420D-01	
A(23)/CPI =	-0.94496D-02	-0.94548D-02	-0.95068D-02	
A(25)/CPI =	-0.73754D-02	-0.73815D-02	-0.74664D-02	
A(27)/CPI =	-0.58661D-02	-0.58734D-02	-0.44225D-01	
A(29)/CPI =	-0.47420D-02	-0.47509D-02	-0.35468D-01	
A(31)/CPI =	-0.38877D-02	-0.38989D-02		
A(33)/CPI =	-0.32270D-02	-0.32423D-02		
A(35)/CPI =	-0.27081D-02	-0.27326D-02		
A(37)/CPI =	-0.22951D-02	-0.22988D-01		
A(39)/CPI =	-0.19623D-02	-0.19562D-01		
A(41)/CPI =	-0.16915D-02			
A(43)/CPI =	-0.14694D-02			
A(45)/CPI =	-0.12873D-02			
A(47)/CPI =	-0.14040D-01			
A(49)/CPI =	-0.12363D-01			

Table 4

CT = 0.10000D 01

NO. OF COEFF. =	N = 25	N = 20	N = 15	N = 10
MAX. (Y/C)/CPI =	0.25190D 00	0.25189D 00	0.25192D 00	0.25181D 00
CPI/SQRT((L-C)/C) =	0.25072D 01	0.25067D 01	0.25058D 01	0.25034D 01
A(M)/CPI M=ODD				
A(1)/CPI =	0.20625D 00	0.20625D 00	0.20625D 00	0.20625D 00
A(3)/CPI =	-0.48390D-01	-0.48390D-01	-0.48390D-01	-0.48391D-01
A(5)/CPI =	-0.37839D-02	-0.37839D-02	-0.37840D-02	-0.37846D-02
A(7)/CPI =	-0.14999D-02	-0.14999D-02	-0.15000D-02	-0.15005D-02
A(9)/CPI =	-0.70011D-03	-0.70013D-03	-0.70018D-03	-0.70067D-03
A(11)/CPI =	-0.38246D-03	-0.38247D-03	-0.38252D-03	-0.38306D-03
A(13)/CPI =	-0.23147D-03	-0.23148D-03	-0.23153D-03	-0.23221D-03
A(15)/CPI =	-0.15063D-03	-0.15065D-03	-0.15070D-03	-0.15176D-03
A(17)/CPI =	-0.10348D-03	-0.10349D-03	-0.10355D-03	-0.51911D-03
A(19)/CPI =	-0.74132D-04	-0.74143D-04	-0.74209D-04	-0.36899D-03
A(21)/CPI =	-0.54916D-04	-0.54927D-04	-0.55008D-04	
A(23)/CPI =	-0.41809D-04	-0.41821D-04	-0.41930D-04	
A(25)/CPI =	-0.32564D-04	-0.32577D-04	-0.32752D-04	
A(27)/CPI =	-0.25856D-04	-0.25871D-04	-0.19420D-03	
A(29)/CPI =	-0.20872D-04	-0.20890D-04	-0.15623D-03	
A(31)/CPI =	-0.17091D-04	-0.17113D-04		
A(33)/CPI =	-0.14172D-04	-0.14202D-04		
A(35)/CPI =	-0.11882D-04	-0.11932D-04		
A(37)/CPI =	-0.10060D-04	-0.10062D-03		
A(39)/CPI =	-0.85939D-05	-0.85774D-04		
A(41)/CPI =	-0.74005D-05			
A(43)/CPI =	-0.64206D-05			
A(45)/CPI =	-0.56123D-05			
A(47)/CPI =	-0.61373D-04			
A(49)/CPI =	-0.54101D-04			

Table 5

CT = 0.50000D 01

NO. OF COEFF. =	N = 25	N = 20	N = 15	N = 10
MAX. (Y/C)/CPI =	0.27814D-01	0.27814D-01	0.27818D-01	0.27803D-01
CPI/SQRT((L-C)/C) =	0.22138D 02	0.22132D 02	0.22120D 02	0.22090D 02

A(M)/CPI M=ODD

A(1)/CPI =	0.23468D-01	0.23468D-01	0.23468D-01	0.23468D-01
A(3)/CPI =	-0.48314D-02	-0.48314D-02	-0.48314D-02	-0.48314D-02
A(5)/CPI =	-0.63414D-03	-0.63414D-03	-0.63414D-03	-0.63411D-03
A(7)/CPI =	-0.21357D-03	-0.21357D-03	-0.21357D-03	-0.21355D-03
A(9)/CPI =	-0.97472D-04	-0.97471D-04	-0.97469D-04	-0.97455D-04
A(11)/CPI =	-0.52604D-04	-0.52604D-04	-0.52602D-04	-0.52590D-04
A(13)/CPI =	-0.31608D-04	-0.31607D-04	-0.31606D-04	-0.31597D-04
A(15)/CPI =	-0.20472D-04	-0.20472D-04	-0.20470D-04	-0.20469D-04
A(17)/CPI =	-0.14017D-04	-0.14016D-04	-0.14015D-04	-0.69840D-04
A(19)/CPI =	-0.10017D-04	-0.10017D-04	-0.10016D-04	-0.49906D-04
A(21)/CPI =	-0.74067D-05	-0.74066D-05	-0.74060D-05	
A(23)/CPI =	-0.56308D-05	-0.56307D-05	-0.56307D-05	
A(25)/CPI =	-0.43806D-05	-0.43804D-05	-0.43820D-05	
A(27)/CPI =	-0.34749D-05	-0.34748D-05	-0.26029D-04	
A(29)/CPI =	-0.28029D-05	-0.28028D-05	-0.20989D-04	
A(31)/CPI =	-0.22935D-05	-0.22936D-05		
A(33)/CPI =	-0.19006D-05	-0.19008D-05		
A(35)/CPI =	-0.15925D-05	-0.15932D-05		
A(37)/CPI =	-0.13476D-05	-0.13468D-04		
A(39)/CPI =	-0.11505D-05	-0.11495D-04		
A(41)/CPI =	-0.99010D-06			
A(43)/CPI =	-0.85822D-06			
A(45)/CPI =	-0.74892D-06			
A(47)/CPI =	-0.82087D-05			
A(49)/CPI =	-0.72422D-05			

Table 6

CT = 0.10000D 02

NO. OF COEFF. =	N = 25	N = 20	N = 15	N = 10
MAX. (Y/C)/CPI =	0.13166D-01	0.13166D-01	0.13168D-01	0.13161D-01
CPI/SQRT((L-C)/C) =	0.46629D 02	0.46616D 02	0.46590D 02	0.46524D 02

A(M)/CPI M=ODD

A(1)/CPI =	0.11143D-01	0.11143D-01	0.11143D-01	0.11143D-01
A(3)/CPI =	-0.22607D-02	-0.22607D-02	-0.22607D-02	-0.22607D-02
A(5)/CPI =	-0.31001D-03	-0.31001D-03	-0.31001D-03	-0.30999D-03
A(7)/CPI =	-0.10379D-03	-0.10379D-03	-0.10378D-03	-0.10377D-03
A(9)/CPI =	-0.47267D-04	-0.47267D-04	-0.47265D-04	-0.47253D-04
A(11)/CPI =	-0.25479D-04	-0.25479D-04	-0.25478D-04	-0.25467D-04
A(13)/CPI =	-0.15298D-04	-0.15298D-04	-0.15297D-04	-0.15287D-04
A(15)/CPI =	-0.99036D-05	-0.99034D-05	-0.99023D-05	-0.98932D-05
A(17)/CPI =	-0.67784D-05	-0.67782D-05	-0.67772D-05	-0.33750D-04
A(19)/CPI =	-0.48429D-05	-0.48427D-05	-0.48418D-05	-0.24132D-04
A(21)/CPI =	-0.35802D-05	-0.35800D-05	-0.35791D-05	
A(23)/CPI =	-0.27214D-05	-0.27212D-05	-0.27203D-05	
A(25)/CPI =	-0.21169D-05	-0.21167D-05	-0.21161D-05	
A(27)/CPI =	-0.16790D-05	-0.16789D-05	-0.12573D-04	
A(29)/CPI =	-0.13542D-05	-0.13540D-05	-0.10141D-04	
A(31)/CPI =	-0.11080D-05	-0.11079D-05		
A(33)/CPI =	-0.91810D-06	-0.91798D-06		
A(35)/CPI =	-0.76925D-06	-0.76923D-06		
A(37)/CPI =	-0.65092D-06	-0.65044D-05		
A(39)/CPI =	-0.55568D-06	-0.55527D-05		
A(41)/CPI =	-0.47815D-06			
A(43)/CPI =	-0.41442D-06			
A(45)/CPI =	-0.36156D-06			
A(47)/CPI =	-0.39642D-05			
A(49)/CPI =	-0.34978D-05			

Table 7

GENERAL ARRANGEMENT OF THE BLOWER WIND-TUNNEL

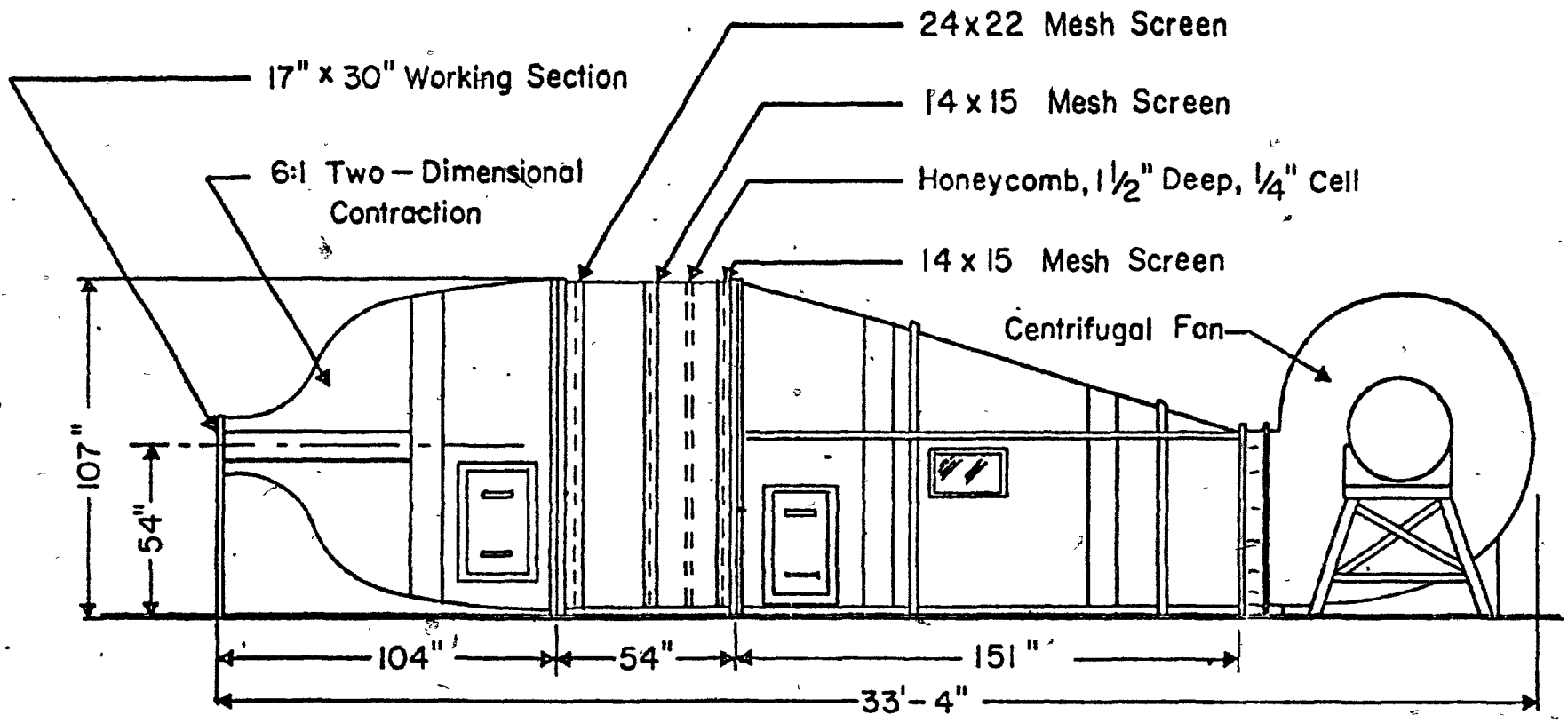

Fig. 1 General arrangement of the blower wind-tunnel

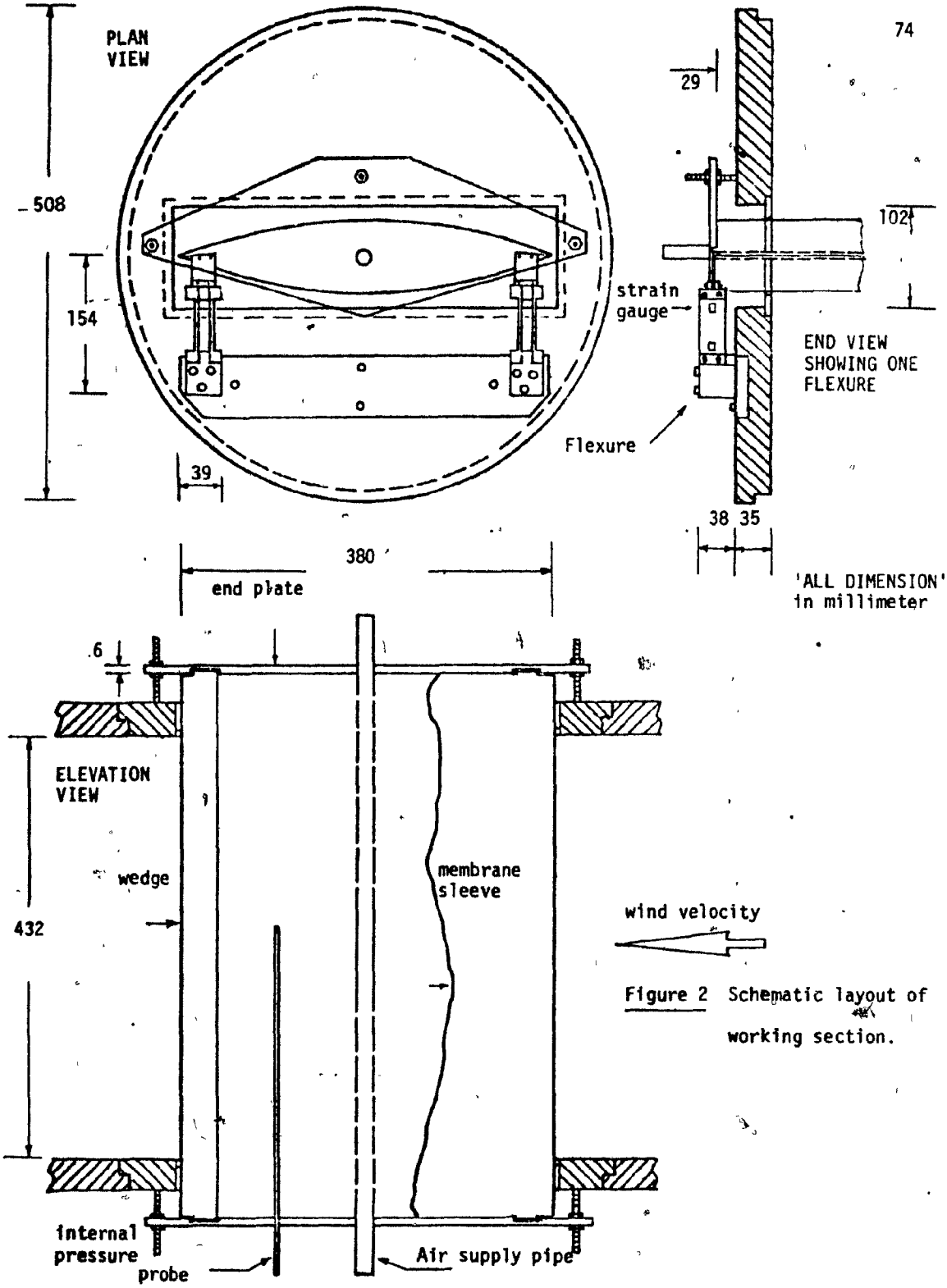

Figure 2 Schematic layout of working section.

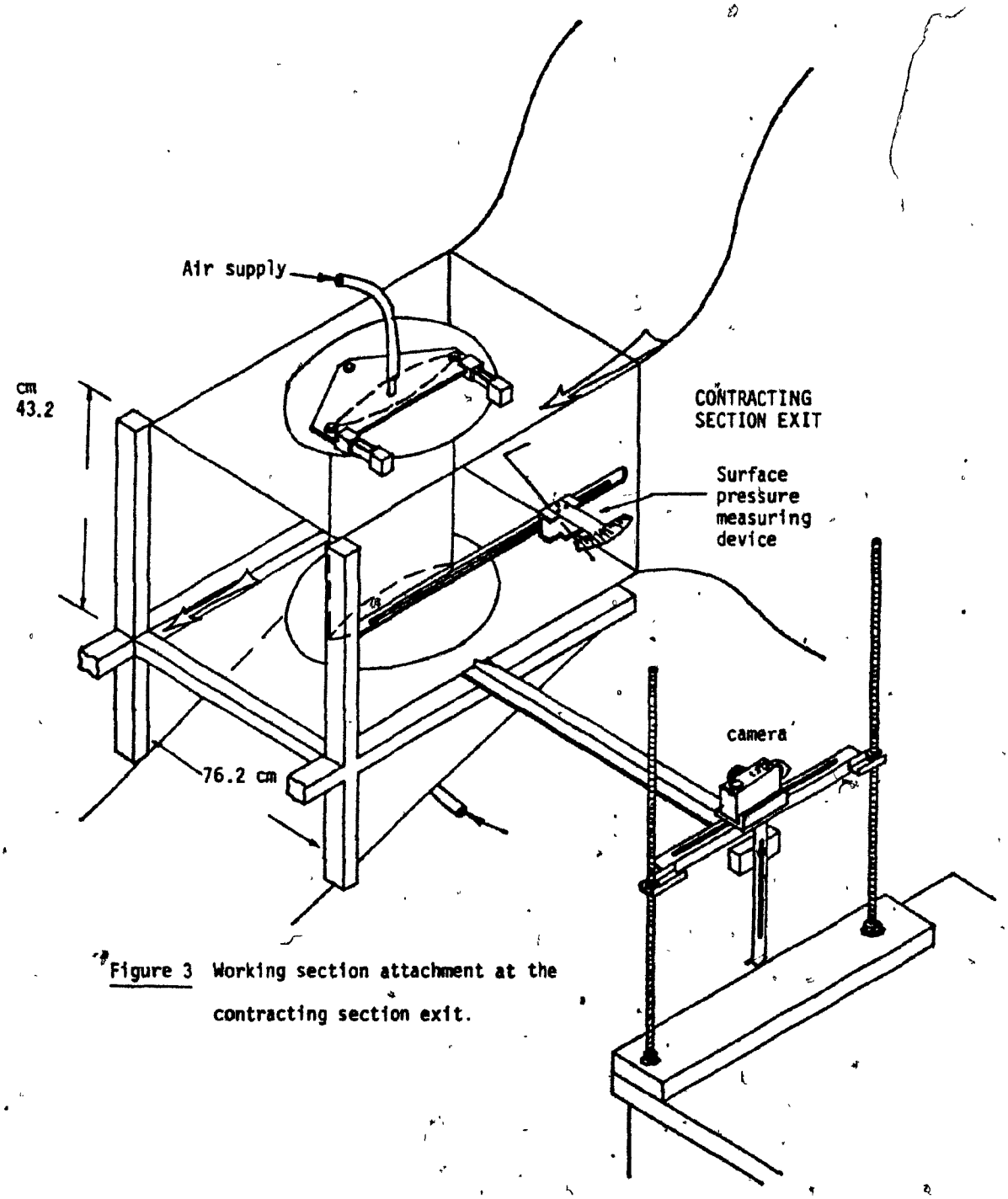

Figure 3 Working section attachment at the contracting section exit.

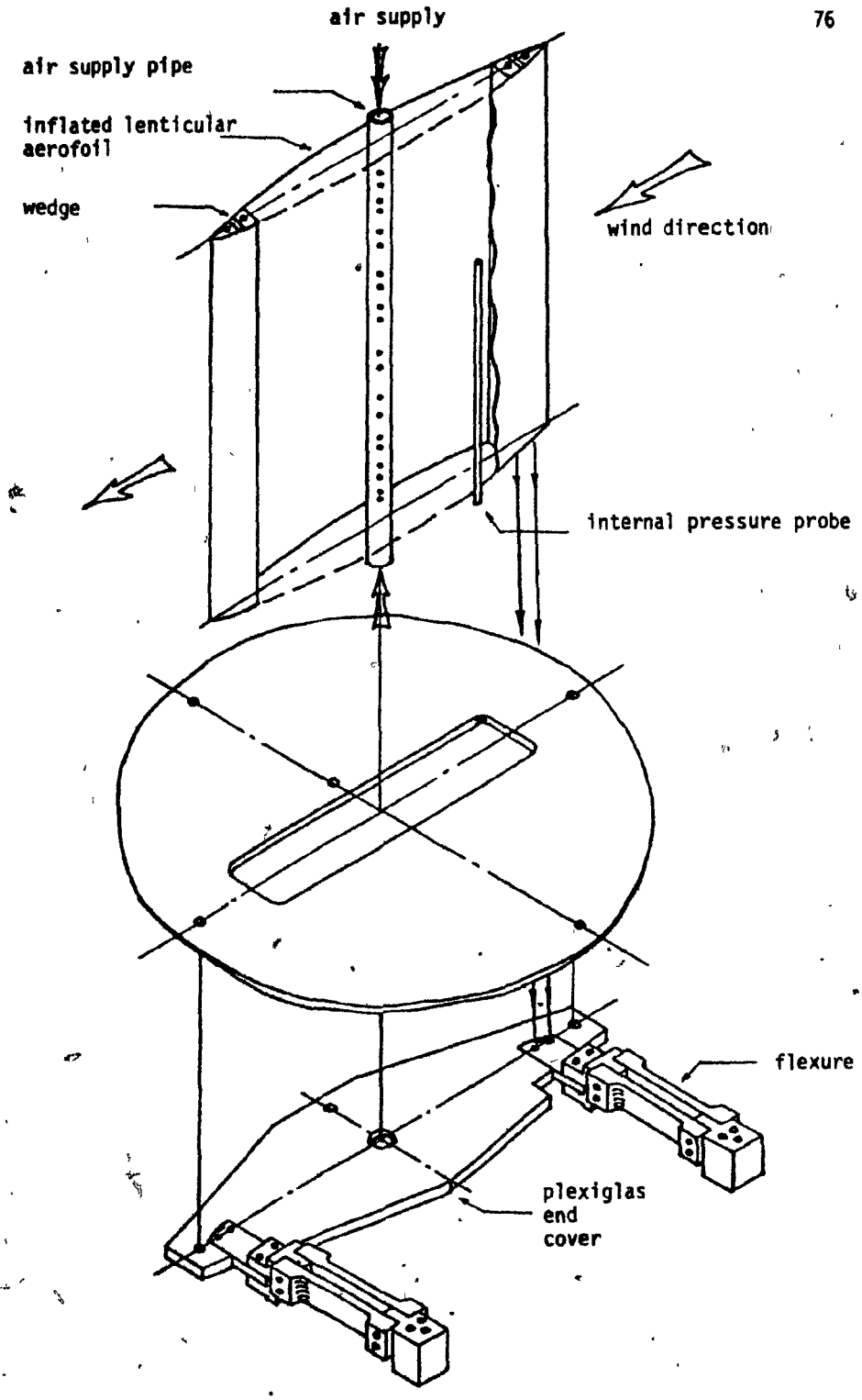

Figure 4 Design of inflated aerofoil.

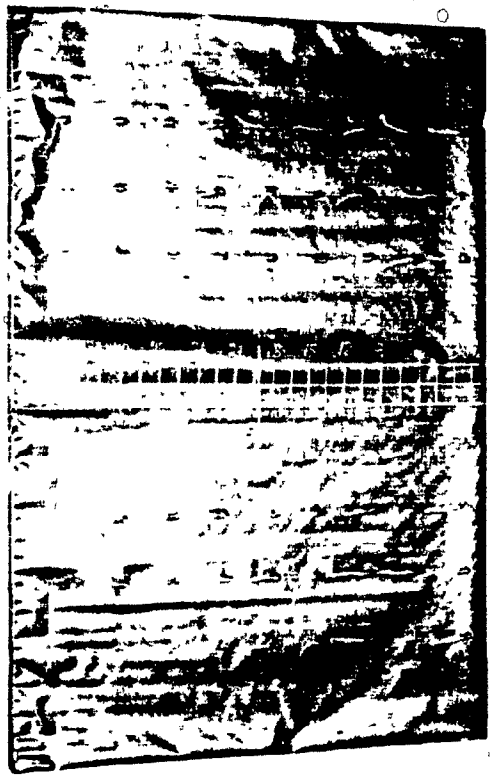

Figure 5a Envelope made of flexible impervious rip-stop nylon 25 g/m^2.

Figure 5b Configuration of wedges, air supply tube and static pressure tubes.

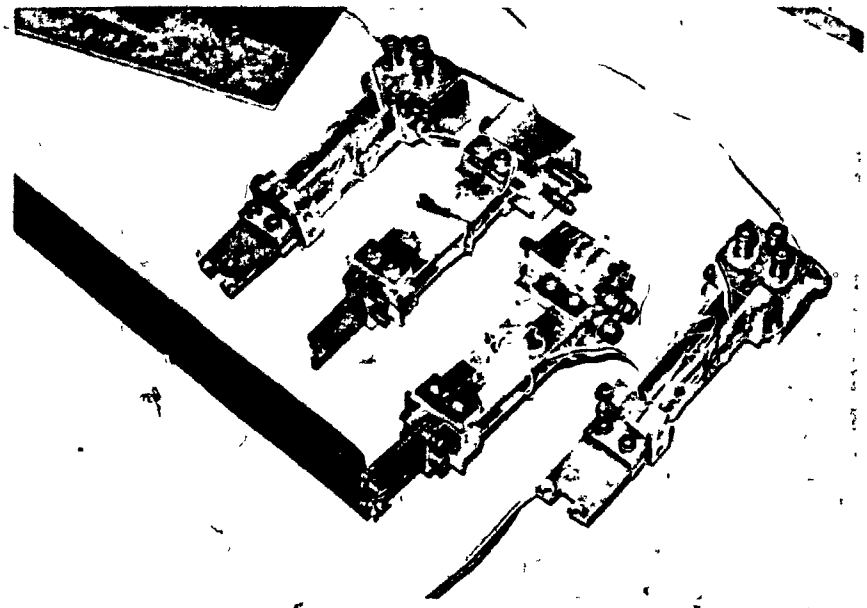

Figure 6 Flexures assembly. (Calibrated flexures, and attachment of wedge on flexure)

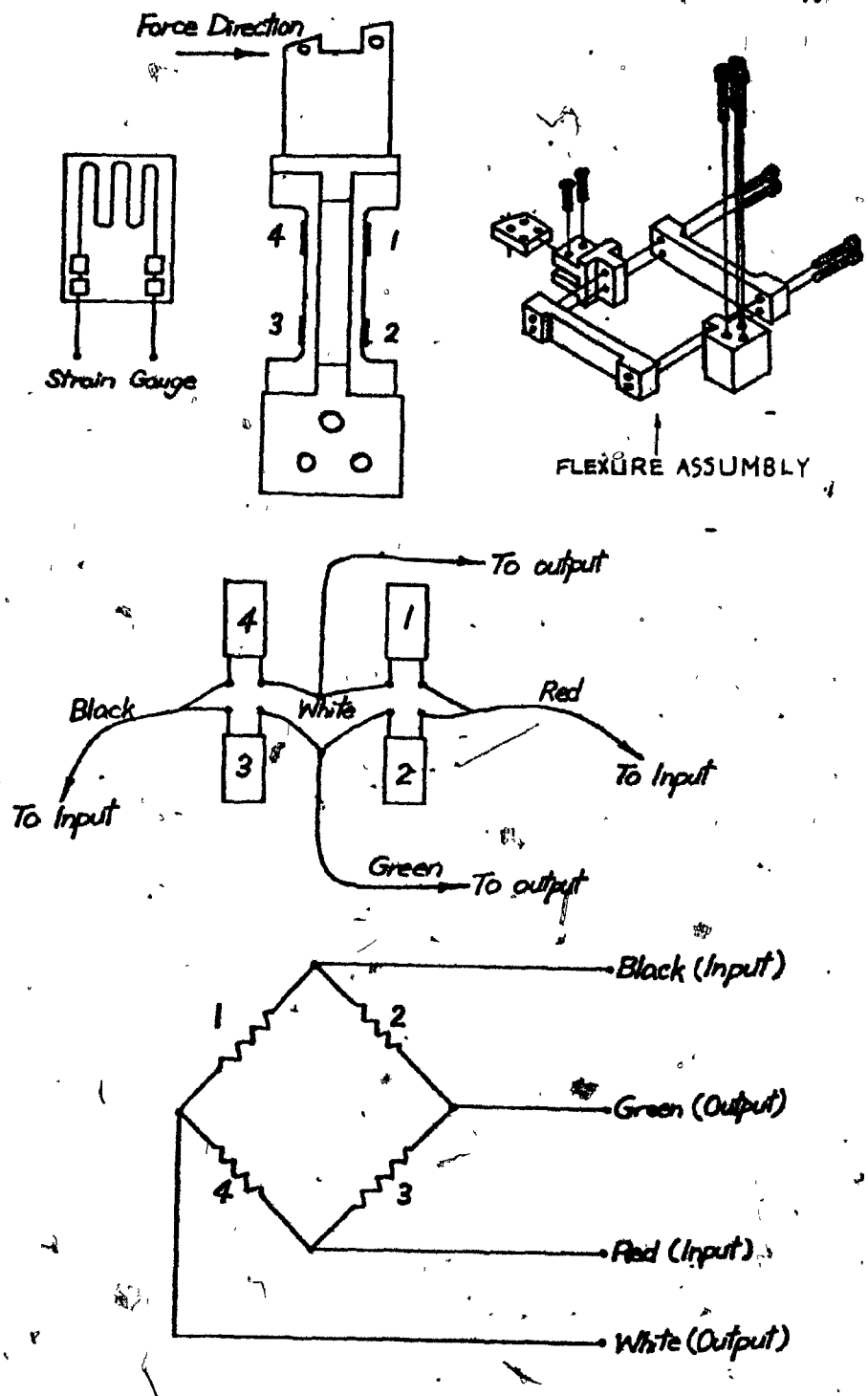

Figure 7 Schematic layout of strain gauges attachment on the flexures.

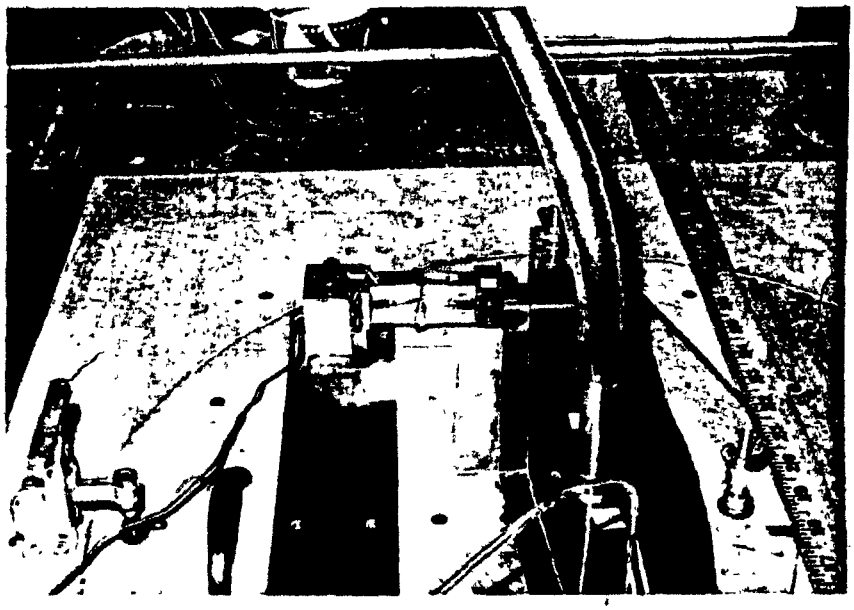

Figure 8 Flexure attachment on roof.

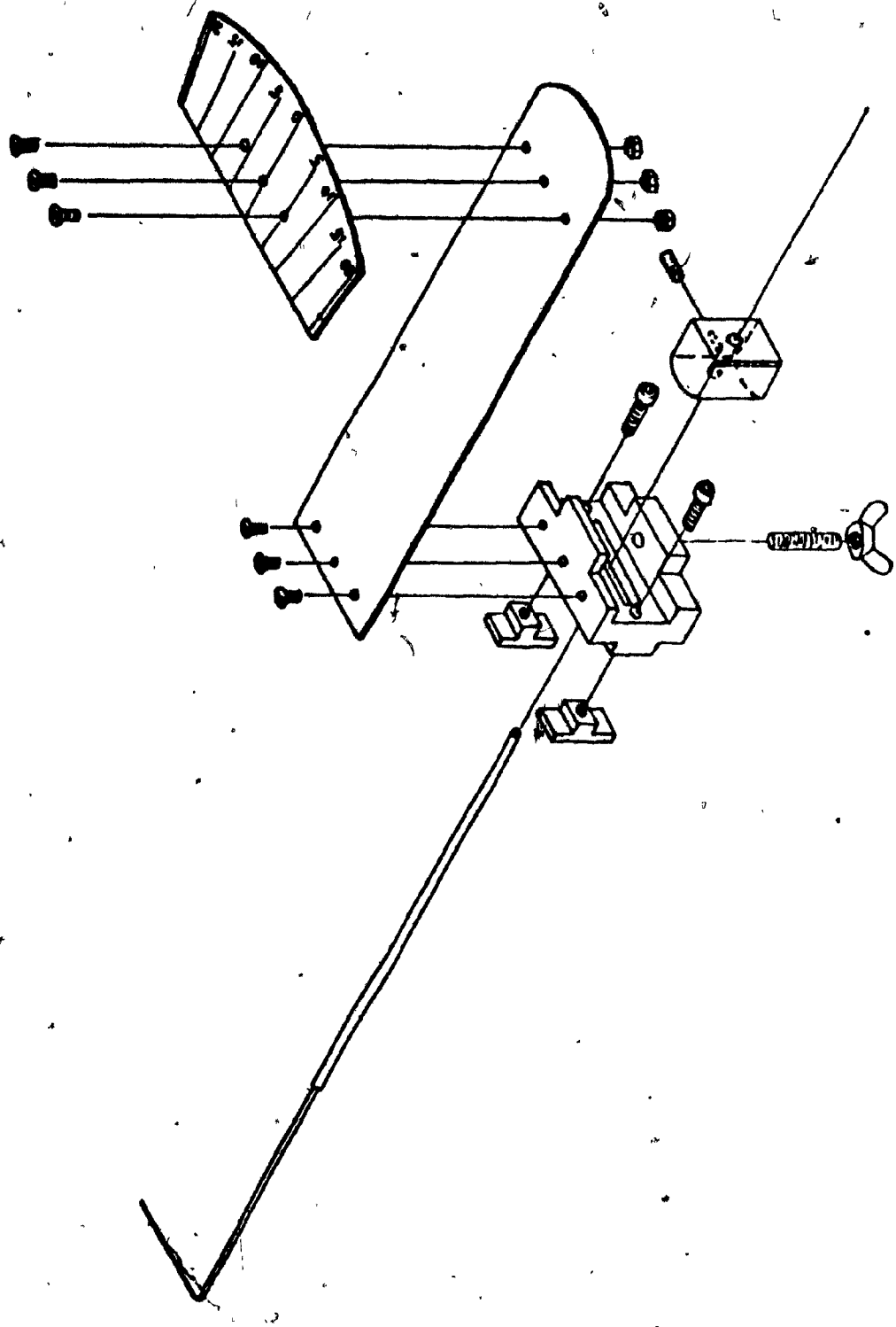

Figure 9A Surface static pressure measuring device.

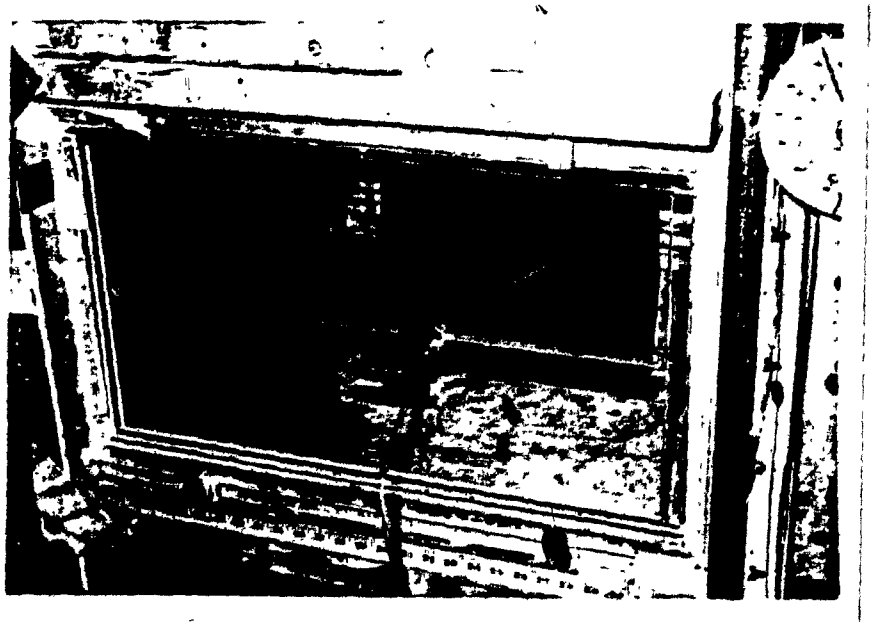

Figure 9B Surface static pressure measuring device.

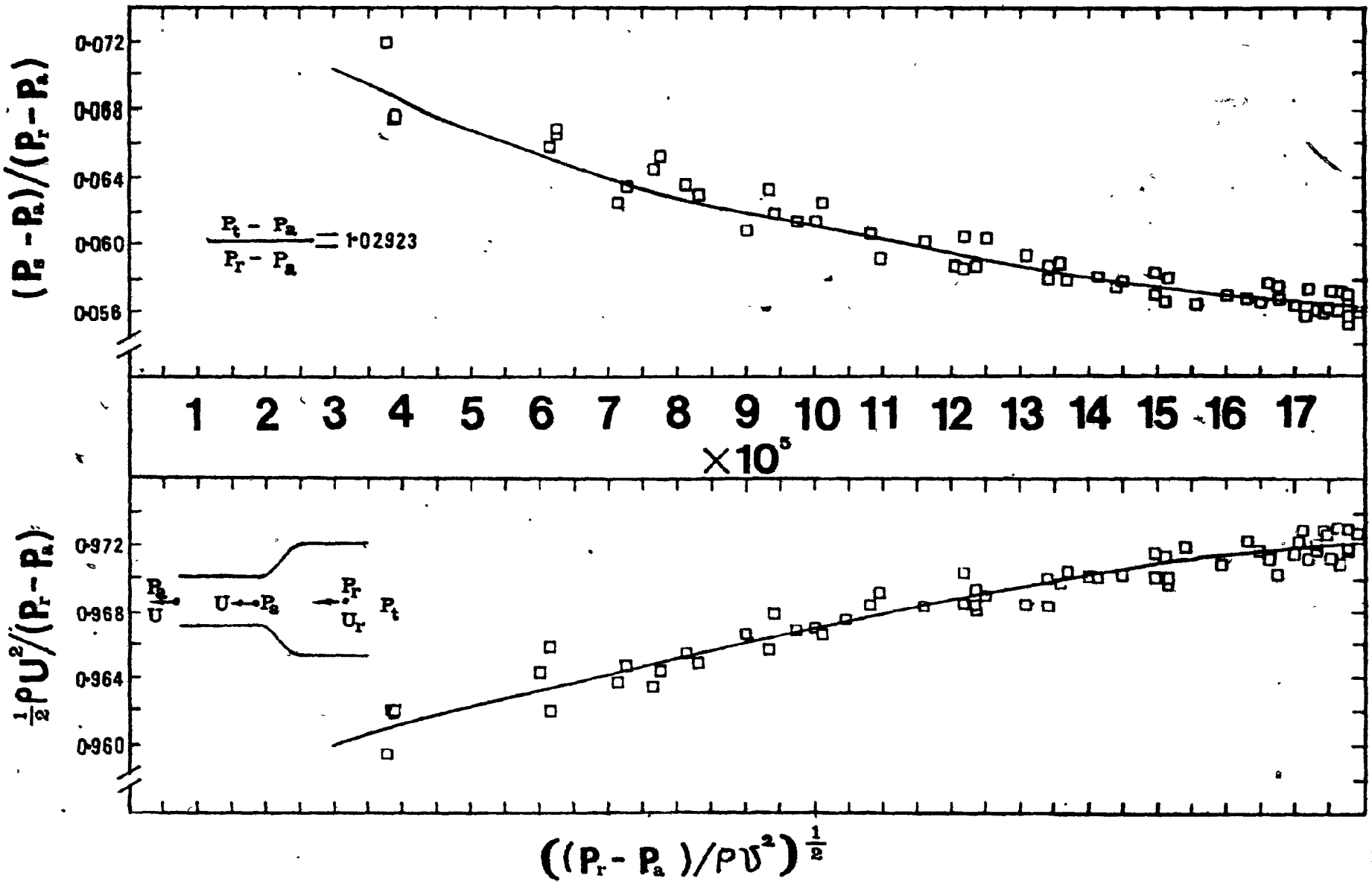

Figure 10 Wind tunnel calibration.

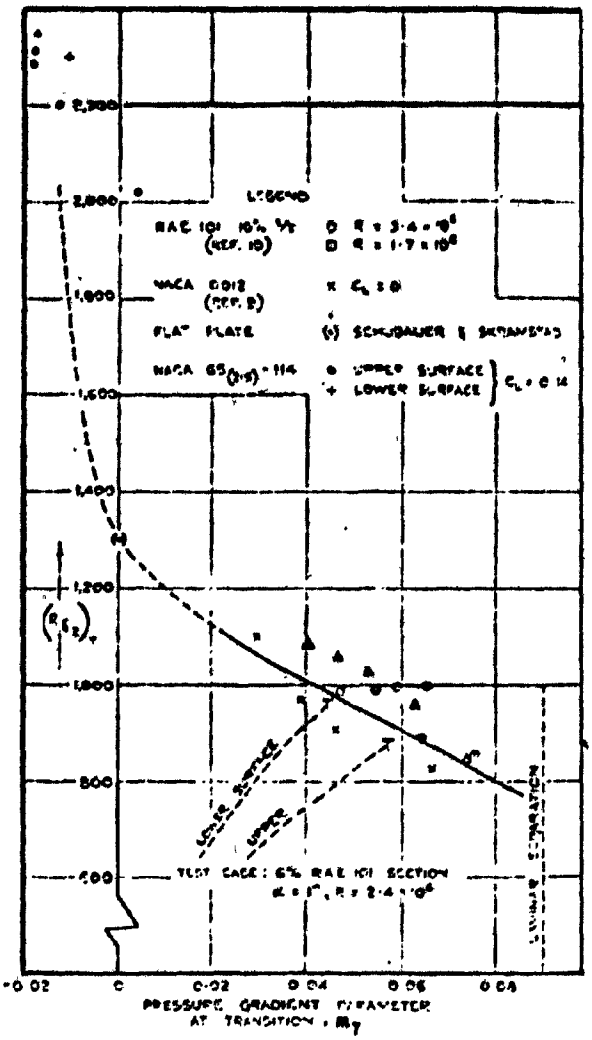

Figure 11 Boundary layer Reynolds number at transition plotted against the pressure gradient parameter.

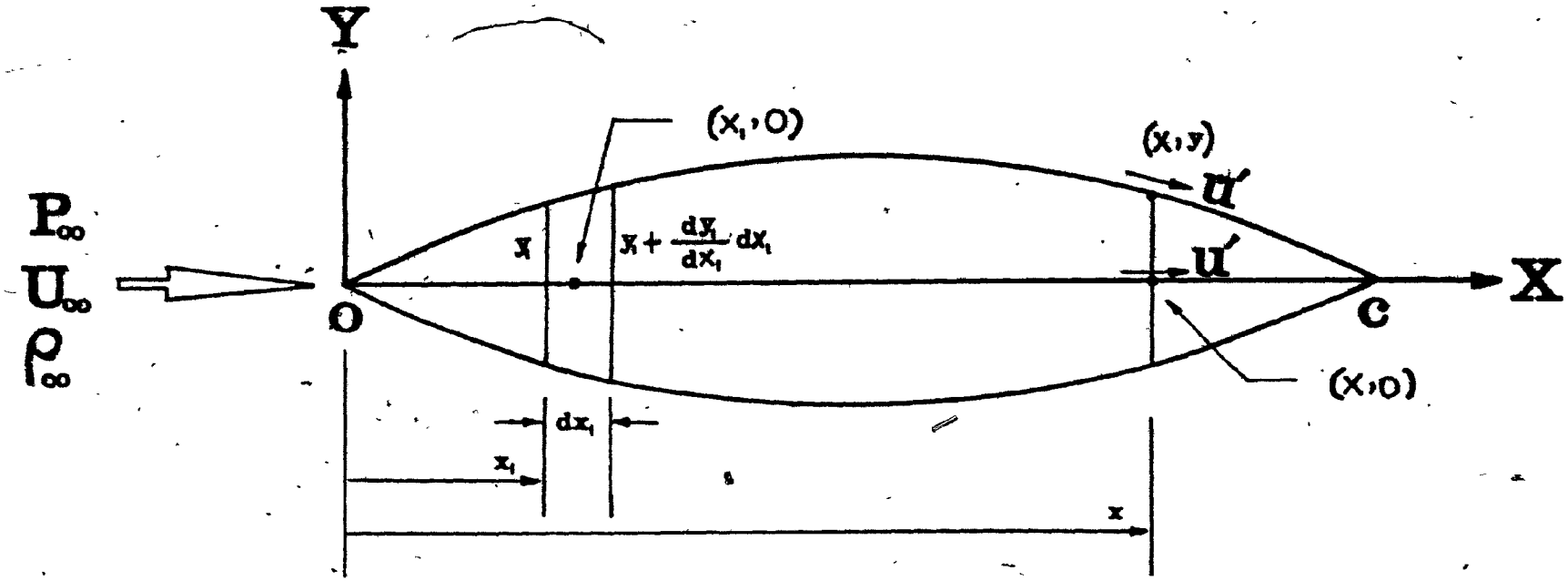

Figure 12 Inflated lenticular aerofoil at zero incidence.

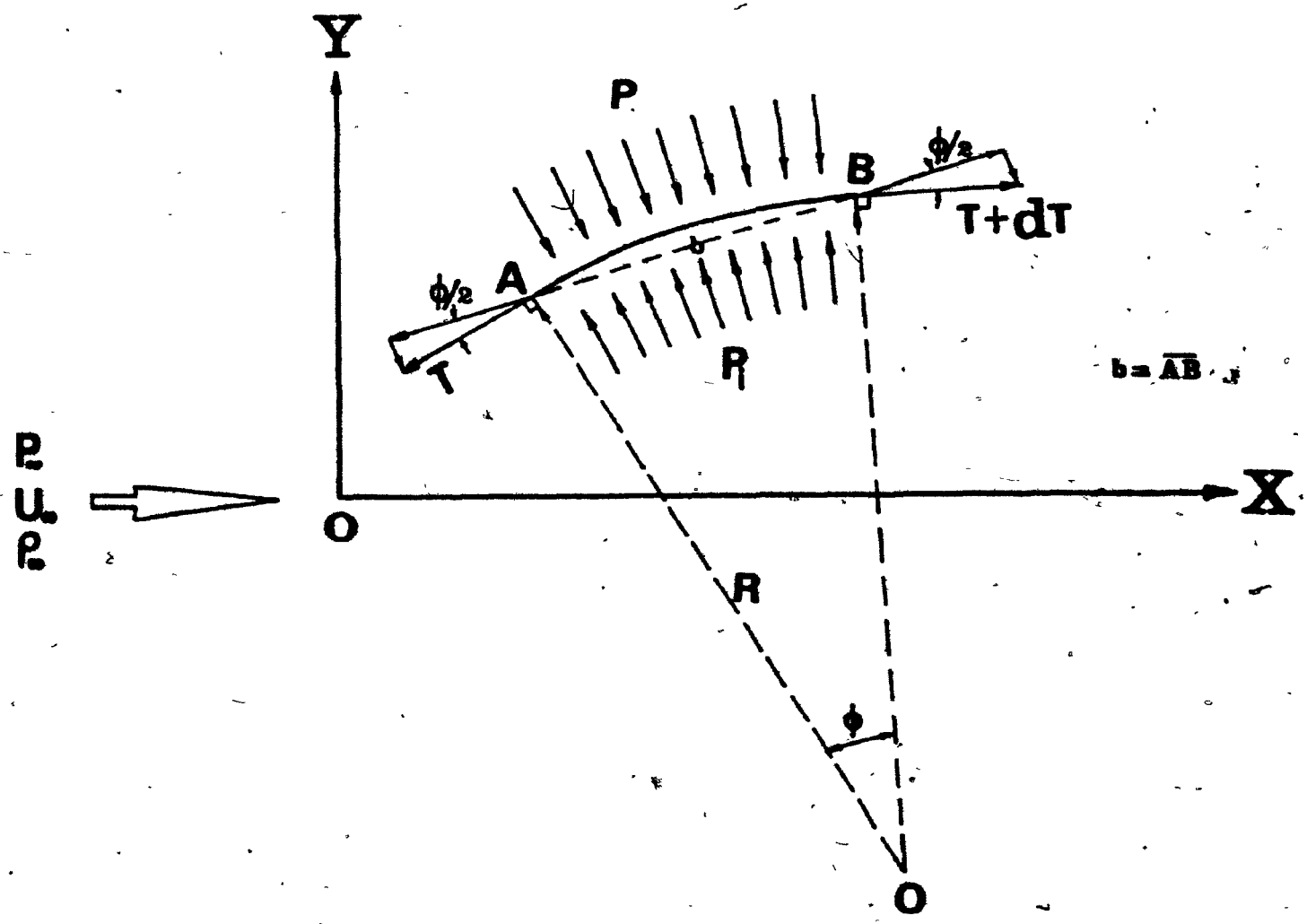

Figure 13 Force balance of the membrane element.

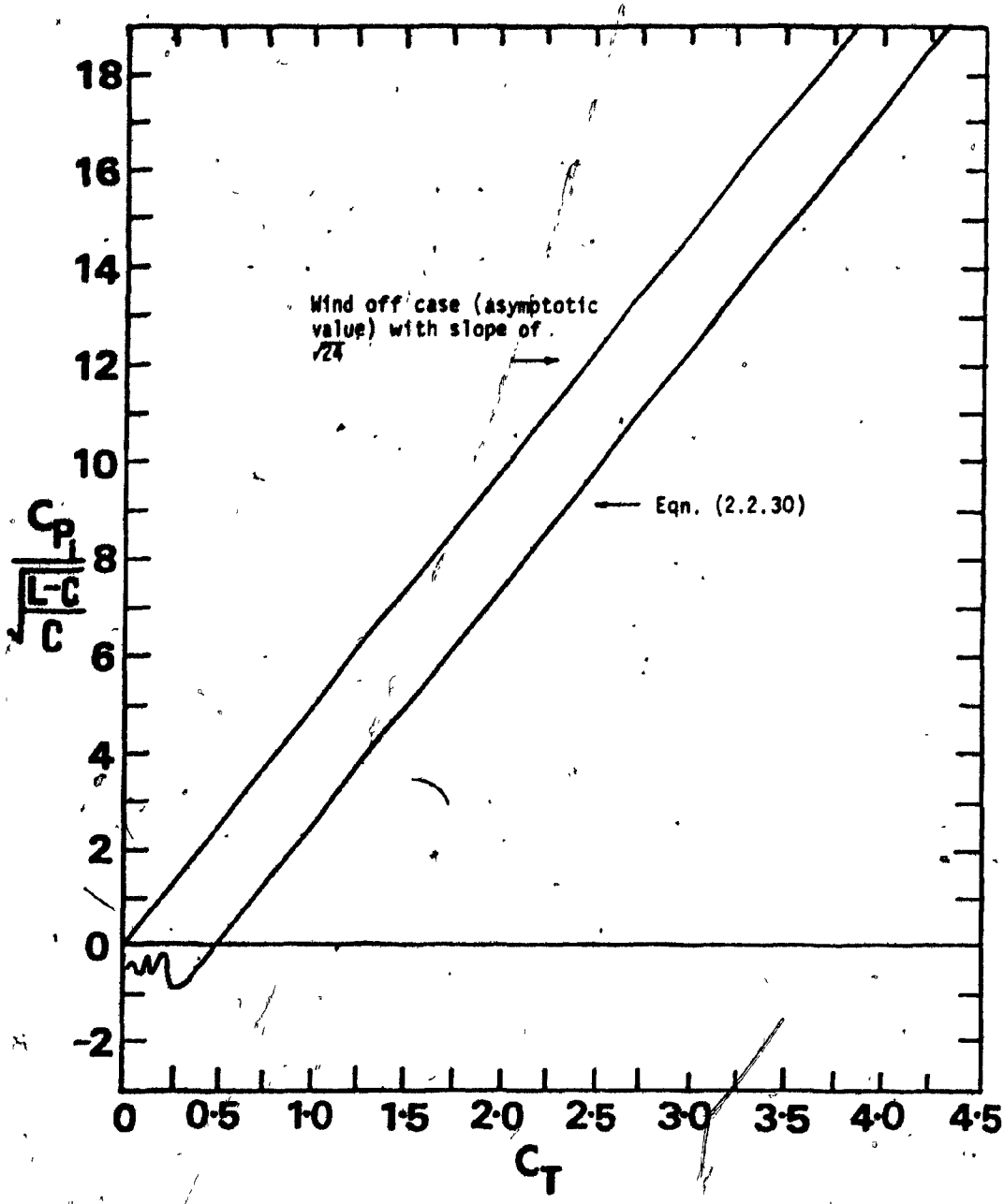

Figure 14 Normalized inflation pressure coefficient plotted against tension coefficient (Theory).

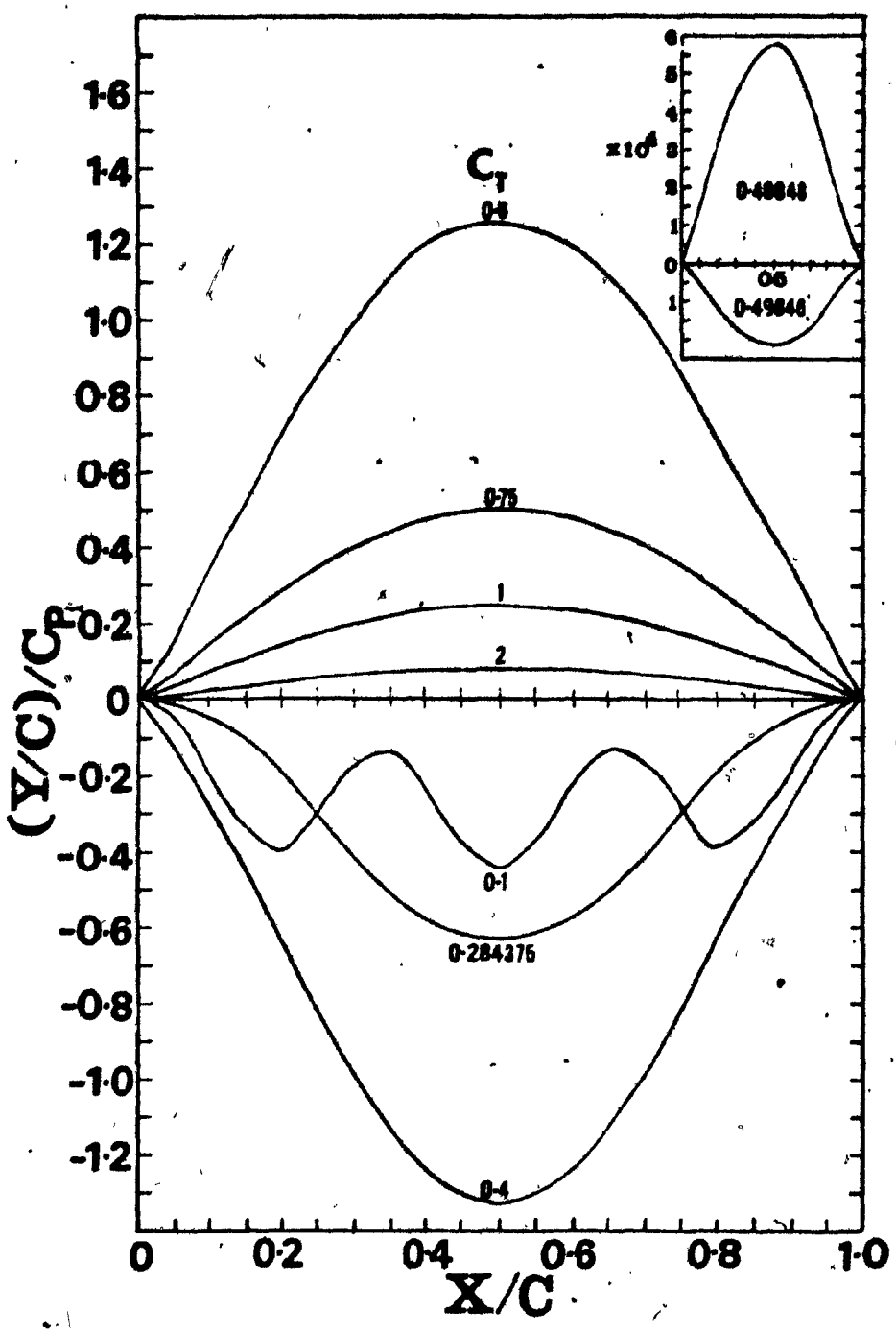

Figure 15 Theoretical membrane shapes for various C_T.

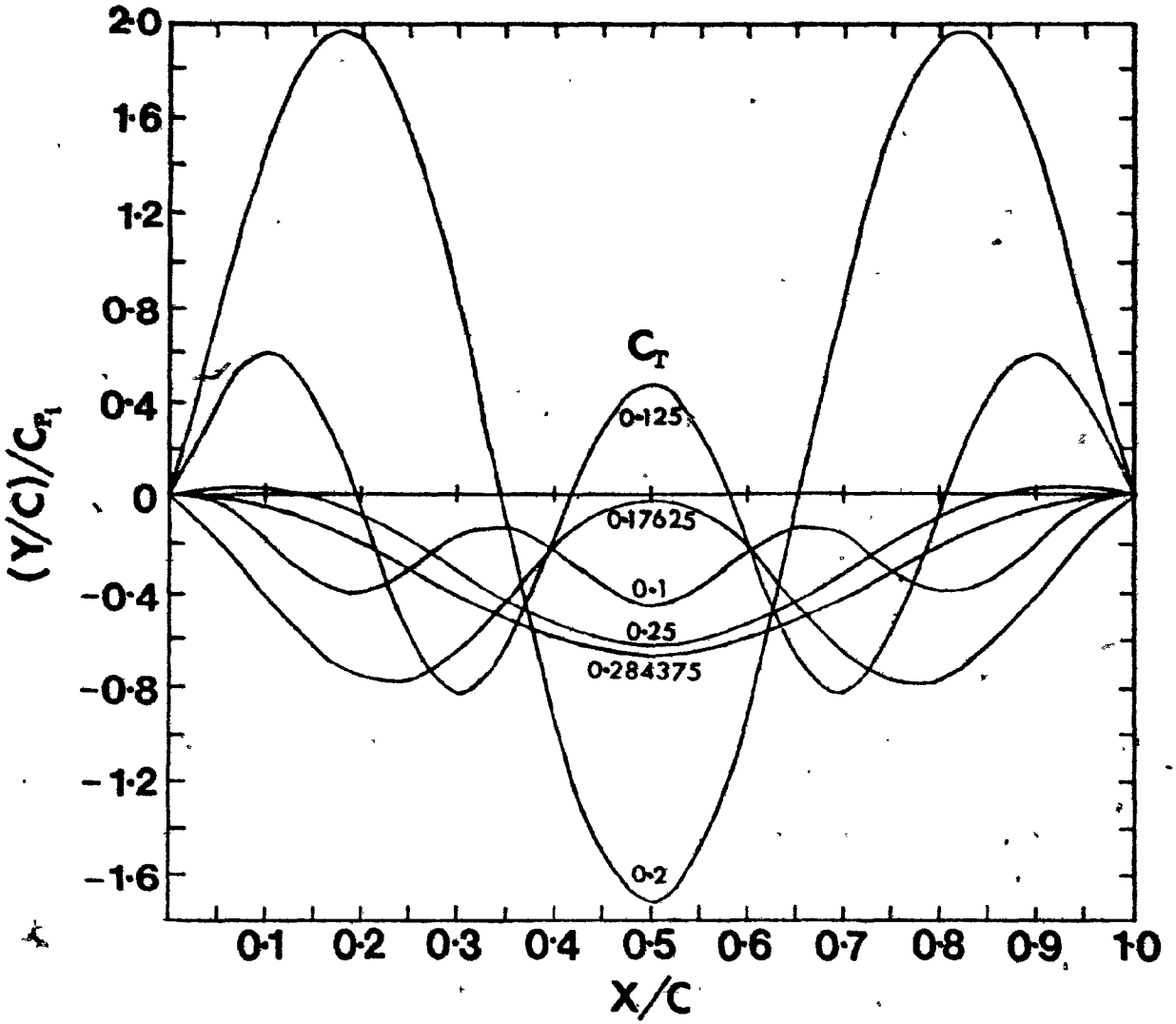

Figure 16 Theoretical membrane shapes for various C_T and negative Cp_i.

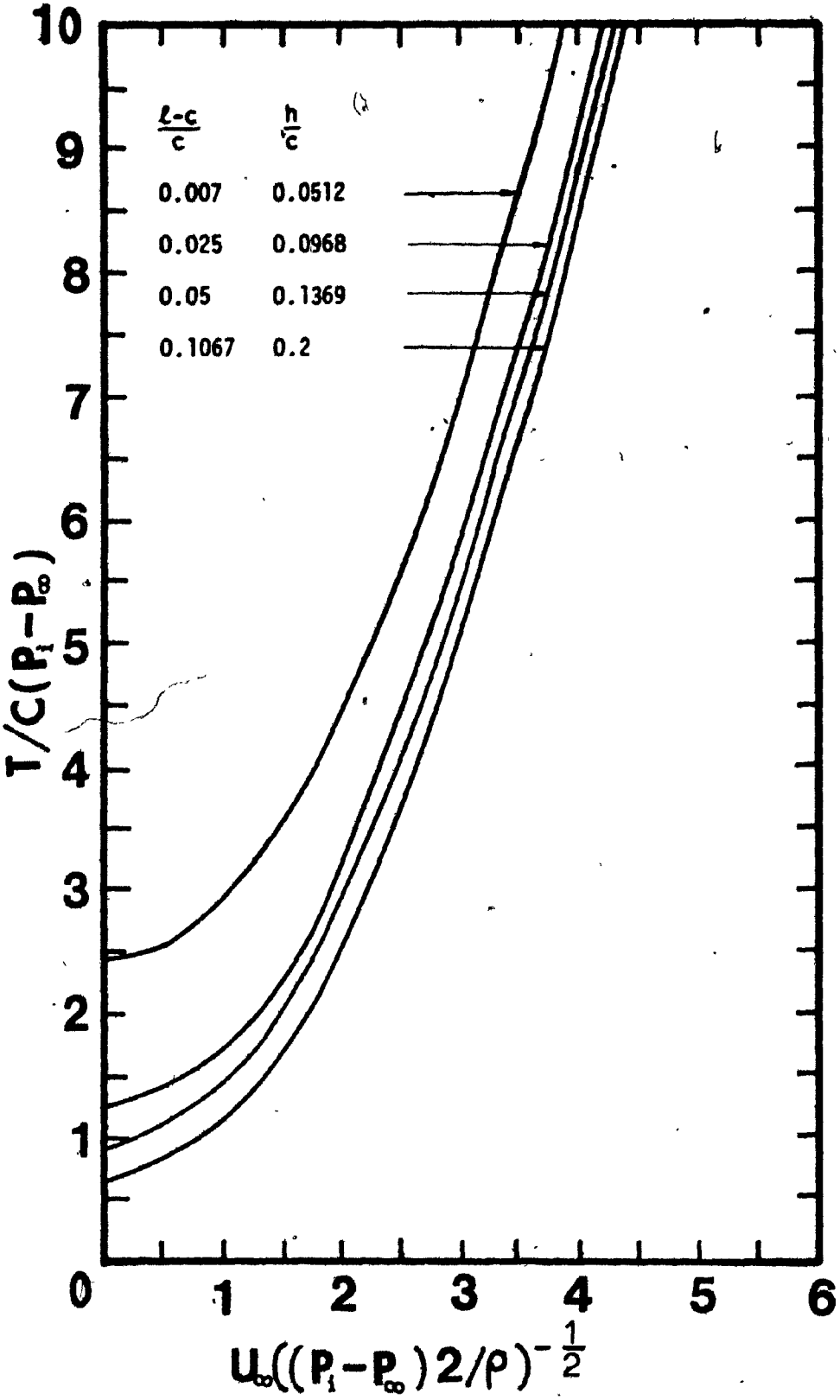

Figure 17 Induced tension as a function of flow velocity for different heights.

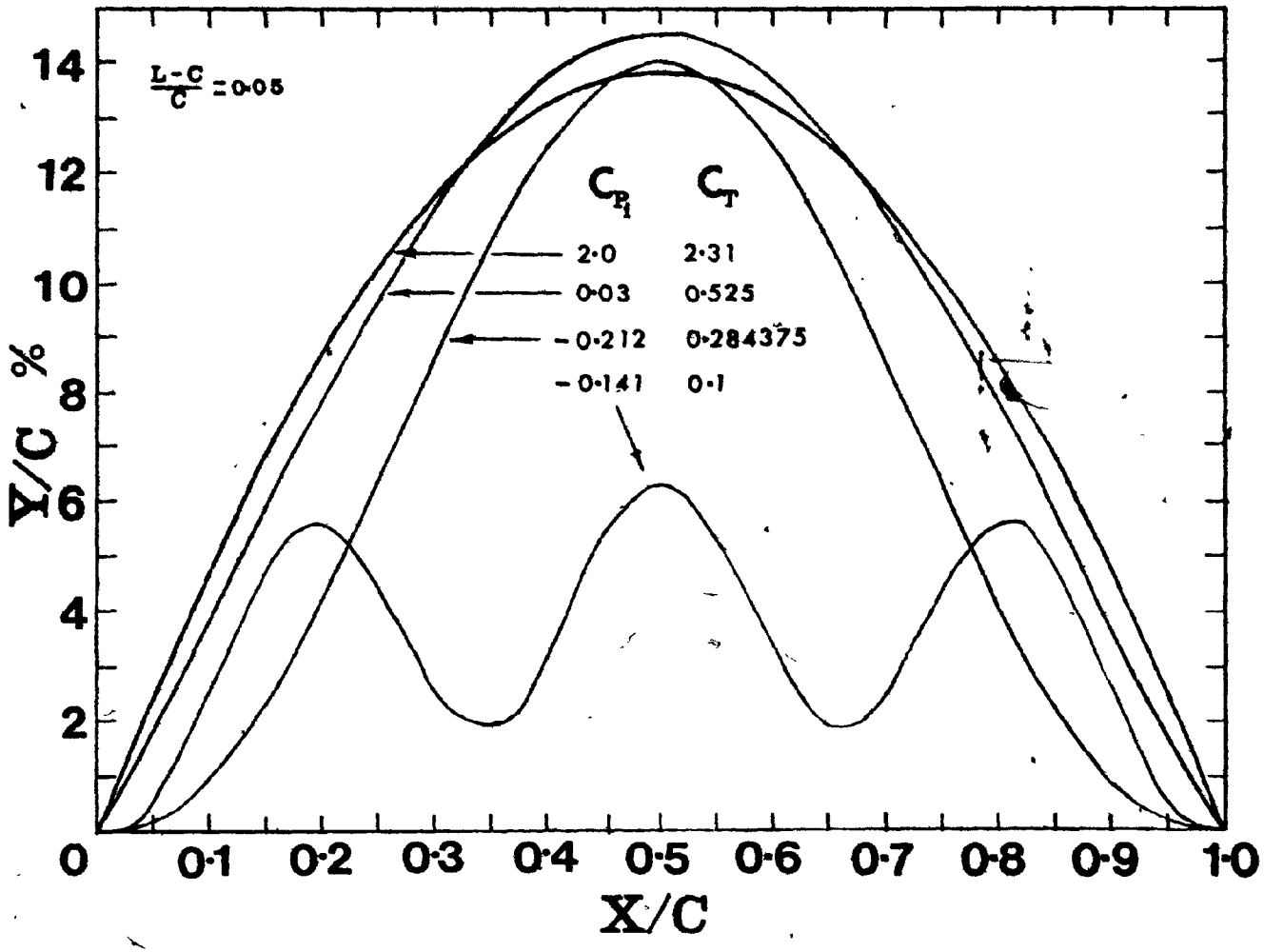

Figure 18 Theoretical membrane coordinates for a fixed membrane length.

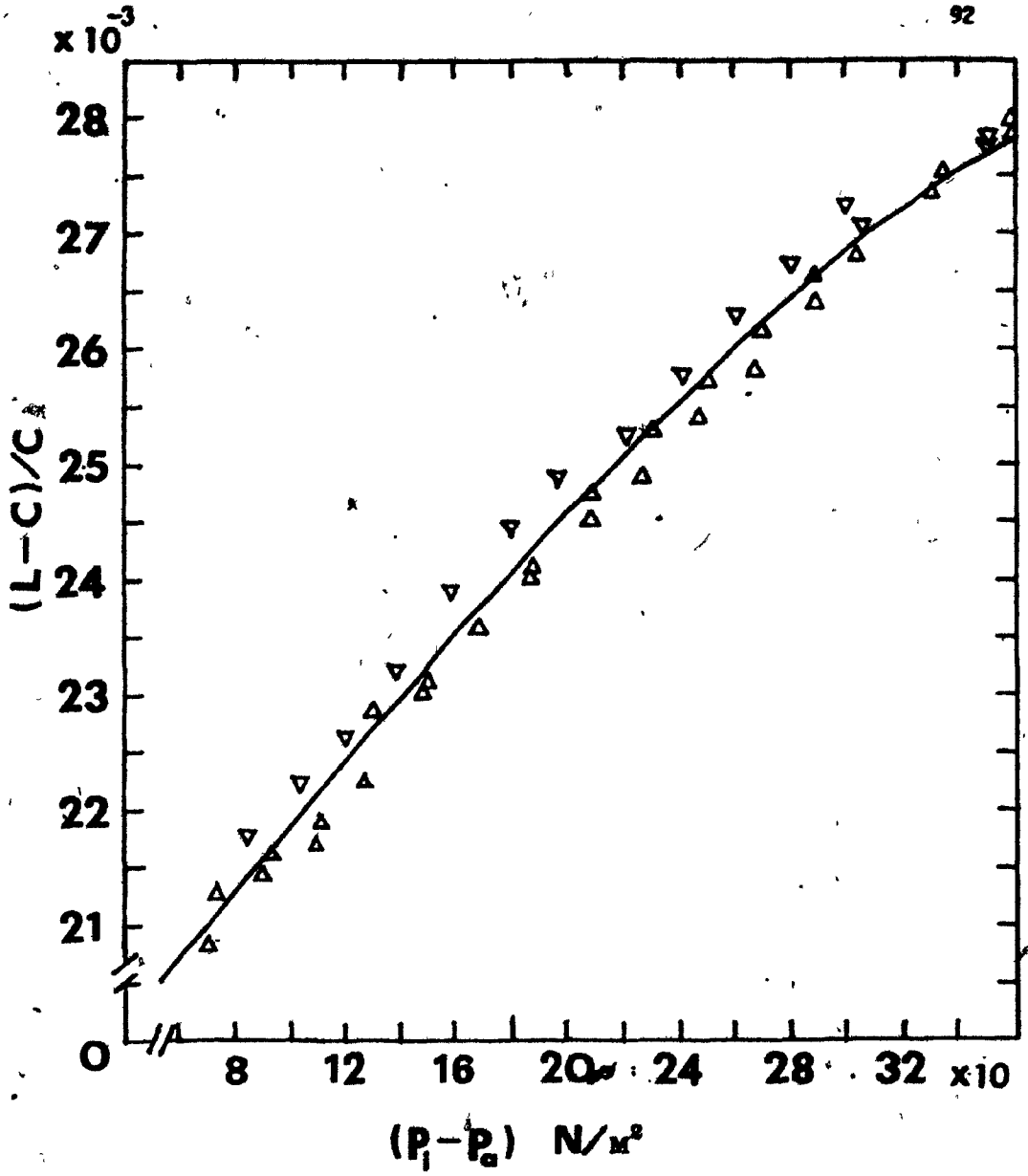

Figure 19A Calibration of excess length to chord ratio plotted against the inflation pressure at wind off.

$$\frac{\ell - c}{c} = (18.744 + 0.02932.07\ \Delta P - 0.3393227 \times 10^{-7}\ \Delta P^3) \times 10^{-3}$$

$$71 < \Delta P < 360$$

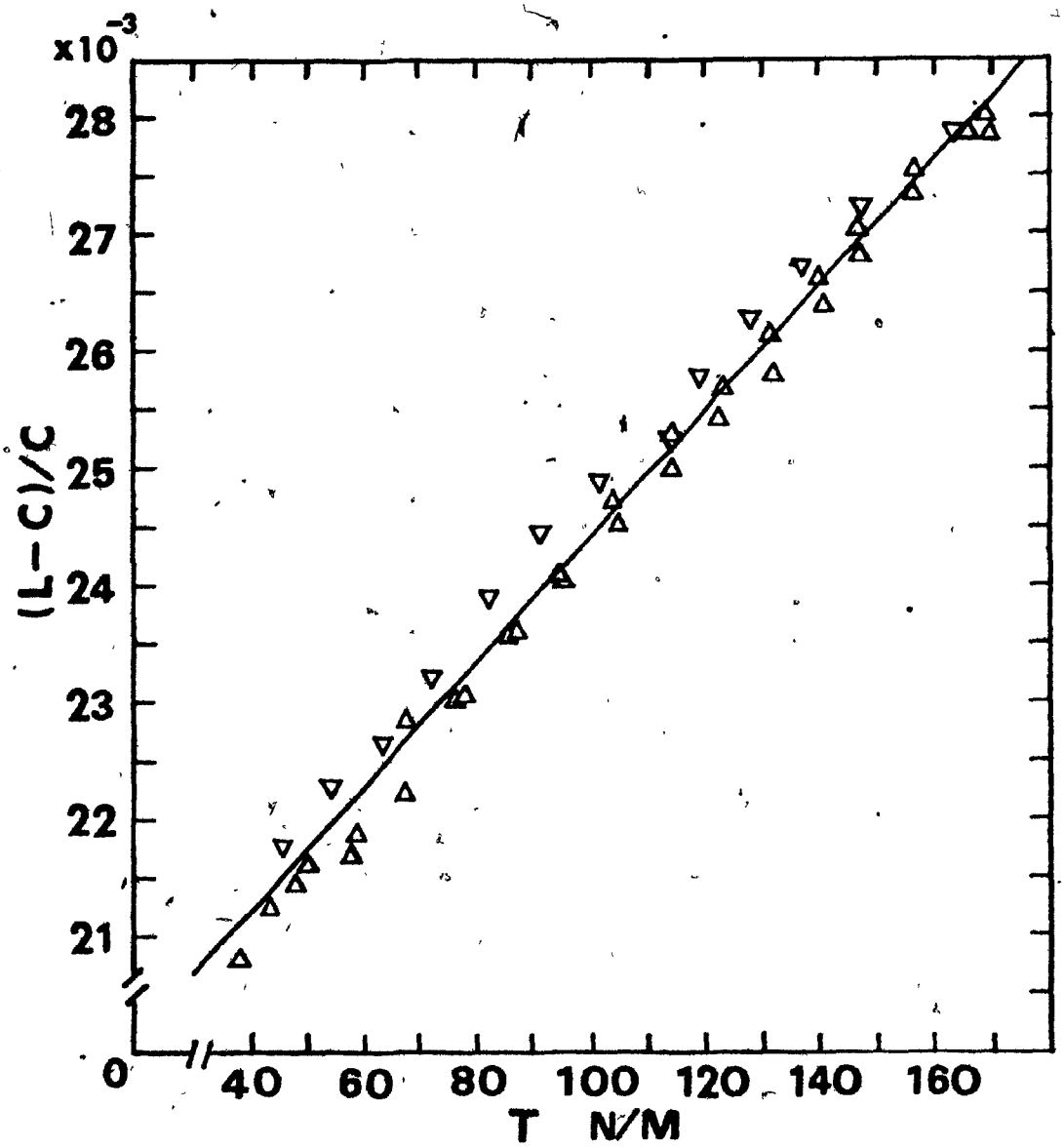

Figure 19B Calibration of excess length to chord ratio plotted against the induced tension at wind off.

$$\frac{\ell - c}{c} = (19.09275 + 0.0532003\ T) \times 10^{-3}$$

$$38.5 < T < 169.555$$

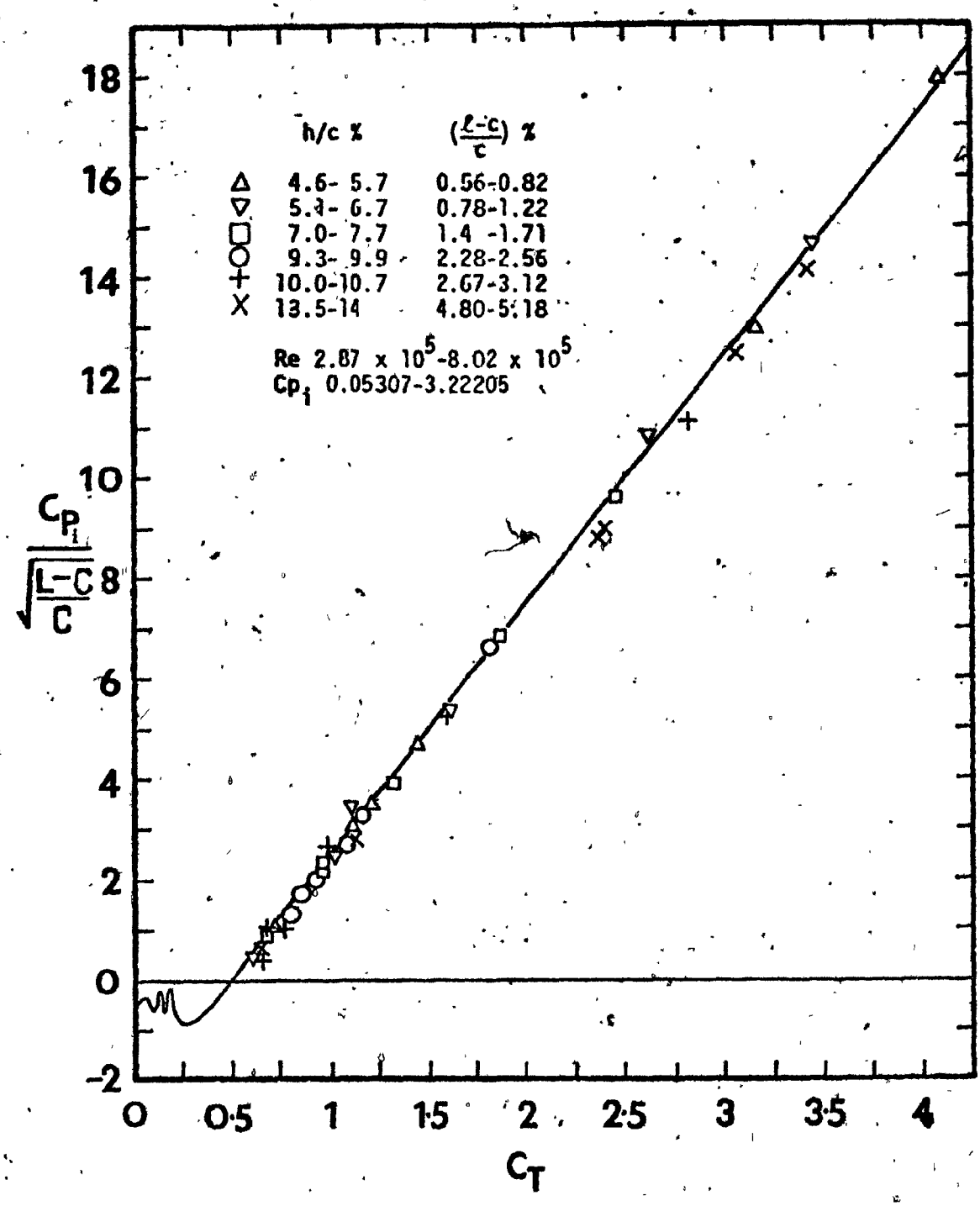

Figure 20 Comparison between theory and experiment for C_T when $Cp_i > 0$.

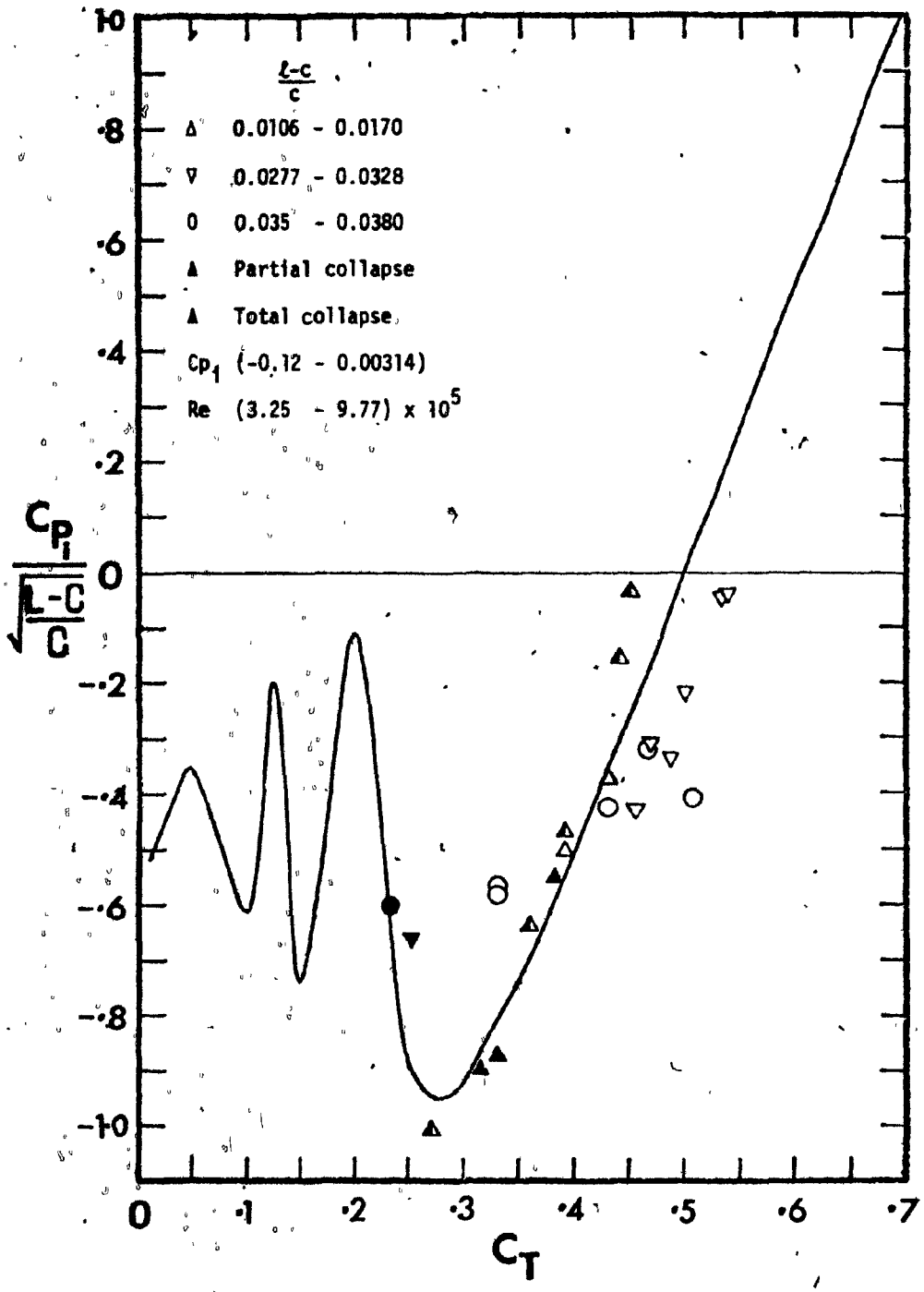

Figure 21 Comparison between theory and experiment for C_T when $Cp_1 < 0$.

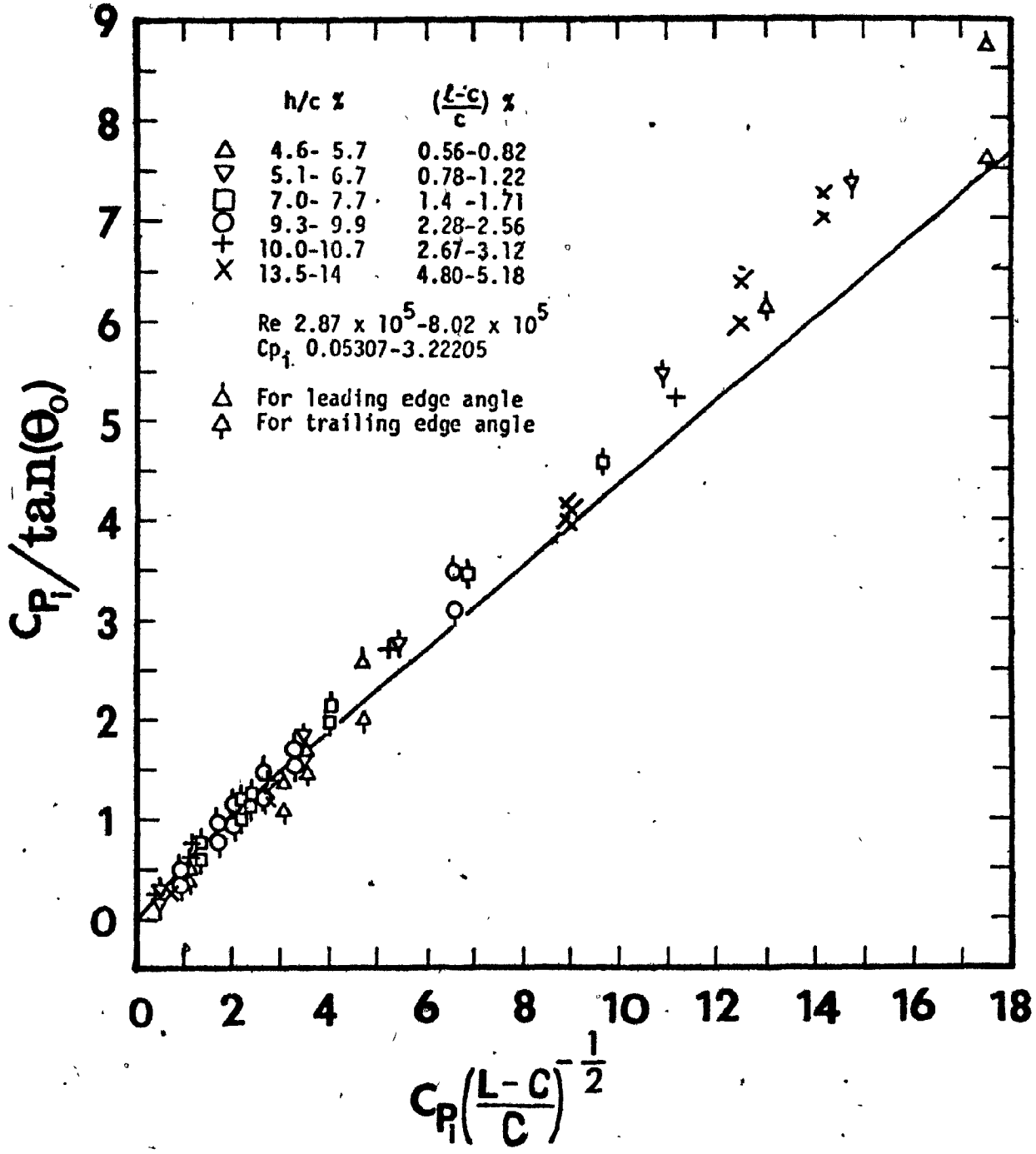

Figure 22 Comparison between theory and experiment for edge slopes at various normalized inflation pressure coefficient.

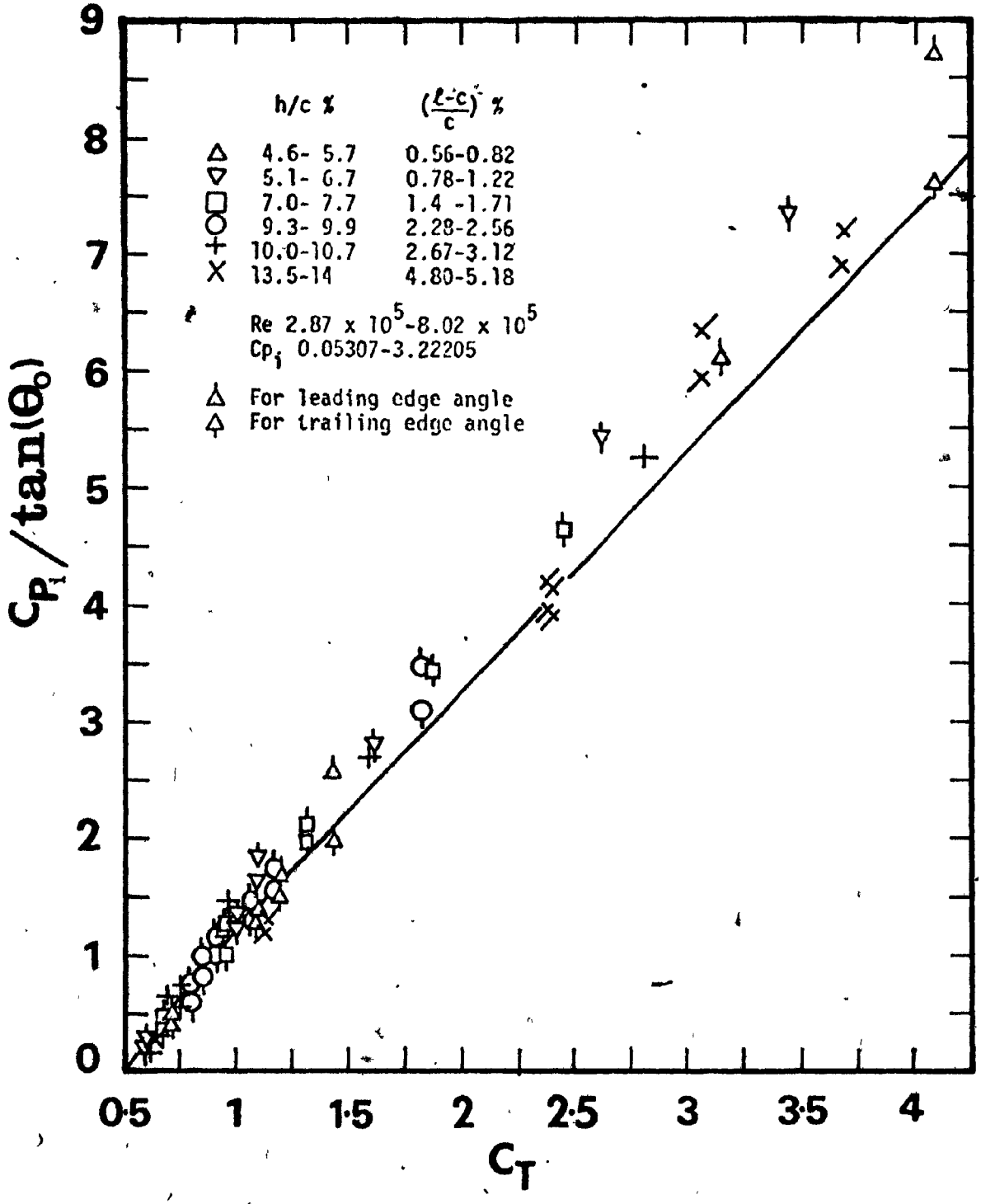

Figure 23 Comparison between theory and experiment for edge slopes at various tension coefficient.

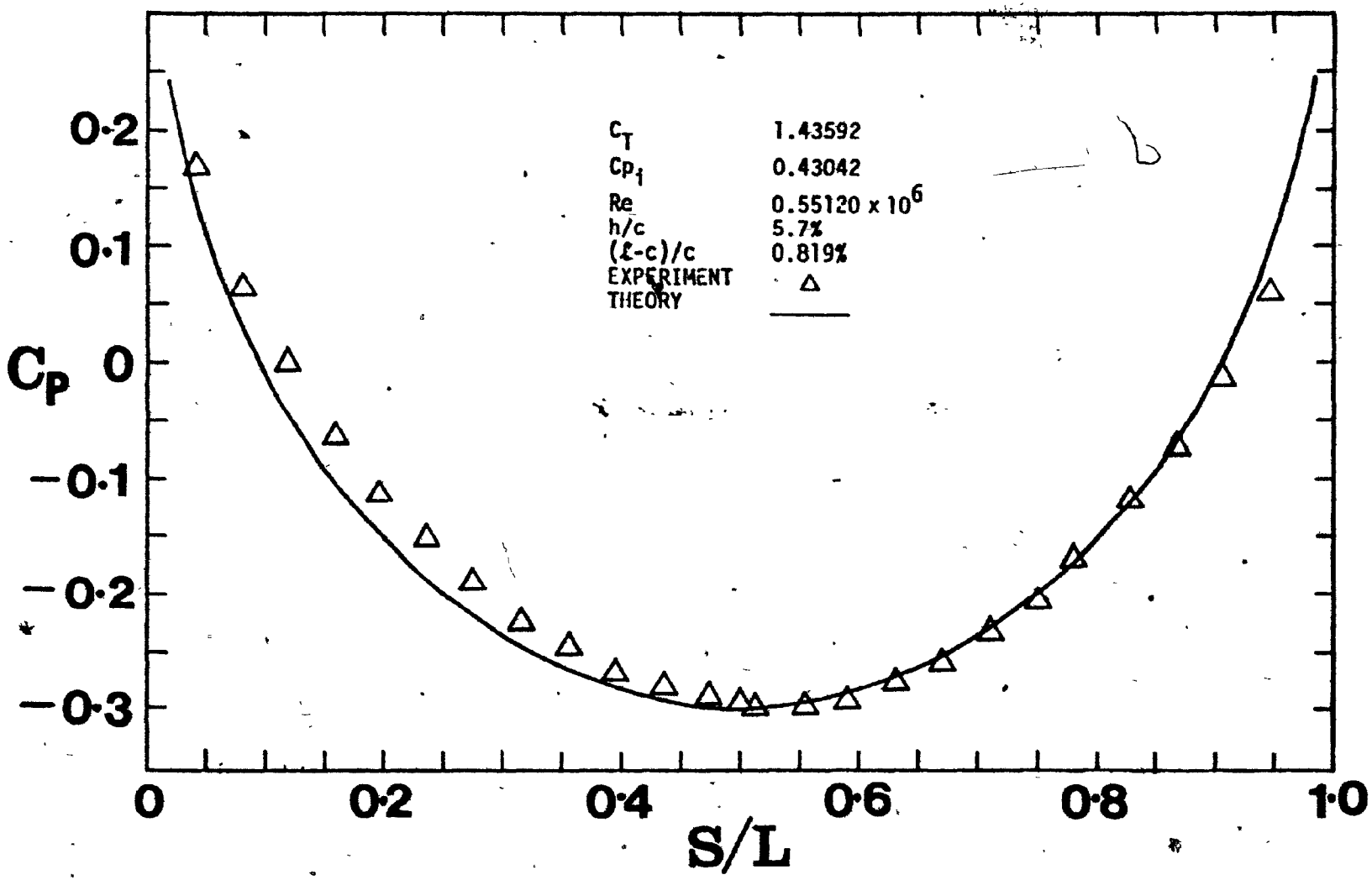

Figure 24 Comparison between theory and experiment for pressure distribution.

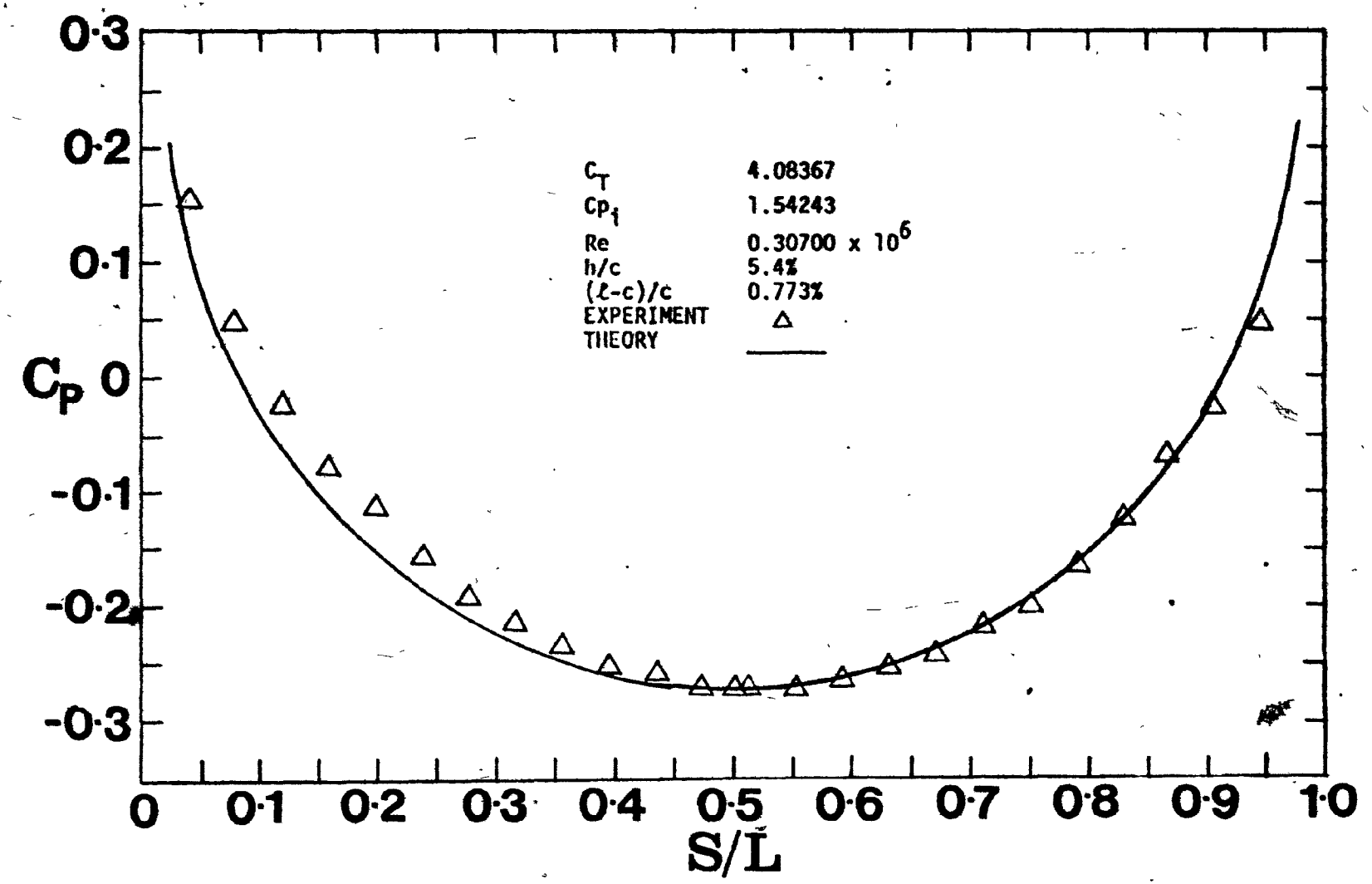

Figure 25 Comparison between theory and experiment for pressure distribution.

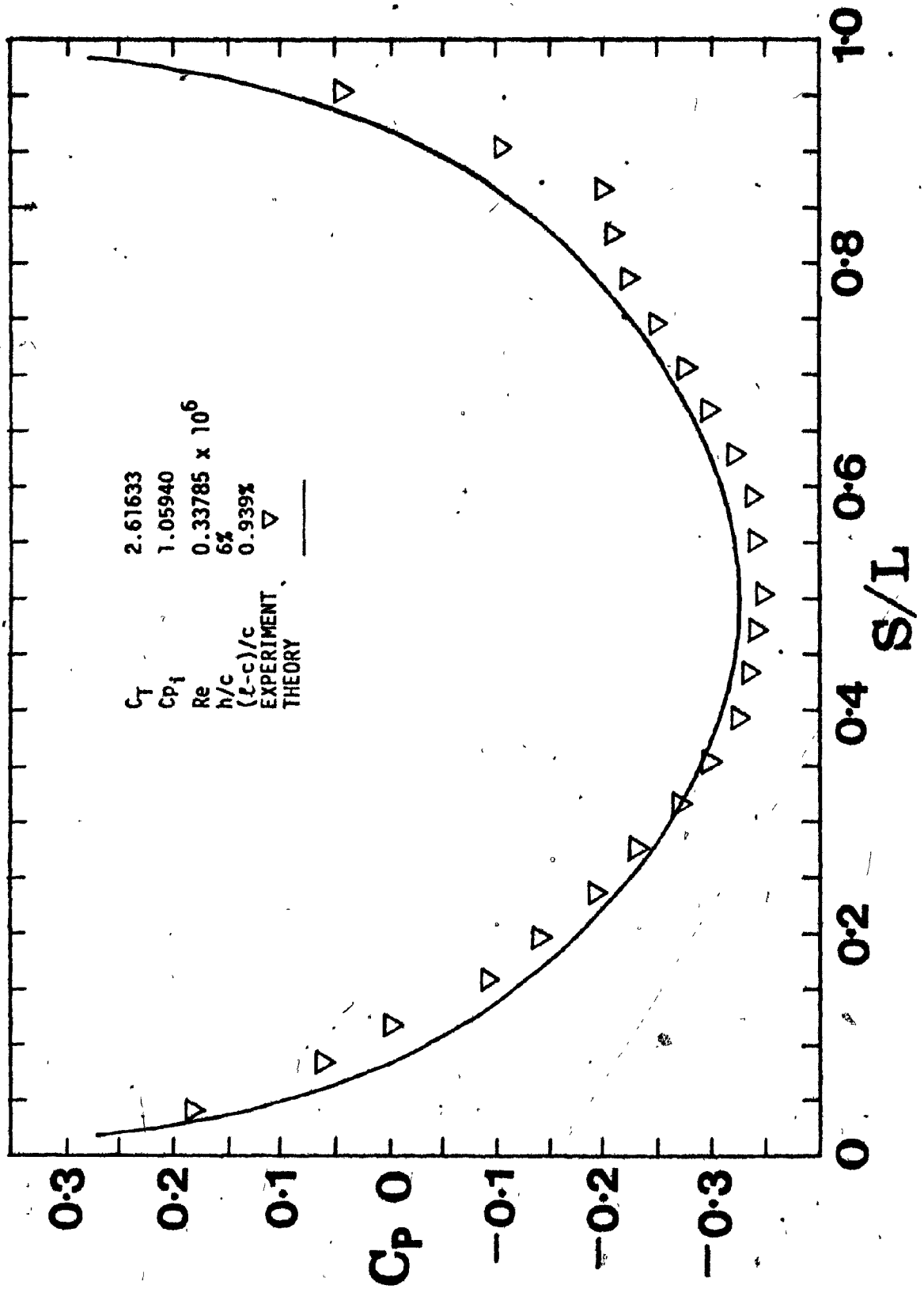

Figure 26 Comparison between theory and experiment for pressure distribution.

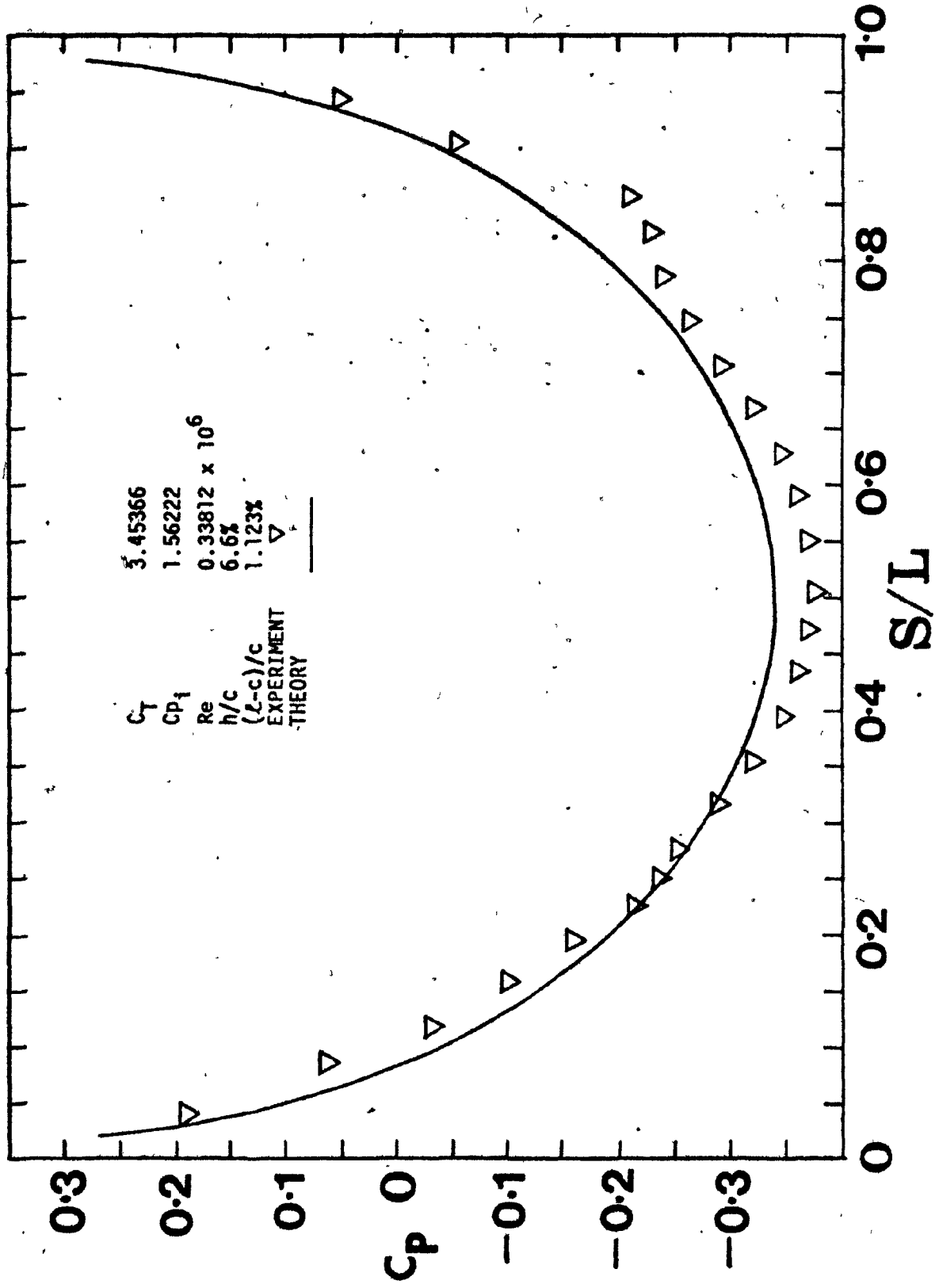

Figure 27 Comparison between theory and experiment for pressure distribution.

Figure 28 Comparison between theory and experiment for pressure distribution.

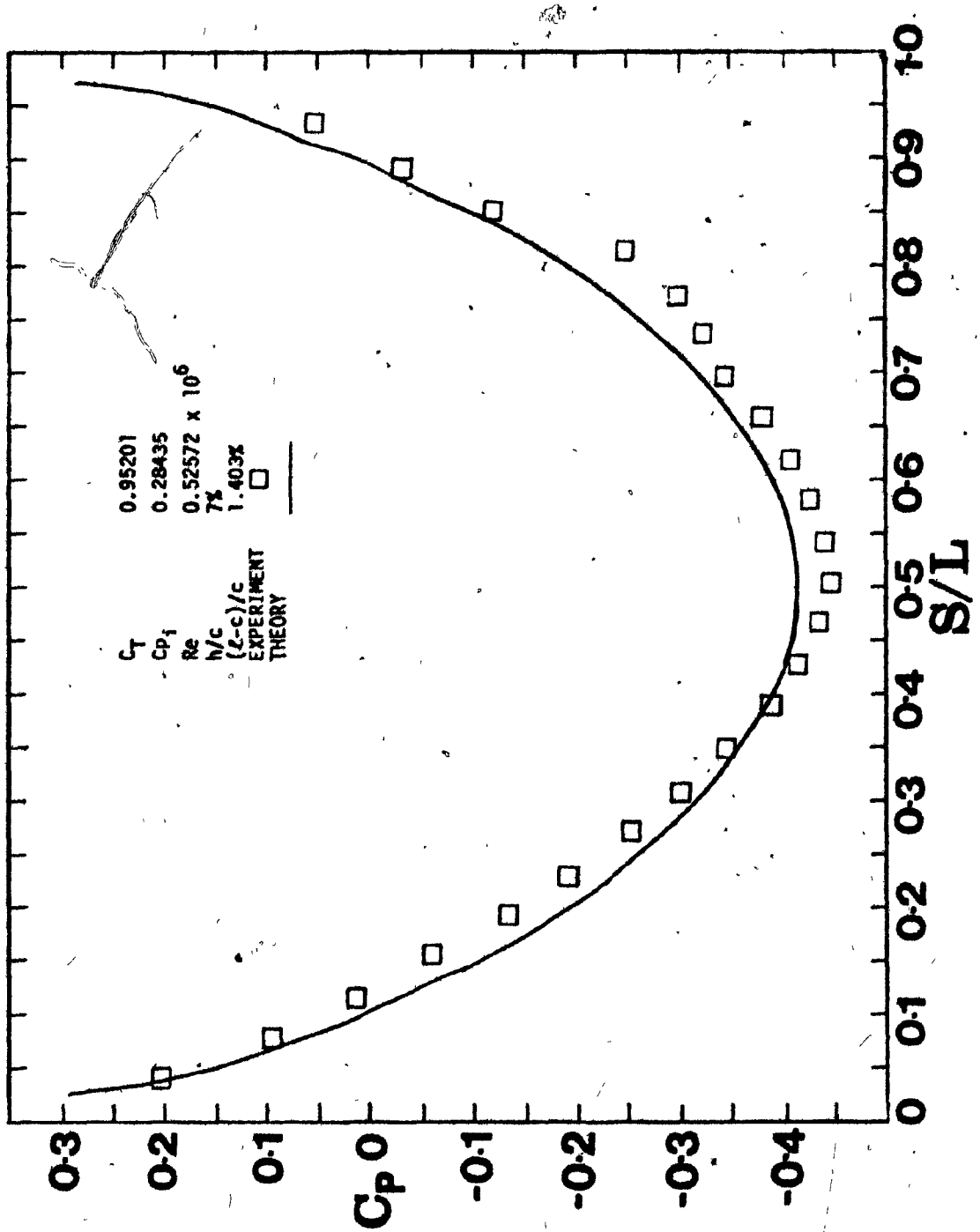

Figure 29 Comparison between theory and experiment for pressure distribution.

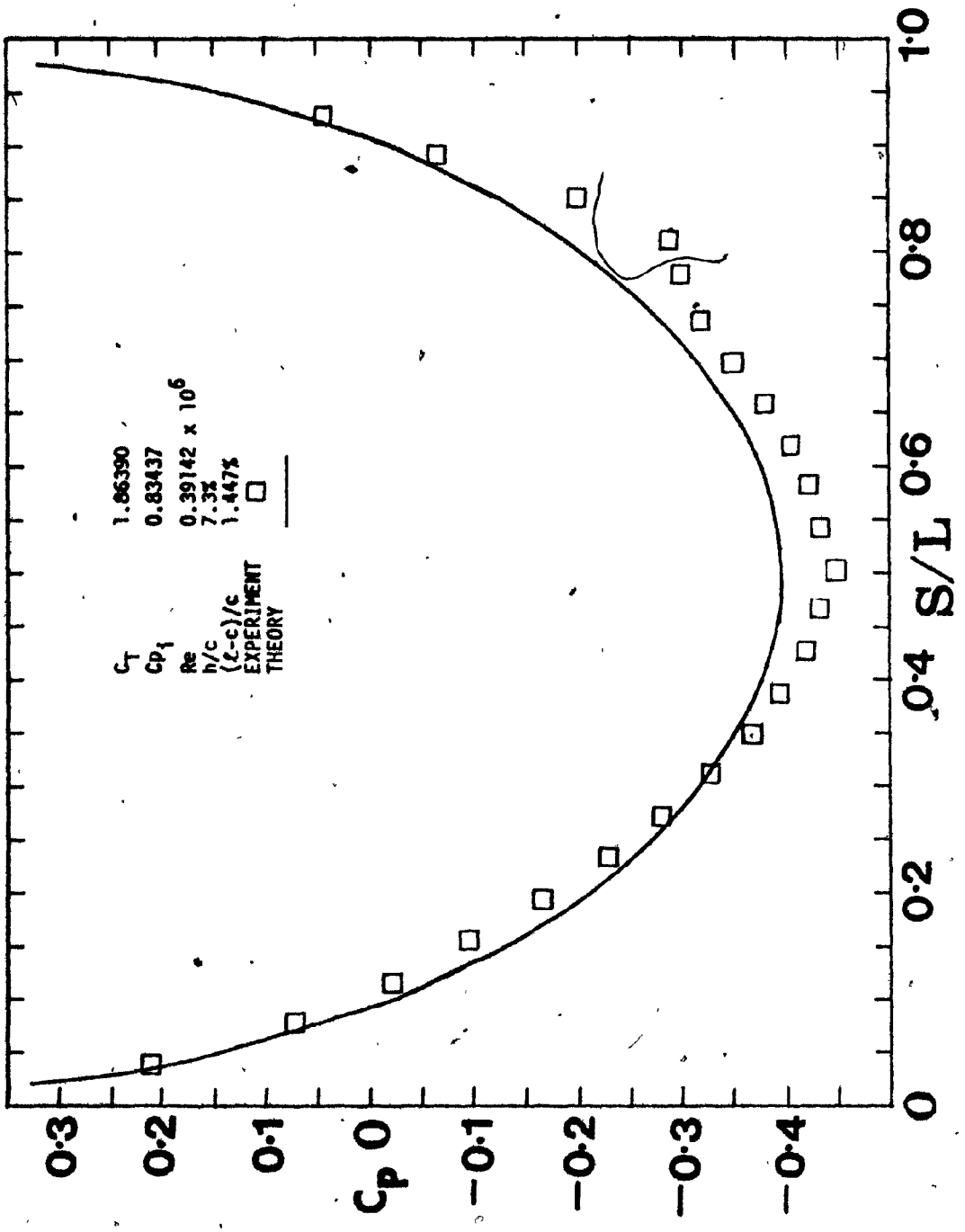

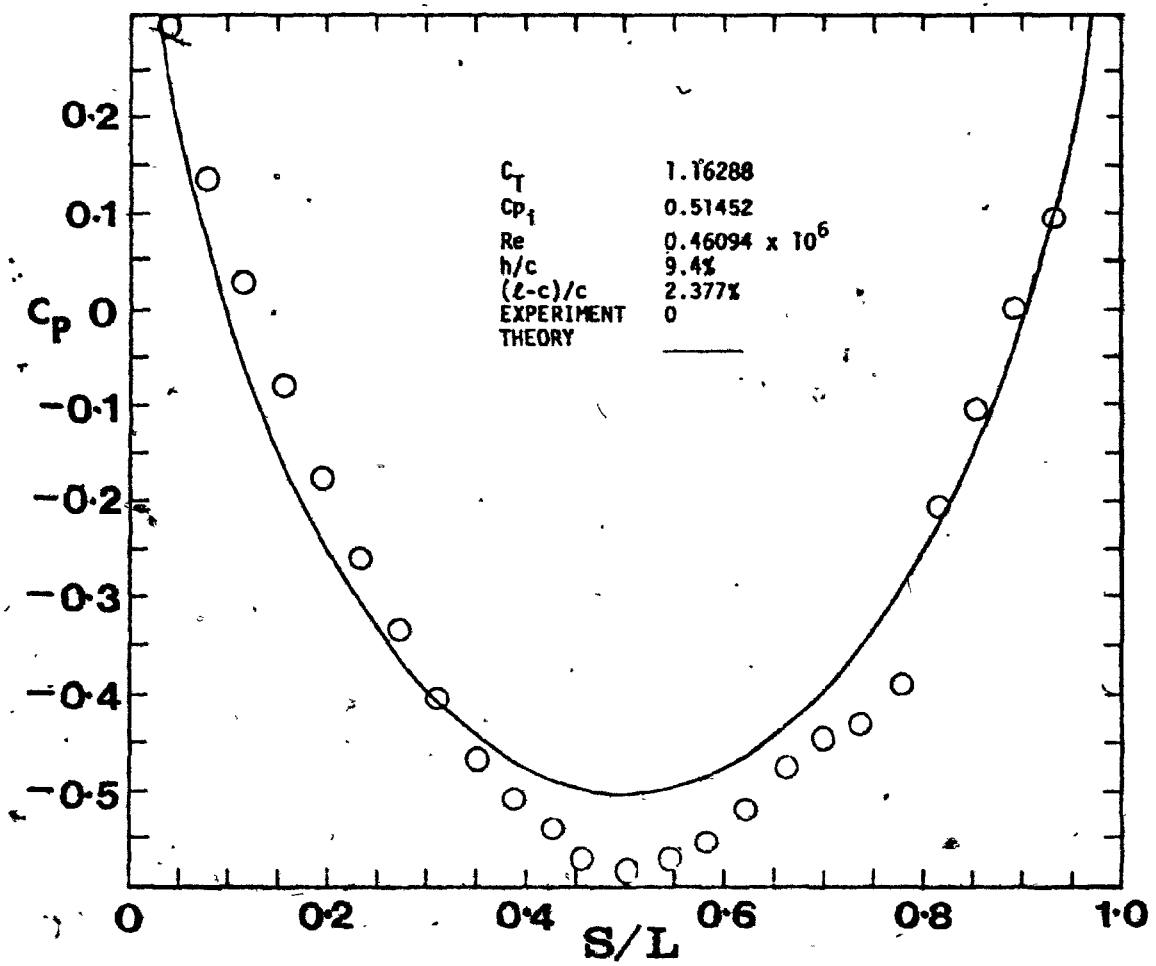

Figure 30 Comparison between theory and experiment for pressure distribution.

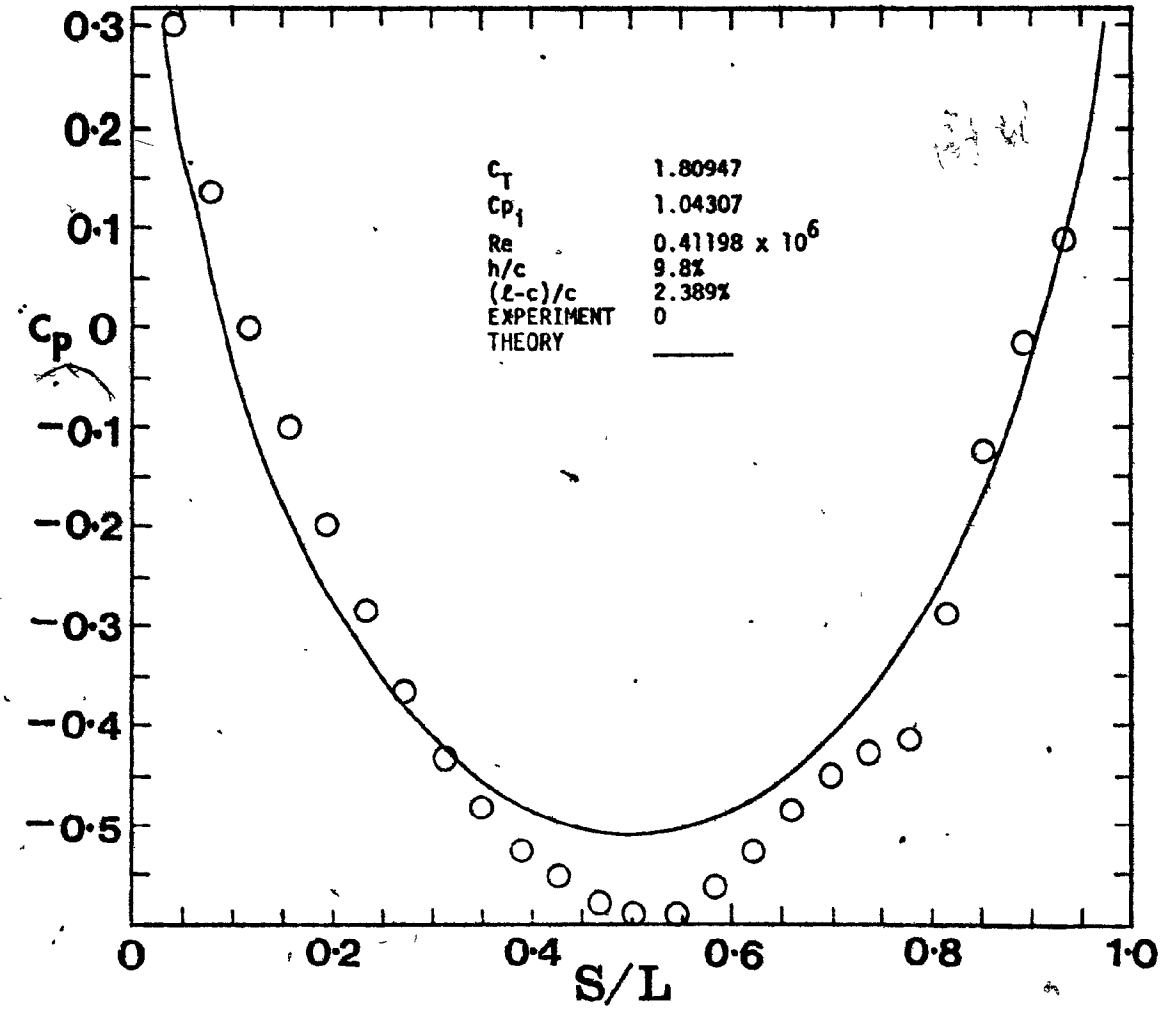

Figure 31 Comparison between theory and experiment for pressure distribution.

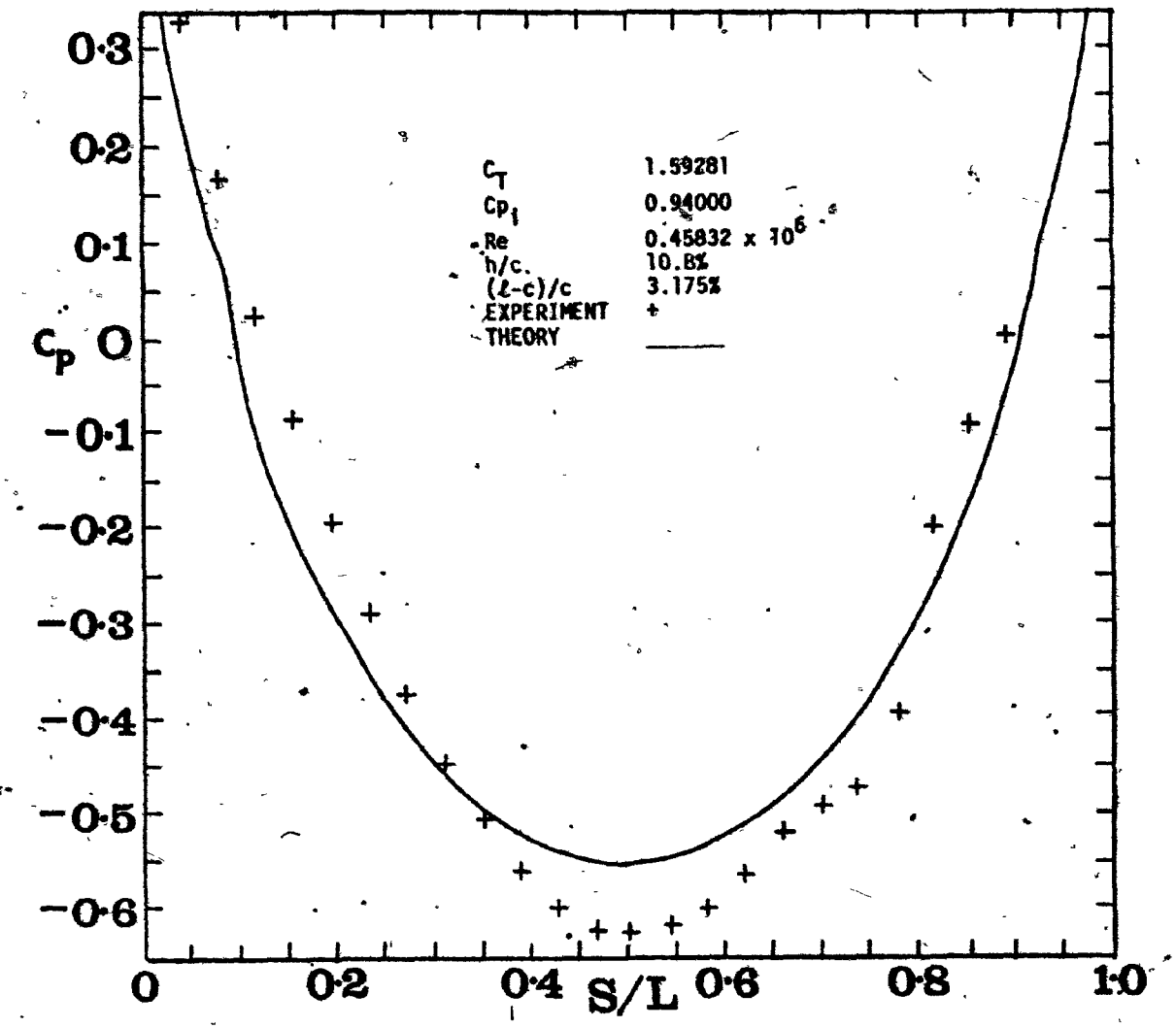

Figure 32 Comparison between theory and experiment for pressure distribution.

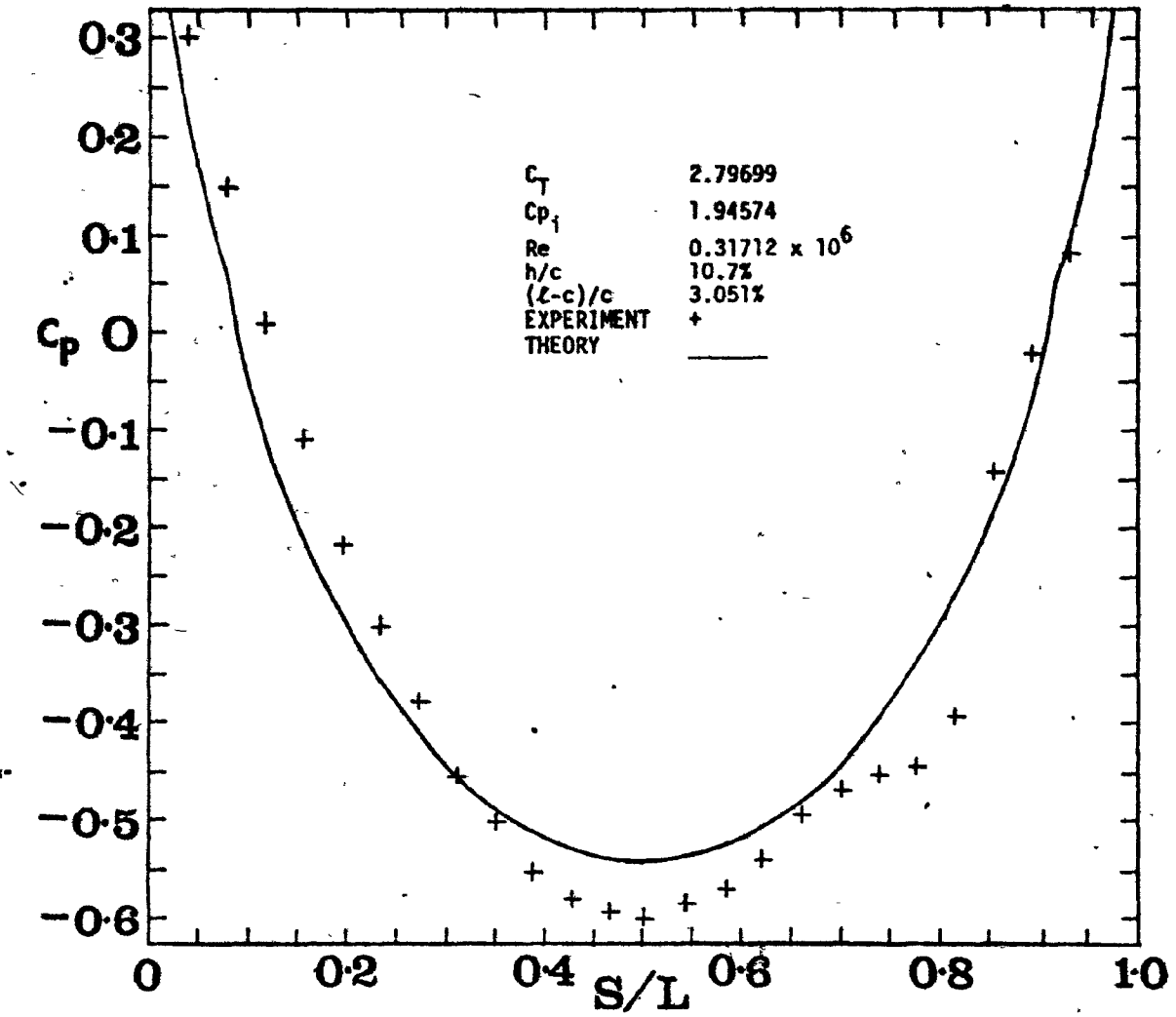

Figure 33 Comparison between theory and experiment for pressure distribution.

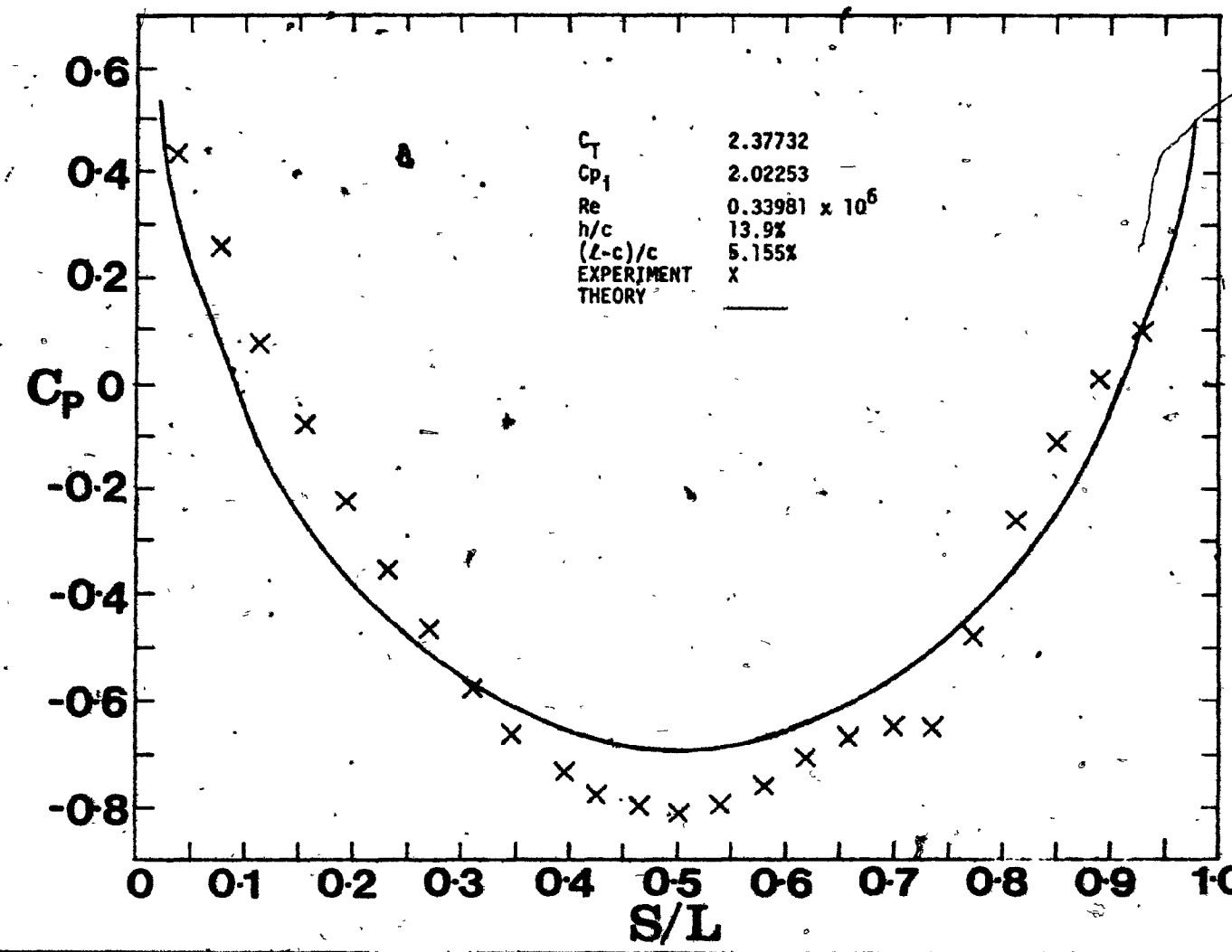

Figure 34 Comparison between theory and experiment for pressure distribution.

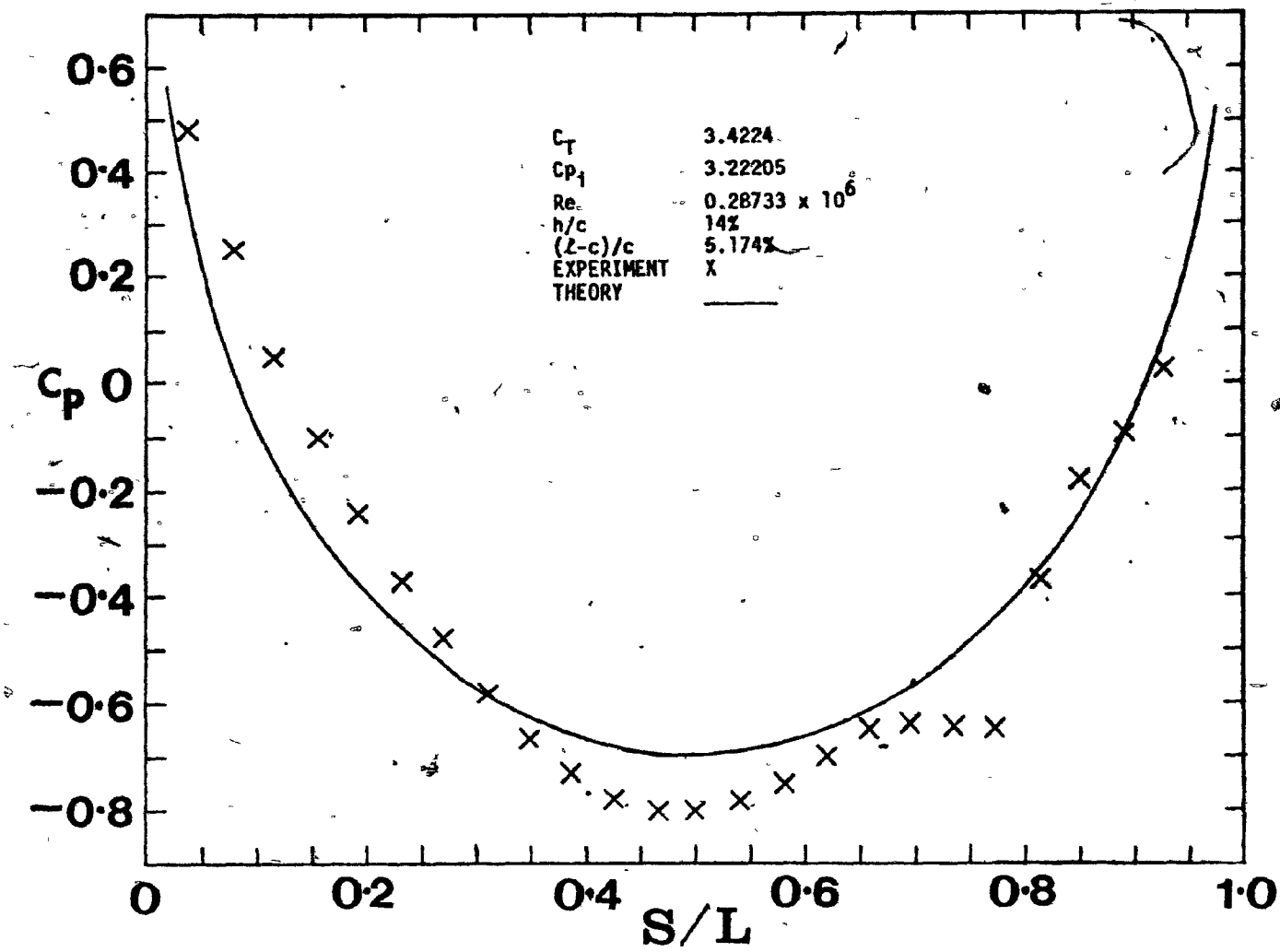

Figure 35 Comparison between theory and experiment for pressure distribution.

Figure 36 Comparison between present method and Karman-Trefft's method for pressure distribution applied for a lenticular aerofoil.

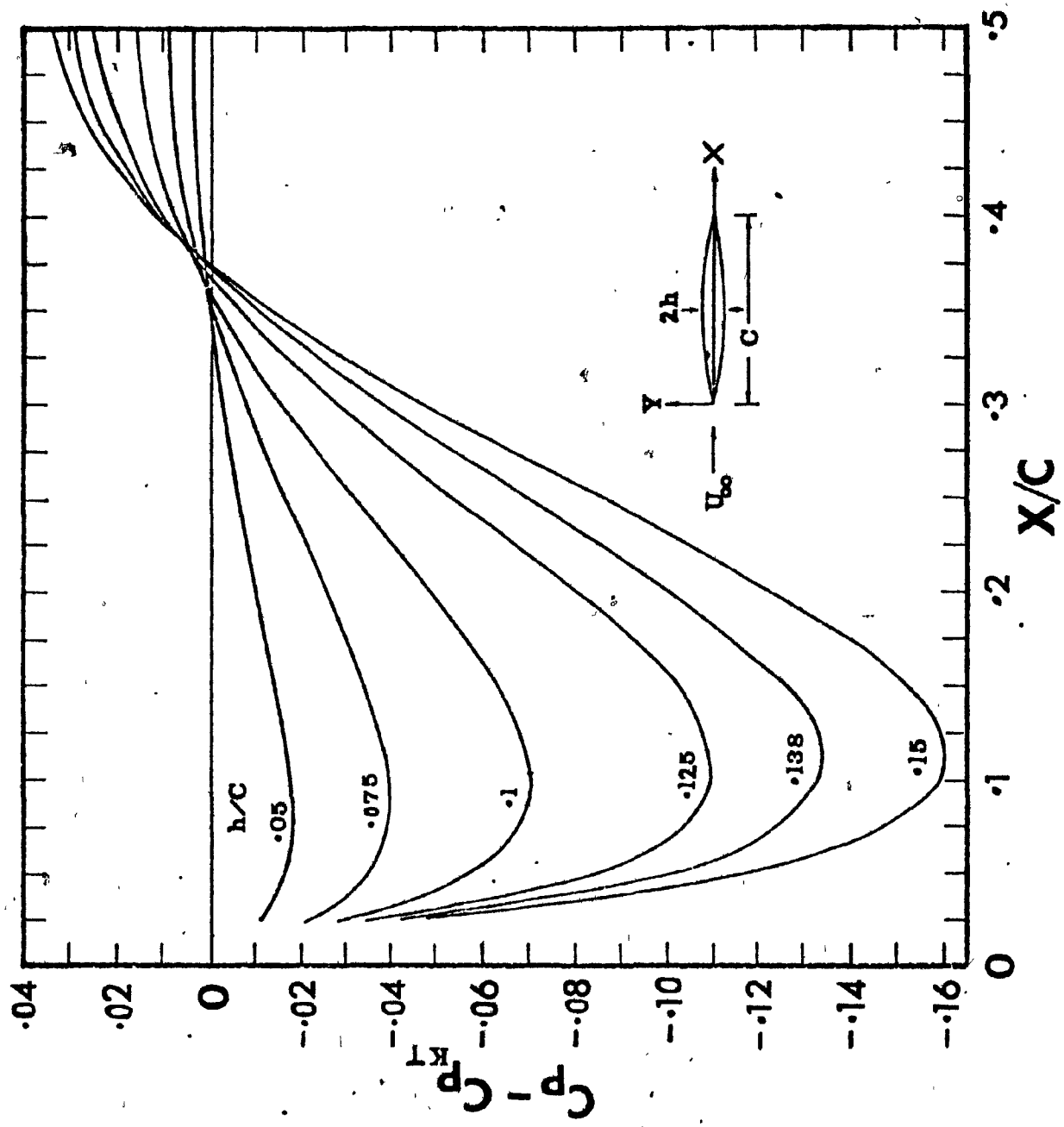

Figure 37a Overall wind tunnel.

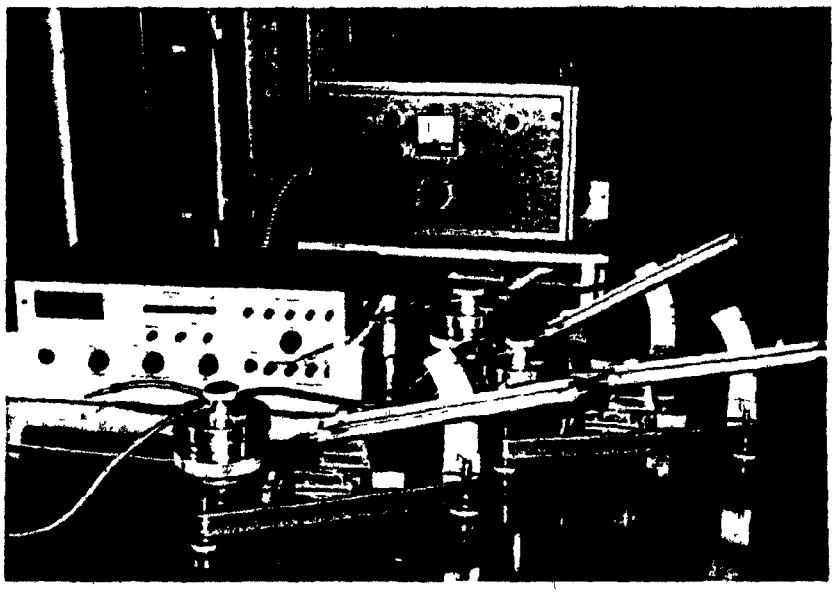

Figure 37b Measuring instruments (inclined manometers and strain indicator 1526).

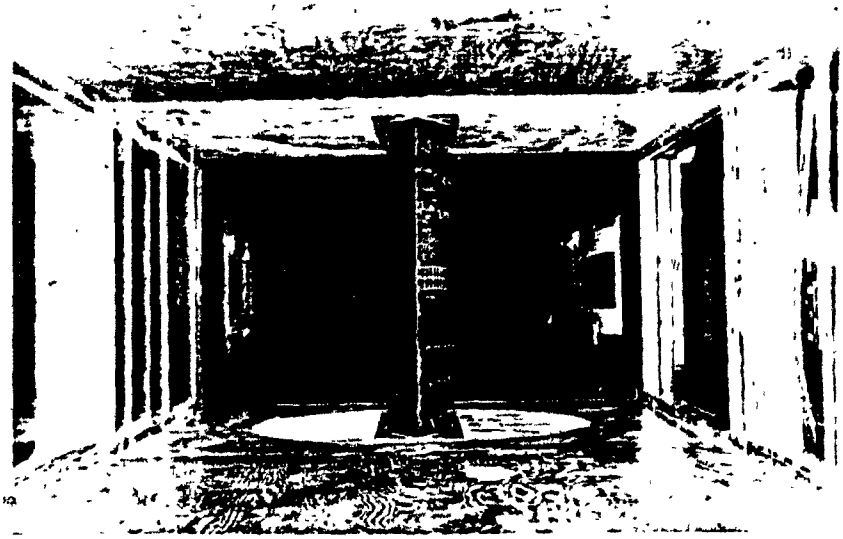

Figure 38a Inflated envelope at wind off (front view).

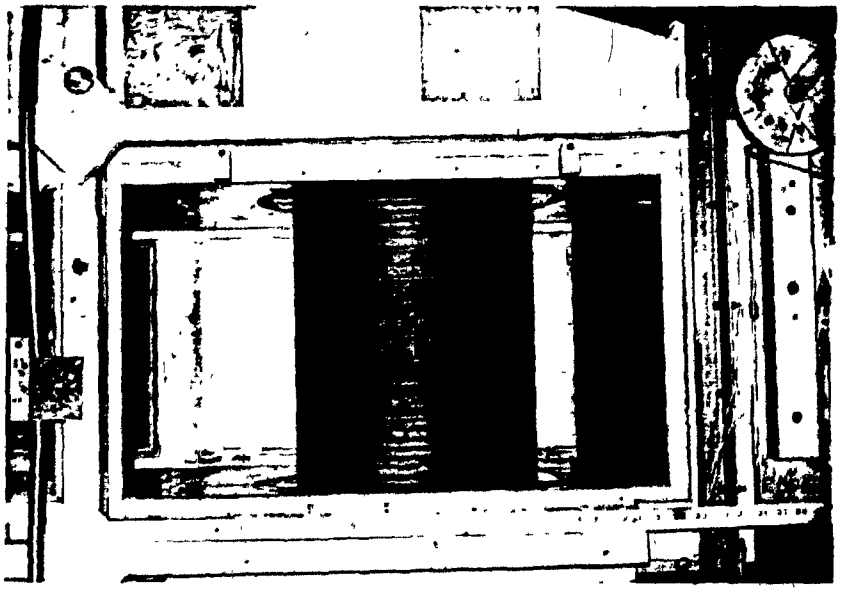

Figure 38b Inflated envelope at wind off (side view).

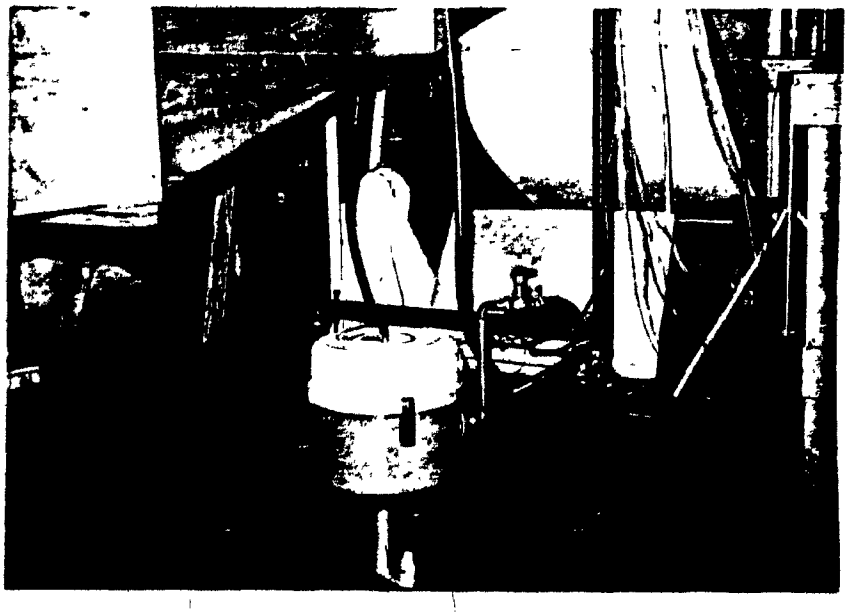

Figure 39 Inflated pressure supply pump.

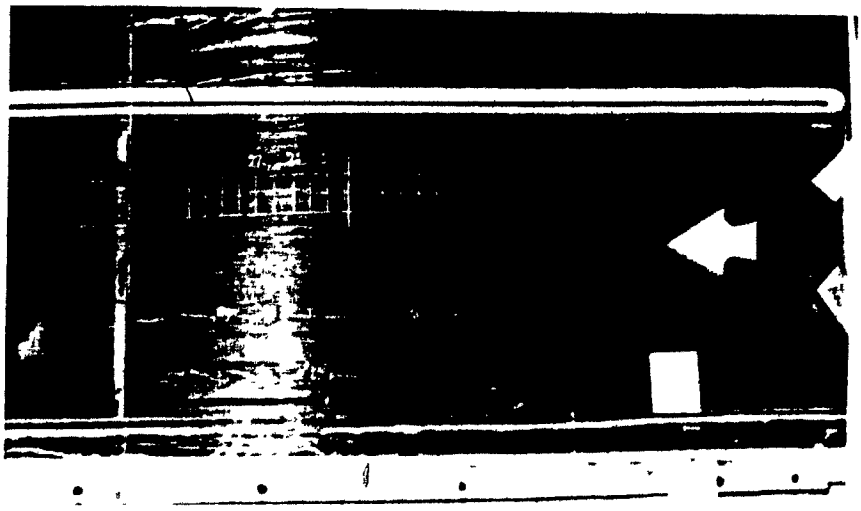

Figure 40a

Re = 7.34×10^5

Cp_i = 0.015

C_T = 0.5698

t/c = 0.2 (wind-off)

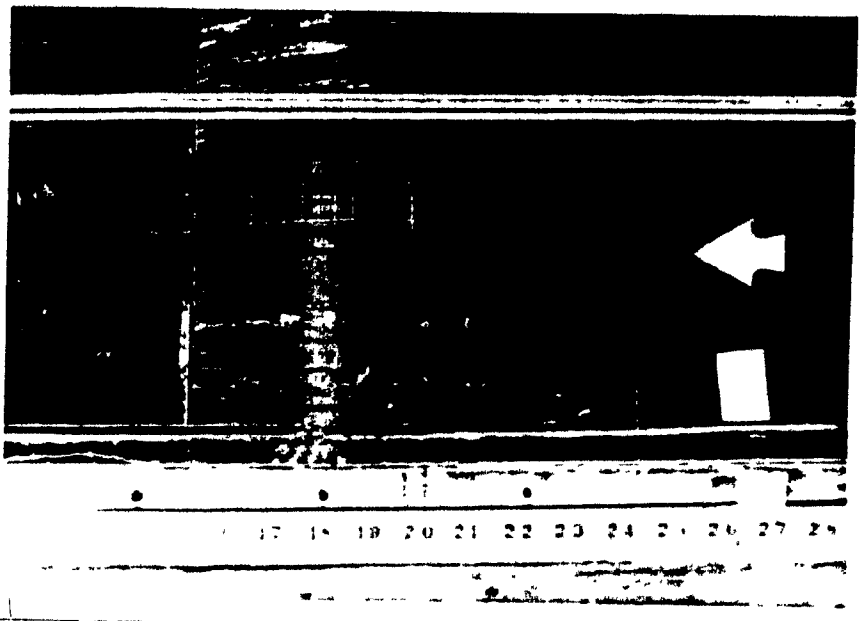

Figure 40b

Re = 3.77×10^5

Cp_i = -0.09817

C_T = 0.41375

t/c = 0.2 (wind-off)

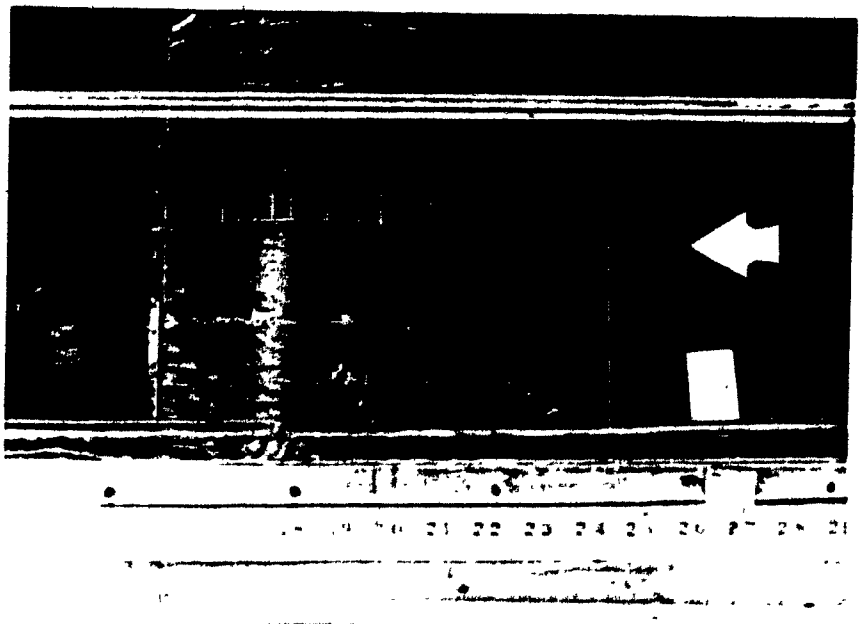

Figure 40c

Re = 3.28×10^5

Cp_i = -0.10865

C_T = 0.25086

t/c = 0.2 (wind-off)

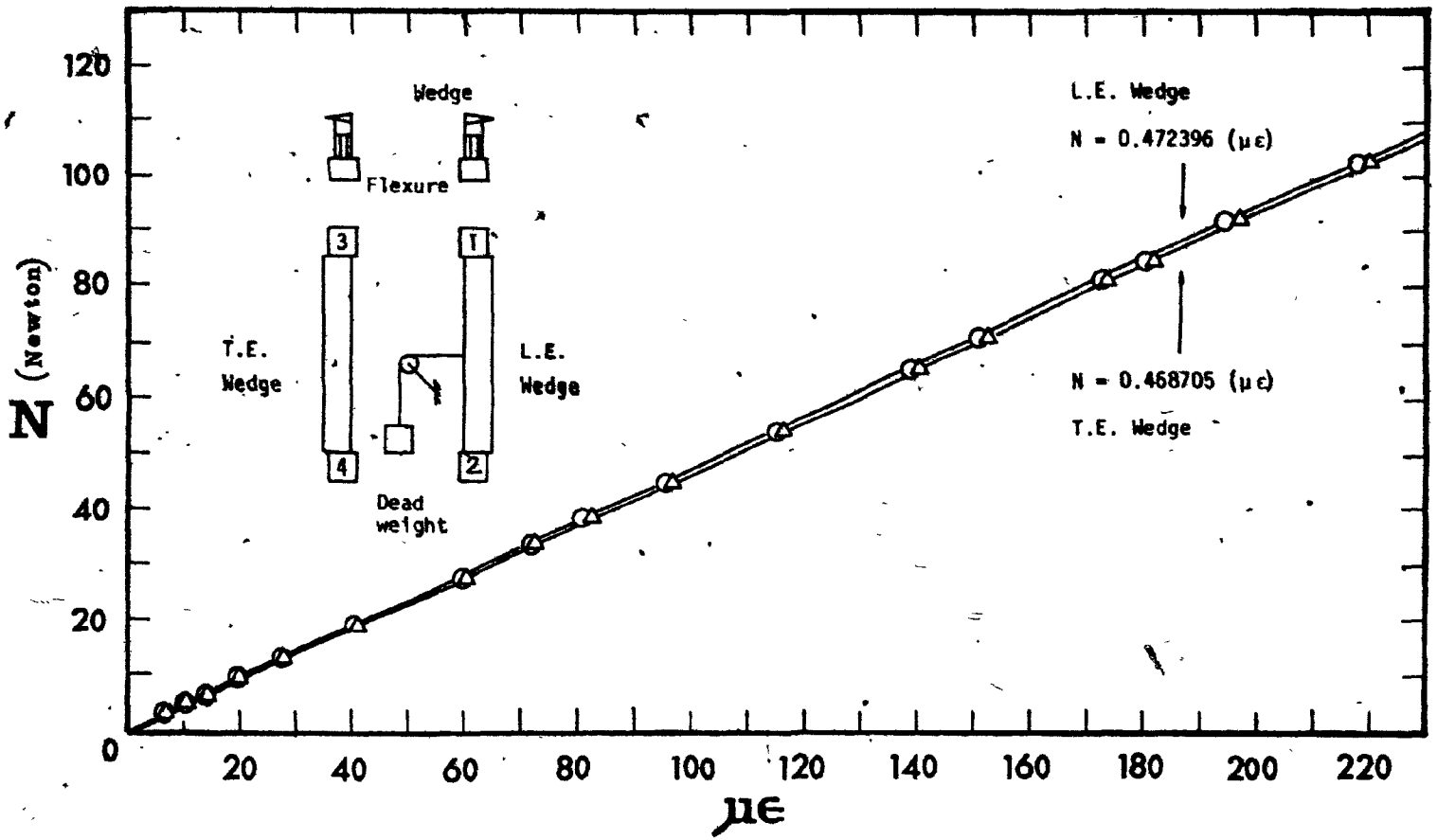

Figure 41 Wedge calibration.